Deterministic and Stochastic Population Invasions

Minors, Kevin

Award date:
2018

Awarding institution:
University of Bath

Deterministic and Stochastic Population Invasions

submitted by

Kevin Minors

for the degree of Doctor of Philosophy

of the

University of Bath

Department of Mathematical Sciences

September 2017

Kevin Minors
August 2016

Acknowledgments

"No man is an island, entire of itself;
every man is a piece of the continent"
- John Donne

"Boy, bye"
- Beyoncé

To my supervisors, Tim Rogers and Jonathan Dawes, thank you for supporting and guiding me through the last few years. You were the best pair of supervisors I could have had. Tim, you are the new-school, "Just put it in Mathematica", "There's an approximation for that" supervisor while Jon, you're the old-school, "Let me just grab a pen and some paper", "Can you prove that rigorously?" supervisor. Together, it meant that I got the best of both worlds. It also meant that you always both contradicted each other when you gave me advice. Somehow it worked. Thank you. Also, thank you to Richard James, Darren Croft, Safi Darden, and Kit Yates for the collaboration.

"Ethnomathematics is the mathematics practiced by cultural groups, such as urban and rural communities, groups of workers, professional classes, children in a given age group, and indigenous societies. In addition to this anthropological character, ethnomathematics has an undeniable political focus. Ethnomathematics is imbedded in ethics, focused on the recovery of the cultural dignity of the human being. The dignity of the individual is violated by social exclusion, which often occurs as a result of failing to pass the discriminatory barriers established by the dominant society, including, and principally, in the school system;

but also by making costumes of the traditional garb of marginalised peoples; folklore of their myths and religions; crimes of their medical practices; and for making of their traditional practices and their mathematics, mere curiosity, when not the target of derision."
- Ubiratan D' Ambrosio in 'Ethnomathematics: Link between Traditions and Modernity'

"In this chapter, I call on the revolutionary function of the Negro spiritual to draw out the "light" of hidden liberatory discourse about teaching, to rally mathematics educators and mathematics teachers of Black children in Bermuda, and elsewhere, toward excellence in teaching."
- Dr. Lou Matthews in ' "This Little Life of Mine!" Entering Voices of Cultural Relevancy into the Mathematics Teaching Conversation' in the collection 'Mathematics Teaching, Learning, and Liberation in the Lives of Black Children'

To my parents, Carol Minors and Kevin Minors Sr., I love you so much. Thank you for having me, raising me, and being there for me. I hope that one day I can repay you for all the sacrifices you made for me. As far as I'm concerned there are no better parents in the whole world. Also, in a few months, my scholarship is gonna run out and I'm gonna need a place to stay. Could I possibly move back home please? Did I say how much I love you? To my brother, Keevon Minors, I'm so proud of you and grateful to have you in my life. I know you don't like it when I tell you how I feel about you, in public or in private, but once again I want to let you know that I love you. You really are the cooler brother and I'm excited to continue to watch you grow into the amazing person you are. Keep doing your thing boss. To my puppy, Cocoa, I can't wait to see you again. I'm sorry I've been gone for so long. I promise I'll be there soon to open my bedroom door when you scratch on it.

"The contribution that falls to us, the exploited and backward of the world, is to eliminate the foundations sustaining imperialism...The fundamental element of that strategic objective, then, will be the real liberation of the peoples..."
- Che Guevara in 'Message to the Tricontinental' (1967)

"I am a feminist, and what that means to me is much the same as the meaning of the fact that I am Black: it means that I must undertake to love myself and to respect myself as though my very life depends upon self-love and self-respect."
- June Jordan

To my extended family, thank you for being a wider support network for me. To my Granny, Carol Raymond, and my Nana, Hilda Minors, I am so grateful to have both of you in my life. To all my aunts, Aunt Rhonda, Aunt Judy, Aunt Beda, Aunt Karen, to all my uncles, Uncle Ivor, Uncle Wallace, Uncle Kendall, Uncle Arnold, Uncle William, Uncle Karl, to all my cousins, Trae, Tasia, Wallicia, David, Renita, Breanna, Brandon, Corey, Natasha, Ronisha, Jamel, Jashun, Jahvon, Jashae, Sherika, Jeelise, to all my 'cousins', who are too many to list here, to all my godparents, Godma Brenda, Godma Shirley, Godma Melody, Godma Zina, Godma Pearline, Godma Ronni, Godpa Llewelyn, Godpa Leon, Godpa Kevin, Godpa Craig, Godpa Benjamin, and to all my family friends, I love you and appreciate you all. To my church family at Vernon Temple AME, I will always be grateful for the people who helped raise me there. To all my teachers at Warwick Academy, thank you for your dedication. In particular, thank you Mr. Rothwell for pushing me in mathematics and physics and thank you Ms. Mathias for guiding me into university and life in general. To the Class of 2010, what's up? Shout out to us! One time for Waltz, Scoop, Oats, Sou, Lush, Wally, Chub, CorCor, and everyone else in that ridiculous group chat. We made it! To my basketball family, I will never forget the experiences, the rivalries, and the team spirit. I look forward to it all picking right back up when I get back. In particular, thank you Chris Crumpler for taking me under your wing and mentoring me. I appreciate it. I'll never forget the fact that you don't feel sorry for me. To my barber Mr. Cromwell Shakir, I learned so much sitting in your chair. Thank you.

"Post-colonialism as a political philosophy means first and foremost the right to autonomous self-government of those who still find themselves in a situation of being controlled politically and administratively by a foreign power. With sovereignty achieved, post-colonialism seeks to change the basis of that state itself,

actively transforming the restrictive, centralising hegemony of the cultural nationalism that may have been required for the struggle against colonialism"

- Robert Young in 'Post-colonialism: A Very Short Introduction'

"Our aim is simple: to be a government for all of Bermuda, whether it be the haves or have-nots, whether it is Front Street or North Village"

- Bermuda Premier David Burt

To my country, Bermuda, thank you for being another world, for better, for worse, and for everything in between. To my fellow Bermudian academics that I've crossed paths with along the way, Emily, Rosy, Kristy, and Alexa, those trips to Oxford and London meant the world to me. Thank you. Special thank you to the Bermuda Oxford and Cambridge Society and to Jay for helping me with practice interviews. To my Oxford family, what a wild ride undergrad was. Shout out to everyone in Teddy Hall, in the mathematics department, in the Oxford University Basketball Club, and in the African and Caribbean Society. In particular, thank you Brian Kwoba for introducing me to white supremacy and oppression and also to black liberation and decolonisation. I am truly grateful. To my Bath family, these last few years have been fun. Shout out to everyone in the basketball club, everyone in the undergraduate African and Caribbean Society, everyone in the postgraduate African and Caribbean Society (which I founded), and everyone in the mathematics department, particularly the Centre for Networks and Collective Behaviour. Shout out to Miranda and Amy, you are both amazing. One time for everyone at the Wellbeing Service, your support has been invaluable.To everyone on social media, thank you so much for coming on this journey with me. I appreciate every like, comment, share, repost, retweet, hashtag, 'Haha' react, and 'Love' react. Social media got me through some tough times. Thank you.

"We may be tired of carrying our heavy hearts,
but we will always march forth."

- Liana Hall

"The first act of violence that patriarchy demands of males is not violence toward women. Instead patriarchy demands of all males

that they engage in acts of psychic self-mutilation, that they kill off
the emotional parts of themselves. If an individual is not successful
in emotionally crippling himself, he can count on patriarchal men to
enact rituals of power that will assault his self-esteem."
- bell hooks

To all the black women in my life, words cannot describe how exceptional you all are. I appreciate each and everyone of you. In particular, thank you to Chloe, Sooto, Dimpho, Ashleigh, Shara, Nafisa, Sheila, Kelly, Euella, Shmona, and Jahnaie. I hope that you achieve all the successes in the world. Shout out to my best friend Mukovhe Masutha. I'm so glad we've been able to connect and survive postgraduate university life together. I am going to miss you when I leave. Please hurry up and come back to England so we can celebrate!

"Praise Black women like religion, I Hail Mary Prince.
Forgive me for letting you down, but never again.
You provided me with life and in my early years,
I was trained to shame you, I see my ways and I repent.

We as men wage war, greenlight genocide,
Sexual, physical violence, ain't never lied.
Ain't it ironic, how we blame and shame rape victims,
And do our best to protect the offenders lives?"
- Makeem Bartley A.K.A Haz the Human

In 2004, Katura Horton-Perinchief represented Bermuda in the
Olympic Games in Athens. She made Olympic history by being the
first black woman to compete in diving and was Bermuda's first
female diver. She is an all-around superhero. #BlackGirlMagic
#BlackBermudianWomanAreAmazing

Finally, shout out to myself. These last few years have been wild. My mental, physical, and emotional health have all faced significant challenges. I've learned the importance of solitude in small doses, the hazards of solitude in large doses, the benefits of writing in my journal, and the joy of going to therapy. On to the next one!

"One of the biggest lessons I learnt was that our collective potential is limitless."

- Ryan Perinchief, founder of the Future Leaders Programme

In Loving Memory
Dakarai Tucker
1992-2008

Summary

This thesis concerns three models of deterministic and stochastic population invasions, starting from individual-level interactions and deducing population-level behaviour.

Firstly, we model a bacteria population near obstacles using the 2D Fisher-Kolmogorov-Petrovskii-Piscounov (FKPP) equation with mixed boundary conditions along a corridor and in the half-plane. For a deterministic population, we calculate the smallest corridor width required for survival, the angle the population level sets make with the boundaries, and the population speed. As the hostility of the mixed boundaries increases, the condition for collapse behind the front is achieved before the condition to achieve speed zero ahead of the front.

Secondly, we model an invasive fish population using the 1D FKPP equation and explore the effect that sexual conflict between individuals has on the diffusion rate, and hence the invasion speed, of the population. After introducing a stochastic model for the microscopic movement, we demonstrate how sexual conflict can increase the effective diffusion rate of a pair of individuals by determining the mean speed, separation, and time required for a direction change. In large populations, sexual conflict can increase the diffusion rate ahead of the front, where the speed of the invasion is determined.

Finally, we model the spread of an opinion using the voter model with nonlocal interaction and diffusion. Individuals can either persuade others who are close by very strongly or persuade others who are far away very weakly. In low density populations, we determine the probability of either individual persuading the other when two different individuals meet in a pair. In a high density population, a small noise expansion determines whether the proportion of either type in the population increases or decreases on average. In both regimes, we find that wide and weakly persuading individuals have an advantage.

List of Publications

K. Minors and J. H. P. Dawes,
Invasions Slow Down or Collapse in the Presence of Reactive Boundaries.
Bull Math Biol (2017) https://doi.org/10.1007/s11538-017-0326-x

K. Minors, T. Rogers, R. James, D. Croft, and S. Darden,
Sexual Conflict Accelerates Species Invasion.
In preparation.

K. Minors, T. Rogers, and C. Yates,
Noise-Driven Bias in the Non-Local Voter Model.
Submitted to EPL.

Contents

1 General Introduction **12**

1.1 New Results Contained in This Thesis 15

2 Technical Introduction **19**

2.1 Dynamics of One Particle 20

2.1.1 Brownian Motion 20

2.1.2 Fokker-Planck Equations 21

2.1.3 Mean Hitting Time 26

2.2 Dynamics of Many Particles 31

2.2.1 Fisher-Kolmogorov-Petrovskii-Piscounov (FKPP) Equation 32

2.2.2 FKPP Invasion Speed Derivation 42

3 Invasions and Reactive Boundaries **47**

3.1 Ahead of the Front 50

3.1.1 C_L 51

3.1.2 C_∞ 54

3.2 Behind the Front 55

3.2.1 Survival 55

3.2.2 Stability 59

3.3 Simulations 62

3.3.1 Stochastic Models 62

3.3.2 Deterministic Model 70

3.4 Conclusion 70

4 Invasions and Intraspecies Conflict **74**
4.1 One Fish . . . 76
4.2 Two Fish . . . 80
4.3 Many Fish . . . 95
4.4 Experiments . . . 100
4.5 Conclusion . . . 103

5 Invasions and Nonlocal Interaction **104**
5.1 Low-Density Regime . . . 107
5.2 High-Density Regime . . . 115
5.3 Conclusion . . . 134

6 General Conclusion and Outlook for Future Research **137**

A Mean Hitting Time For Alternative Boundary Conditions **143**

B Calculation of Sexual Conflict as a Second Order Interaction **146**

Bibliography **154**

Chapter 1

General Introduction

From the ancient Egyptians [1] to early Chinese dynasties [2], from ancient India [3] to the Native Americans [4], mathematical modelling has been a fundamental tool across time and across cultures. It has been used to track the motion of the planets [5], determine how crops should be planted to maximise return [6], and influence the architecture and engineering of early civilizations [7].

In more recent history, mathematics has continued to play a crucial part in modelling the world around us. It has allowed us to model evolution as a result of natural selection [8], the demand at a call centre [9], the spread of infectious diseases through a population [10], and the harm caused by an invasive species [11]. The creation of models that reflect these situations have allowed a deeper understanding of the underlying interactions and resulting phenomena. This thesis will be concerned with the subset of models that focuses specifically on the development of biological populations, which have been studied in depth [12, 13, 14, 15, 16, 17, 18].

Once such model was created in 1937. It was independently introduced by Fisher [19] and by Kolmogorov, Petrovskii, and Piscounov [20]. The Fisher-Kolmogorov-Petrovskii-Piscounov (FKPP) equation models a population moving into a new territory as a reaction-diffusion equation. For a population with density $u(x,t)$ at location x and time t, growth rate r, and diffusion coefficient D, the FKPP equation in 1D is

$$u_t = Du_{xx} + ru(1-u).$$

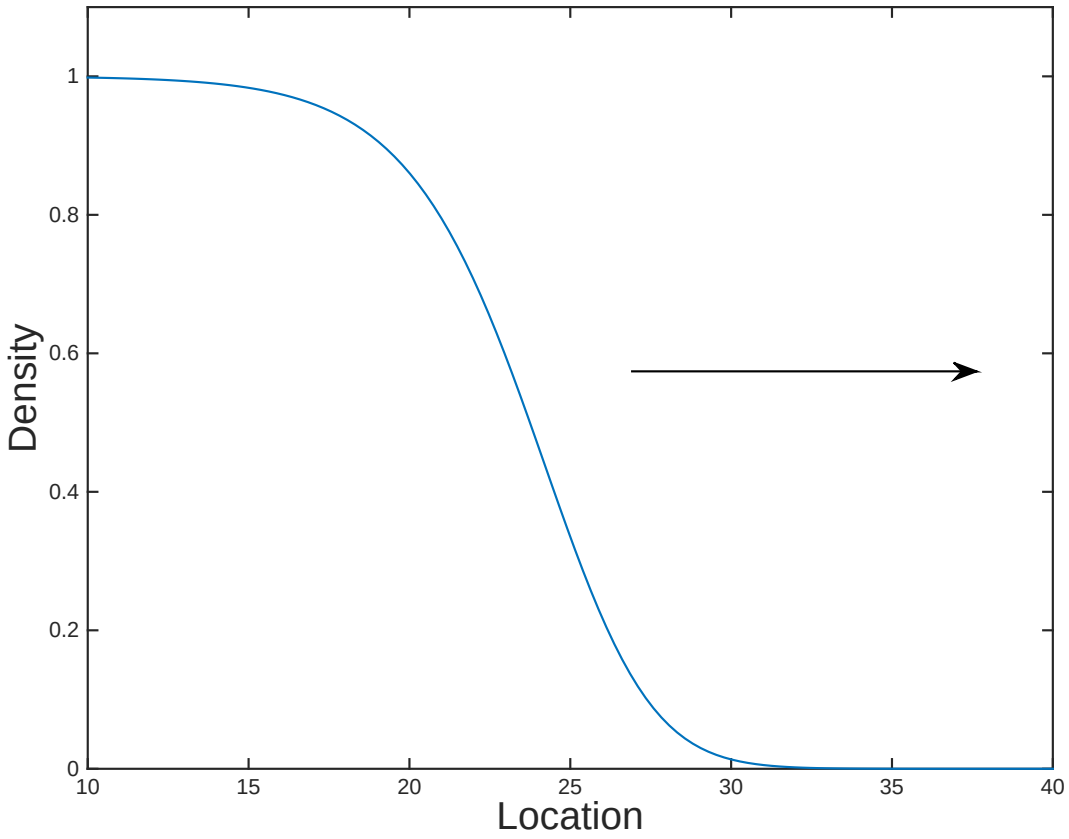

Figure 1-1: The invading population front of the 1D FKPP equation.

It combines diffusion and logistic growth terms and it admits solutions in the form of travelling waves in which the stable high-density $u = 1$ state propagates into the unstable low-density state $u = 0$, shown in Figure 1-1, with speed $c = 2\sqrt{rD}$, which is calculated by the asymptotic linear spreading rate of the low density population ahead of the travelling wave, as the FKPP creates a pulled front [21]. Biologically speaking, this means that only a very small number of 'seed' individuals are required to grow a large population. In fact, the FKPP has travelling wave solutions for all speeds $c \geq 2$ [22] and these limiting speeds depend significantly on the initial conditions [23]. However, these solutions are not physically relevant as they are not robust to small fluctuations. This work has led to a significant amount of research in the area of traveling waves and parabolic systems [24]. Fisher first applied the FKPP equation to the growth of an advantageous gene. It has since been used to model wound closure [25], human dispersion [26], and bacterial growth [27].

The FKPP equation has been studied in depth in 1D. However, many biological invasions occur in 2D but not so much work has been done on the FKPP equation in 2D [28, 29, 30]. Analysing the FKPP equation in 2D provides room to more accurately model realistic biological invasions. This extra dimension allows more complicated diffusion and growth, which determines how quickly the population invades a new territory. This can be seen in both theoretical and experimental work [31, 32, 33, 34]. Extending the FKPP equation to 2D also allows models to have more complicated heterogeneous environments, such as spatially fragmented environments [35].

For example, the recent work of Möbius et. al. [36] on the movement of bacteriophage T7 focuses on the effect of environmental heterogeneities on population fronts and genetic structure. In particular, they consider a 2D bacteria invasion in the presence of obstacles that the population must invade around. The environmental heterogeneity introduced by these obstacles creates a kink in the population front. They also find that this kink is independent of the shape of the obstacle. Motivated by this work, this thesis will analyse the 2D FKPP equation with a mixed boundary condition in both a corridor and the half plane. The mixed boundaries in these two environments simulate the presence of an obstacle.

In addition to new boundary conditions in two dimensions, the FKPP equation can also be used to model the invasion speed of a population, which depends on the growth rate and diffusion coefficient of the population. The diffusion has been modelled in a variety of different ways, including density-dependent diffusion [37, 38], nonlocal diffusion [39], and location-dependent diffusion [40]. It is important to understand the underlying interactions within a population that determine the diffusion coefficient of a population.

This link between diffusion coefficient and invasion speed can be seen at play in fish populations with sexual conflict between individuals. The different behaviours, male fish swimming towards female fish and female fish swimming away from male fish in general, cause a conflict between the two genders, which influences the diffusion coefficient of the population, which in turn determines the invasion speed of the population. This thesis will explore the link between interactions between individuals due to sexual conflict and the population diffusion rate in order to understand how sexual conflict in a population can affect the invasion speed of a population according to the FKPP equation.

As well as individuals, we can also mathematically model the spread of ideas through a population. The voter model is used to simulate the exchange of opinions between neighbours in a population. Also known as an interacting particle system [48], this model has been extended to a biased voter model [49] and a noisy voter model [50]. Research has been done in one dimension [51], in two dimensions [52], on a d-dimensional lattice [53], and on heterogeneous networks [54]. Further applications include genetics [55], tumour growth [56], territory competition [47, 57], and chemical monomer-monomer models [58].

One of the key properties of the voter model is that individuals only interact with their nearest neighbours. That is, all interactions are local. Over time, individuals interact locally until the environment has been conquered by one population. This is called reaching consensus. The condition for only local interactions can be relaxed to allow nonlocal interactions. This thesis will explore the voter model with two types of non-locally interacting individuals: one type of voter can weakly persuade within a very large radius and the other type of voter can strongly persuade within a very short radius.

The main part of this thesis is structured as follows: Chapter 2 will be a technical introduction to the key concepts and definitions used throughout. In particular, the dynamics of single particle and multiple particle systems will be discussed. The interactions between individuals and their environment in the case of bacteria invasions will be explored in Chapter 3 while Chapter 4 will contain an analysis of antagonistic interactions between individuals in the case of sexual conflict between male and female fish. Chapter 5 will be an analysis of competitive interactions between individuals affecting the probability of reaching consensus in the nonlocal voter model and finally a conclusion and outlook for future research will be given in Chapter 6.

1.1 New Results Contained in This Thesis

In Chapter 3, we consider the 2D FKPP equation

$$u_t = u_{xx} + u_{yy} + u(1-u),$$

with mixed boundary condition $u_y = \alpha u$ at $y = 0$. In the corridor $C_L = \{(x, y) : x \in \mathbb{R}, 0 \leq y \leq L\}$, we apply a second mixed boundary condition $u_y = -\beta u$ at $y = L$. On this domain ahead of the front, we calculate that:

- The condition for the population to have invasion speed zero is given by

$$(2 - \alpha\beta)\tan(\sqrt{2}L) = \sqrt{2}(\alpha + \beta).$$

- The critical corridor width required to support a population is given by $L^m_{\infty,\infty} = \pi/\sqrt{2}$. If $L > L^m_{\infty,\infty}$, then the population will have a positive invasion speed for any α, β.

In $C_\infty = \{(x, y) : x \in \mathbb{R}, y \geq 0\}$ ahead of the front, we calculate that:

- An explicit equation for the low density population is given by

$$u(x, y, t) = u_0 \exp(-(x - 2t))(1 + \alpha y).$$

- Level sets meet the $y = 0$ boundary with gradient $1/\alpha$, which is independent of the level set chosen.

Behind the front, we show that:

- Nonzero steady states exist in C_L for all $L > 0$ and in C_∞.

- The condition for stability of the nonzero steady state behind the front in C_L is given by

$$(1 - \alpha\beta)\tan(L) = \alpha + \beta.$$

Finally, we show that, as the reaction rate α increases in C_L, the condition for the steady state behind the front becoming unstable is always achieved before the condition for the population to achieve speed zero ahead of the front. This is confirmed by simulations.

Chapter 4 concerns the effect of sexual conflict in an invading population. We calculate the diffusion coefficient D for an individual fish assuming a 'run and tumble' model of fish motion. After the introduction of sexual conflict in a male-female pair of fish when the male fish has sexual aggression characterised by a parameter $A > 0$, we show that:

- The effective diffusion coefficient D_{eff} is given by

$$D_{\text{eff}} = 4\sqrt{\frac{D\pi}{A+1}}\left(\frac{A}{A+1}\right)^2 \sinh\left(\frac{1}{4D(A+1)}\right),$$

  which can be significantly larger than D for particular values of D, A.

In populations with many male and female fish and sexual conflict, we show that:

- The diffusion coefficient of a male fish ahead of the front is higher than a male fish behind the front.
- The diffusion coefficient of a fish switching from diffusion coefficient D_1 to D_2 with rate λ_1 and back with rate λ_2 is given by

$$D_{\text{swt}} = \frac{D_1\lambda_2 + D_2\lambda_1}{\lambda_1 + \lambda_2}.$$

Given that the 1D FKPP equation creates a pulled front and so the invasion speed is determined by the dynamics ahead of the front, this shows that sexual conflict can increase the invasion speed of the population.

In Chapter 5, we consider the nonlocal voter model with diffusion with two types. Individuals of type W are weakly interacting over a wide domain and individuals of type S are strongly interacting over a small domain. The interaction ranges are r_W, r_S and the interaction rates are λ_W, λ_S for type W, S respectively. We assume $r_S < r_W$, $\lambda_W < \lambda_S$, and that individuals have diffusion coefficient D. In a low density population, we calculate that:

- The probability p_S of a type S individual converting a type W individual in a pairwise interaction, for $\mu_1 = \sqrt{(\lambda_S + \lambda_W)/D}, \mu_2 = \sqrt{\lambda_W/D}$, is given by

$$p_S = \frac{2\mu_1\lambda_S(e^{2\mu_1 r_S} - 1)e^{\mu_2(r_S + r_W)}}{(\lambda_S + \lambda_W)((\mu_1 - \mu_2)(e^{2r_S(\mu_1+\mu_2)} - e^{2\mu_2 r_W}) + (\mu_1 + \mu_2)(e^{2\mu_1 r_S + 2\mu_2 r_W} - e^{2\mu_2 r_S}))}.$$

- When we assume $\lambda_S r_S = 1/2 = \lambda_W r_W$, $p_S < 1/2$. This means that a type W individual is more likely to convert a type S individual when they meet as a pair.

- In a population of N individuals with N_S^0 initially of type S, the probability P_S of type S individuals reaching consensus is given by

$$P_S = \frac{p_S^{N-N_S^0}}{p_S^{N-N_S^0} + (1-p_S)^{N_S^0}}.$$

  When $N_S^0 = N/2, P_S < 1/2$. This means that, given a low density population of size N with half of type S and half of type W, the type W individuals are more likely to survive to consensus.

In a high density population with diffusion rates D_W, D_S, we show that:

- For infinite populations, there exists a linearly stable state of the system, in which a proportion τ are of type W and the remaining $1-\tau$ are of type S for all $\tau \in [0,1]$.

- For large but finite N and the addition of noise in the system, the fluctuations in the steady state for the proportion of type W individuals in the population satisfies

$$\frac{d}{dt}\tau = \frac{\tau(1-\tau)}{N\pi^2} \sum_{k\neq 0} \frac{\frac{1}{2r_W}\sin(kr_W) - \frac{1}{2r_S}\sin(kr_S)}{(D_W+D_S)\frac{k^3}{2} - 4k[(\frac{1}{2kr_W}\sin(kr_W)+1/2)(1-\tau) + (\frac{1}{2kr_S}\sin(kr_S)+1/2)\tau]}.$$

- When we assume $\lambda_S r_S = 1/2 = \lambda_W r_W$, $\frac{d}{dt}\tau > 0$ for all τ. This means that, on average, the noise in the system causes the proportion of type W individuals to increase. Over time, this results in the type W individuals surviving to consensus in a high density population.

Chapter 2

Technical Introduction

In this Chapter, the key concepts and definitions used throughout the rest of this thesis will be introduced. In order to understand individual interactions within a population in various environments, we must first have a framework for how individuals behave on their own.

The first part of this framework begins with one individual exhibiting random motion. Random motion is useful here because it is unbiased and it provides a general starting point as we introduce interactions between individuals. We define Brownian motion, Gaussian white noise, and derive the Fokker-Planck equations, all of which will be used in Chapter 4 to describe the motion of fish at an individual level. We will also use Gaussian white noise in Chapter 5 to model fluctuations in a population density.

The second part of this framework focuses on the movement of many individuals with interactions between them, particularly births and deaths. From these individual-level interactions, we derive the population-level FKPP partial differential equation and the associated linearised invasion speed. The FKPP equation will be used in Chapter 3 to model the bacteria population and in Chapter 4 to model the fish population. The method used to derive the FKPP equation will be used in Chapter 5 to determine which type reaches consensus in the high density population case.

This framework can be summarised as being a combination of two phenomena: collective motion and pairwise interaction. Pairwise interactions take the form of microscopic events between individuals over a very short time scale that can cumulatively influence population motion. Collective motion is a macroscopic

event that arises from the actions of individuals in the population viewed on a long time scale.

2.1 Dynamics of One Particle

We begin by defining the framework for the movement of one particle in a 1D domain. This particle may, for example, represent an individual bacterium, fish, or voter. We assume on short time scales that the particle exhibits Brownian motion. Once Brownian motion and Gaussian white noise has been defined, we will derive the forward and backward Fokker-Planck equations, which determine the development of a probability density function for the location of the particle both forwards and backwards in time. We will use the backward Fokker-Planck equation to calculate an equation for the mean time required for a particle to hit a given boundary, which will be needed in Chapter 4, and we will use Gaussian white noise in Chapter 5 to model fluctuations in a population density.

2.1.1 Brownian Motion

Consider a single particle. At time t, let this particle have location $x(t)$ in a 1D environment. The movement of the particle is called Brownian motion, or a Wiener process, with diffusion coefficient D when the following three properties hold:

- Firstly, for two chronological points in time t_1, t_2 with $t_1 < t_2$, the change in location of the particle $x(t_2) - x(t_1)$ is distributed according to a normal distribution with mean zero and variance $D(t_2 - t_1)$ (known as stationary Gaussian increments).

- Secondly, for n chronological points in time $t_1, t_2, \ldots, t_n$ with $t_1 \leq t_2 \leq \cdots \leq t_n$, the changes in location over the disjoint intervals $x(t_2) - x(t_1)$, $x(t_3) - x(t_2), \ldots, x(t_n) - x(t_{n-1})$ are independent (known as independent increments).

- Finally, the function $t \to x(t)$ that maps time $t > 0$ to location $x(t)$ is

continuous with probability 1. That is,

$$P\left[\lim_{t\to t'}|x(t)-x(t')|=0\right]=1.$$

These are the rules the movement of the particle satisfies on an individual level, which is summarised from [59]. In the main part of this thesis, we will also need the definition of Gaussian white noise. A process $\xi(t)$ is called Gaussian white noise when the following properties hold:

- $\xi(t)$ has mean zero, that is $\mathbb{E}[\xi(t)]=0$
- For all $t\neq t'$, $\xi(t),\xi(t')$ are statistically independent, that is $\mathbb{E}[\xi(t)\xi(t')]=\delta(t-t')$,
- $\int_0^t \xi(t')dt'=x(t)$, where $x(t)$ satisfies the requirements of Brownian motion.

These conditions follow from [60]. We will use Brownian motion and Gaussian white noise to model the motion of the fish in Chapter 4 and the fluctuations in population densities in Chapter 5.

2.1.2 Fokker-Planck Equations

We have introduced Brownian motion and Gaussian white noise to describe the random motion of a particle. In the main part of this thesis, we will also need equations that determine how the probability density for the location of a particle develops over time, that is, both forwards and backwards in time. These equations will allow us to calculate the mean time required for a particle to hit a given boundary later in this technical introduction. In Chapter 4, we will use the mean hitting time to determine the mean time required for two fish chasing each other in one direction to switch sides and chase each other in the opposite direction.

We begin by deriving Itô's formula using [60]. Let $a(x,t),b(x,t)$ be two arbitrary functions of location $x(t)$ and time t, let $W(t)$ be Brownian motion or a Wiener process, and let a small change in the location of the particle $\Delta x(t)$ develop according to the stochastic differential equation

$$\Delta x(t)=a(x,t)\Delta t+b(x,t)\Delta W(t).$$

If $f[x(t)]$ is an arbitrary function of $x(t)$, then expanding $f[x(t)]$ to second order gives

$$\begin{aligned}\Delta f[x(t)] =& f[x(t)+\Delta x(t)] - f[x(t)] \\ =& f'[x(t)]\Delta x(t) + \frac{1}{2}f''[x(t)]\Delta x(t)^2 + \mathcal{O}(\Delta x(t)^3) \\ =& f'[x(t)]\left\{a(x,t)\Delta t + b(x,t)\Delta W(t)\right\} + \frac{1}{2}f''[x(t)]b(x,t)^2\Delta W(t)^2,\end{aligned}$$

after ignoring higher order terms. Using the result $\Delta W(t)^2 = \Delta t$ then gives

$$\Delta f[x(t)] = \left\{f'[x(t)]a(x,t) + \frac{1}{2}f''[x(t)]b(x,t)^2\right\}\Delta t + f'[x(t)]b(x,t)\Delta W(t),$$

which is called Itô's formula. It shows that changing variables from x to $f[x(t)]$ is not given by standard chain rule for stochastic differential equations and it will be needed to derive the Fokker-Planck equations.

Using Brownian motion, Gaussian white noise, and Itô's formula, we can now derive the forward and backward Fokker-Planck equations. These equations are partial differential equations that determine how the probability density of a particle being at a given location at a given time varies as time progresses either forwards or backwards. They are useful because they allow us to determine where the particle is likely to be as a function of the particle's underlying dynamics. We will use the Fokker-Planck equations later in this Section to calculate the mean time for a particle to hit a given boundary.

We now derive the forward Fokker-Planck equation using [60]. For this derivation, we need the following conditions for all $\epsilon > 0$:

$$\begin{aligned}&\lim_{\Delta t\to 0}\frac{1}{\Delta t}p(x,t+\Delta t|z,t) = 0 \text{ for } |x-z| > \epsilon, \\ &\lim_{\Delta t\to 0}\frac{1}{\Delta t}\int_{|x-z|<\epsilon}(x-z)p(x,t+\Delta t|z,t)dx = A(z,t) + \mathcal{O}(\epsilon) \\ &\lim_{\Delta t\to 0}\frac{1}{\Delta t}\int_{|x-z|<\epsilon}(x-z)^2p(x,t+\Delta t|z,t)dx = B(z,t) + \mathcal{O}(\epsilon).\end{aligned} \tag{2.1}$$

The first condition ensures the movement of the particle is continuous. The second and third conditions serve as definitions for the drift and diffusion coefficients respectively. Now, let $f(x)$ be an arbitrary twice differentiable function. The time

derivative of the expectation of f can be written as

$$\begin{aligned}\frac{\partial}{\partial t}\mathbb{E}[f(y)] &= \frac{\partial}{\partial t}\int f(x)p(x,t|y,t')dx \\ &= \lim_{\Delta t\to 0}\frac{1}{\Delta t}\int f(x)[p(x,t+\Delta t|y,t') - p(x,t|y,t')]dx,\end{aligned}$$

where we have applied the time derivative to p. We now need to use the Chapman-Kolmogorov equation, which states, for locations x_1, x_2, x_3 and times $t_1 < t_2 < t_3$,

$$p(x_3,t_3|x_1,t_1) = \int_{-\infty}^{\infty} p(x_3,t_3|x_2,t_2)p(x_2,t_2|x_1,t_1)dx_2.$$

Applying the Chapman-Kolmogorov equation to the positive p term gives

$$\begin{aligned}&\frac{\partial}{\partial t}\int f(x)p(x,t|y,t')dx \\ &= \lim_{\Delta t\to 0}\frac{1}{\Delta t}\left\{\int\int f(x)p(x,t+\Delta t|z,t)p(z,t|y,t')dzdx - \int f(z)p(z,t|y,t')dz\right\}.\end{aligned} \tag{2.2}$$

We have assumed that $f(x)$ is twice differentiable so, for $|x-z| < \epsilon$, we have

$$\begin{aligned}&f(x) \\ &= f(z) + \frac{\partial f(z)}{\partial z}(x-z) + \frac{1}{2}\frac{\partial^2 f(z)}{\partial z^2}(x-z)^2 + \mathcal{O}(|x-z|^3).\end{aligned} \tag{2.3}$$

Separating the double integral domain into $|x-z| < \epsilon$ and $|x-z| \geq \epsilon$ and then substituting this equation into (2.2) gives

$$\begin{aligned}&\frac{\partial}{\partial t}\int f(x)p(x,t|y,t')dx = \\ &\lim_{\Delta t\to 0}\frac{1}{\Delta t}\left\{\iint_{|x-z|<\epsilon}\left[f(z) + \frac{\partial f(z)}{\partial z}(x-z)\right.\right. \\ &\left.+\frac{1}{2}\frac{\partial^2 f(z)}{\partial z^2}(x-z)^2 + \mathcal{O}(|x-z|^3)\right]p(x,t+\Delta t|z,t)p(z,t|y,t')dzdx \\ &\left.+\iint_{|x-z|\geq\epsilon} f(x)p(x,t+\Delta t|z,t)p(z,t|y,t')dzdx - \int f(z)p(z,t|y,t')dz\right\},\end{aligned}$$

and rearranging gives

$$\begin{aligned}
&\frac{\partial}{\partial t}\int f(x)p(x,t|y,t')dx = \\
&\lim_{\Delta t\to 0}\frac{1}{\Delta t}\left\{\iint_{|x-z|<\epsilon}\left[\frac{\partial f(z)}{\partial z}(x-z)+\frac{1}{2}\frac{\partial^2 f(z)}{\partial z^2}(x-z)^2\right]\right. \\
&\qquad\qquad\qquad\qquad\qquad\qquad \times p(x,t+\Delta t|z,t)p(z,t|y,t')dzdx \\
&\iint_{|x-z|<\epsilon}\mathcal{O}(|x-z|^3)p(x,t+\Delta t|z,t)p(z,t|y,t')dzdx \\
&+\iint_{|x-z|\geq\epsilon} f(x)p(x,t+\Delta t|z,t)p(z,t|y,t')dzdx \\
&+\iint_{|x-z|<\epsilon} f(z)p(x,t+\Delta t|z,t)p(z,t|y,t')dzdx \\
&\left.-\int\int f(z)p(x,t+\Delta t|z,t)p(z,t|y,t')dzdx\right\},
\end{aligned} \tag{2.4}$$

where the last line follows by noticing that the integral over x is equal to one. We now consider (2.4) line by line. For the first and second line of the RHS, we assume uniform convergence to bring the limit inside the x integral to get

$$\int\left[A(z)\frac{\partial f}{\partial z}+\frac{1}{2}B(z)\frac{\partial^2 f}{\partial z^2}\right]p(z,t|y,t')dz+\mathcal{O}(\epsilon).$$

For the third line of the RHS, we see that it vanishes as $\epsilon\to 0$. For the final three lines of the RHS, we can simplify them in the following way

$$\begin{aligned}
&\lim_{\Delta t\to 0}\frac{1}{\Delta t}\left\{\iint_{|x-z|\geq\epsilon} f(x)p(x,t+\Delta t|z,t)p(z,t|y,t')\right. \\
&\qquad\qquad\left.-f(z)p(x,t+\Delta t|z,t)p(z,t|y,t')dzdx\right\} \\
&=\iint_{|x-z|\geq\epsilon} f(x)p(z,t|y,t')\lim_{\Delta t\to 0}\frac{1}{\Delta t}p(x,t+\Delta t|z,t) \\
&\qquad\qquad-f(z)p(z,t|y,t')\lim_{\Delta t\to 0}\frac{1}{\Delta t}p(x,t+\Delta t|z,t)dzdx \\
&=0,
\end{aligned}$$

using the first condition in (2.1). Now letting $\epsilon \to 0$ in (2.4), we have

$$\frac{\partial}{\partial t}\int f(x)p(x,t|y,t')dx = \int \left[A(z)\frac{\partial f}{\partial z} + \frac{1}{2}B(z)\frac{\partial^2 f}{\partial z^2}\right] p(z,t|y,t')dz,$$

and integrating by parts and using the fact that f is arbitrary gives

$$\frac{\partial}{\partial t}p(z,t|y,t') = -\frac{\partial}{\partial z}[A(z,t)p(z,t|y,t')] + \frac{1}{2}\frac{\partial^2}{\partial z^2}[B(z,t)p(z,t|y,t')], \tag{2.5}$$

which is called the forward Fokker-Planck equation. This partial differential equation tells us how the probability $p(z,t|y,t')$ develops over time in an ordinary differential equation that depends on $A(z,t), B(z,t)$ given initial conditions y, t'. This equation is very useful if we know the initial conditions and would like to evolve this equation forward in time.

Now, we derive the backward Fokker-Planck equation, which describes the probability of the particle being at a given location at a given time in the past. The following is a summary of [60]. The derivation begins with the Chapman-Kolmogorov equation. Let Δt be a small increment in time that will eventually tend to zero. Then, the Chapman-Kolmogorov equation applied to $p(x',t'|x,t)$ with $t' > t$ gives

$$p(x',t'|x,t-\Delta t) = \int_{-\infty}^{\infty} p(x',t'|z,t)p(z,t|x,t-\Delta t)dz, \tag{2.6}$$

which says that the probability of the particle being at location x' at time t' given that it was at location x at time $t-\Delta t$ is equal to the sum of all probabilities of the particle being at an intermediate location z at time t. In the small time interval $[t-\Delta t, t]$, the particle cannot move very far so we assume the locations x and z are very close to each other. This assumption allows us to Taylor expand the term $p(x',t'|z,t)$ in (2.6) as a function of $(z-x)$. This expansion is given by

$$p(x',t'|z,t) = p(x',t'|x,t) + (z-x)\frac{\partial}{\partial x}p(x',t'|x,t) + \frac{1}{2}(z-x)^2\frac{\partial^2}{\partial x^2}p(x',t'|x,t),$$

which ignores higher order terms in $(z-x)$. Substituting this expansion into

(2.6) and expanding gives

$$\begin{aligned} p(x',t'|x,t-\Delta t) = p(x',t'|x,t)\int_{-\infty}^{\infty} p(z,t|x,t-\Delta t)dz \\ + \left(\frac{\partial}{\partial x}p(x',t'|x,t)\right)\int_{-\infty}^{\infty}(z-x)p(z,t|x,t-\Delta t)dz \\ + \left(\frac{\partial^2}{\partial x^2}p(x',t'|x,t)\right)\int_{-\infty}^{\infty}\frac{1}{2}(z-x)^2 p(z,t|x,t-\Delta t)dz. \end{aligned} \tag{2.7}$$

The first integral in (2.7) integrates to one as we integrate over all probabilities. For the second and third integrals, we define functions $a(x,t), b(x,t)$ such that

$$\begin{aligned} a(x,t-\Delta t) &= \frac{1}{\Delta t}\int_{-\infty}^{\infty}(z-x)p(z,t|x,t-\Delta t)dz \\ b(x,t-\Delta t)^2 &= \frac{1}{\Delta t}\int_{-\infty}^{\infty}(z-x)^2 p(z,t|x,t-\Delta t)dz, \end{aligned}$$

so that (2.7) can be rewritten as

$$\begin{aligned} \frac{p(x',t'|x,t)-p(x',t'|x,t-\Delta t)}{\Delta t} &= -a(x,t-\Delta t)\frac{\partial}{\partial x}p(x',t'|x,t) \\ &\quad -\frac{1}{2}b(x,t-\Delta t)^2\frac{\partial^2}{\partial x^2}p(x',t'|x,t), \end{aligned}$$

and letting $\Delta t \to 0$ gives

$$\frac{\partial}{\partial t}p(x',t'|x,t) = -a(x,t)\frac{\partial}{\partial x}p(x',t'|x,t) - \frac{1}{2}b(x,t)^2\frac{\partial^2}{\partial x^2}p(x',t'|x,t), \tag{2.8}$$

which is called the backward Fokker-Planck equation. It is a partial differential equation which shows how the probability $p(x',t'|x,t)$ develops backwards in time. In the next Section, we will use this equation to calculate the mean time required for the particle to hit a given boundary, which will be used in Chapter 4.

2.1.3 Mean Hitting Time

In Chapter 4, we will need an equation that gives the mean time for a particle to hit a given boundary. In particular, we require a 1D domain with a reflective boundary to the left and an absorbing boundary to the right. The derivation for this equation begins by considering the probability that the particle remains

within some interval, applying the backwards Fokker-Planck equation (2.8), and then defining the mean time for hitting a boundary on the interval. This will give a second-order ordinary differential equation for the mean hitting time that we will solve by direct integration. What follows is a derivation in [60] applied to the scenario in Chapter 4.

Consider a particle at time t with location $x(t)$ in the interval $[A, B]$ for constants $A < B$ with a reflective boundary at $x = A$ and an absorbing boundary at $x = B$ so that, when the particle reaches $x = A$, it is reflected back into the interval and, when the particle reaches $x = B$, it is removed from the system. Let $p(x', t|x, 0)$ be the probability that the particle is at location x' at time t given that the particle was at location x at time 0 in the past. Also, let $\mathcal{P}(x, t)$ be the probability that the particle is located within the interval at time t, i.e. $A \leq x'(t) \leq B$ given that it started at location x. These two probabilities $p(x', t|x, 0), \mathcal{P}(x, t)$ are related by the equation

$$\mathcal{P}(x, t) = \int_A^B p(x', t|x, 0)dx',$$

and taking a time derivative gives

$$\frac{\partial}{\partial t}\mathcal{P}(x, t) = \frac{\partial}{\partial t}\int_A^B p(x', t|x, 0)dx' = \int_A^B \frac{\partial}{\partial t}p(x', t|x, 0)dx',$$

as A, B are constants. We now apply the backwards Fokker-Planck equation, which can be written as

$$\frac{\partial}{\partial t}p(x', t'|x, t) = a(x)\frac{\partial}{\partial x}p(x', t'|x, t) + \frac{1}{2}b(x)^2\frac{\partial^2}{\partial x^2}p(x', t'|x, t).$$

The differences between this version and (2.8) are that the functions $a(x), b(x)$ do not explicitly depend on time and that the sign of both coefficients is positive. We require both for the derivations in Chapter 4. Applying this backwards Fokker-Planck equation to $p(x', t|x, 0)$, noting that the system is homogeneous in time

so $p(x', t|x, 0) = p(x', 0|x, -t)$, gives

$$\begin{aligned}\frac{\partial}{\partial t}\mathcal{P}(x,t) =& \int_A^B a(x)\frac{\partial}{\partial x}p(x',t|x,0) + \frac{1}{2}b(x)^2\frac{\partial^2}{\partial x^2}p(x',t|x,0)dx' \\ =& a(x)\frac{\partial}{\partial x}\int_A^B p(x',t|x,0)dx' + \frac{1}{2}b(x)^2\frac{\partial^2}{\partial x^2}\int_A^B p(x',t|x,0)dx',\end{aligned}$$

and substituting the definition of $\mathcal{P}(x,t)$ gives

$$\frac{\partial}{\partial t}\mathcal{P}(x,t) = a(x)\frac{\partial}{\partial x}\mathcal{P}(x,t) + \frac{1}{2}b(x)^2\frac{\partial^2}{\partial x^2}\mathcal{P}(x,t). \tag{2.9}$$

This is a second order partial differential equation for $\mathcal{P}(x,t)$ with boundary conditions for a reflective boundary at $x = A$ and an absorbing boundary at $x = B$ given by

$$\frac{\partial}{\partial x}\mathcal{P}(A,t) = \mathcal{P}(B,t) = 0, \tag{2.10}$$

for all time t. We choose these boundary conditions here as we will be considering a pair of individuals moving in a 1D environment with a reflective boundary to the left and an absorbing boundary to the right in Chapter 4. We consider this calculation with other boundary conditions in Appendix A. We will use (2.9) with the boundary conditions (2.10) to derive a differential equation for the mean time at which the particle hits a boundary. Let $T(x)$ be the first time that the particle hits the absorbing boundary $x = B$ given that the particle starts at location x. The probability that $T(x) \geq t$ is given by

$$\mathbb{P}[T(x) \geq t] = \int_A^B p(x', t|x, 0)dx' = \mathcal{P}(x,t).$$

Using a definition of expectation, the mean hitting time $\mathbb{E}[T(x)]$ given that the particle starts at location x is then given by

$$\mathbb{E}[T(x)] = \int_0^\infty \mathbb{P}[T(x) \geq t]dt = \int_0^\infty \mathcal{P}(x,t)dt.$$

We now have the mean hitting time $\mathbb{E}[T(x)]$ expressed in terms of $\mathcal{P}(x,t)$. We will now use (2.9) and (2.10) to derive a differential equation for $\mathbb{E}[T(x)]$. Firstly,

we integrate (2.9) from 0 to ∞ to get

$$\int_0^\infty \frac{\partial}{\partial t}\mathcal{P}(x,t)dt' = \int_0^\infty a(x)\frac{\partial}{\partial x}\mathcal{P}(x,t) + \frac{1}{2}b(x)^2\frac{\partial^2}{\partial x^2}\mathcal{P}(x,t)dt.$$

On the left hand side, we have

$$\int_0^\infty \frac{\partial}{\partial t}\mathcal{P}(x,t)dt = \mathcal{P}(x,\infty) - \mathcal{P}(x,0) = -1$$

as the particle eventually leaves the interval if we wait long enough, and the particle initially starts within the interval. On the right hand side, we have

$$\begin{aligned}\int_0^\infty a(x)\frac{\partial}{\partial x}\mathcal{P}(x,t) + \frac{1}{2}b(x)^2\frac{\partial^2}{\partial x^2}\mathcal{P}(x,t)dt& \\ =a(x)\frac{\partial}{\partial x}\int_0^\infty \mathcal{P}(x,t)dt + \frac{1}{2}b(x)^2\frac{\partial^2}{\partial x^2}\int_0^\infty \mathcal{P}(x,t)dt& \\ =a(x)\frac{\partial}{\partial x}\mathbb{E}[T(x)] + \frac{1}{2}b(x)^2\frac{\partial^2}{\partial x^2}\mathbb{E}[T(x)].&\end{aligned}$$

Hence, we have that

$$a(x)\frac{\partial}{\partial x}\mathbb{E}[T(x)] + \frac{1}{2}b(x)^2\frac{\partial^2}{\partial x^2}\mathbb{E}[T(x)] = -1. \tag{2.11}$$

This is a second order ordinary differential equation for the mean hitting time $\mathbb{E}[T(x)]$. Using (2.10), the boundary conditions for $\mathbb{E}[T(x)]$ are given by

$$\frac{\partial}{\partial x}\mathbb{E}[T(A)] = \mathbb{E}[T(B)] = 0. \tag{2.12}$$

We now have a differential equation with boundary conditions for the mean hitting time $\mathbb{E}[T(x)]$. We can solve this equation by direct integration. Define

$$S(x) = \frac{\partial}{\partial x}\mathbb{E}[T(x)],$$

so that (2.11) becomes

$$a(x)S(x) + \frac{1}{2}b(x)^2\frac{\partial}{\partial x}S(x) = -1.$$

Dividing by $b(x)^2/2$ gives

$$\frac{\partial}{\partial x}S(x) + 2\frac{a(x)}{b(x)^2}S(x) = -\frac{2}{b(x)^2},$$

and defining integrating factor

$$\gamma(x) = \exp\left(\int_0^x 2\frac{a(y)}{b(y)^2}dy\right),$$

gives

$$\frac{d}{dx}[\gamma(x)S(x)] = -\frac{2\gamma(x)}{b(x)^2}.$$

Integrating and simplifying gives

$$\frac{\partial}{\partial x}\mathbb{E}[T(x)] = S(x) = -\frac{2}{\gamma(x)}\int_A^x \frac{\gamma(z)}{b(z)^2}dz + \frac{C_1}{\gamma(x)},$$

for some constant C_1, and then integrating again gives

$$\mathbb{E}[T(x)] = -2\int_A^x \frac{1}{\gamma(w)}\int_A^w \frac{\gamma(z)}{b(z)^2}dzdw + \int_A^x \frac{C_1}{\gamma(w)}dw + C_2, \tag{2.13}$$

for some constant C_2. We now have an equation for the mean hitting time $\mathbb{E}[T]$ with two constants C_1, C_2. We define these constants by using the boundary conditions (2.12), which give

$$\begin{aligned}
0 = \frac{\partial}{\partial x}\mathbb{E}[T(A)] =& \frac{\partial}{\partial x}\left[-2\int_A^x \frac{1}{\gamma(w)}\int_A^w \frac{\gamma(z)}{b(z)^2}dzdw + \int_A^x \frac{C_1}{\gamma(w)}dw + C_2\right]\Bigg|_{x=A} \\
=& \left[-\frac{2}{\gamma(x)}\int_A^x \frac{\gamma(z)}{b(z)^2}dz + \frac{C_1}{\gamma(x)}\right]\Bigg|_{x=A} \\
=& \frac{C_1}{\gamma(A)},
\end{aligned}$$

so $C_1 = 0$ and

$$0 = \mathbb{E}[T(B)] = -2\int_A^B \frac{1}{\gamma(w)}\int_A^w \frac{\gamma(z)}{b(z)^2}dzdw + C_2$$

so

$$C_2 = 2\int_A^B \frac{1}{\gamma(w)}\int_A^w \frac{\gamma(z)}{b(z)^2}dzdw.$$

Hence

$$\mathbb{E}[T(x)] = -2\int_A^x \frac{1}{\gamma(w)}\int_A^w \frac{\gamma(z)}{b(z)^2}dzdw + 2\int_A^B \frac{1}{\gamma(w)}\int_A^w \frac{\gamma(z)}{b(z)^2}dzdw,$$

and therefore, the equation for the mean hitting time with a reflective boundary at $x = A$ and an absorbing boundary at $x = B$ is given by

$$\mathbb{E}[T(x)] = 2\int_x^B \frac{1}{\gamma(w)}\int_A^w \frac{\gamma(z)}{b(z)^2}dzdw. \tag{2.14}$$

The calculation of this equation for other combinations of boundary types are in Appendix A. We will use this equation in Chapter 4 to determine the mean time required for a pair of fish swimming in one direction to change directions and swim in the opposite direction.

We now have a framework for the dynamics of one particle. On the microscopic stochastic level, we have defined Brownian motion and Gaussian white noise for the random, unbiased movement of the particle. On the macroscopic deterministic level, we have derived the forward and backward Fokker-Planck equations, second order partial differential equations for the probability density for the location of the particle. Finally, using the Fokker-Planck equation, we calculated an equation for the mean hitting time of an absorbing boundary at $x = B$ on the interval $[A, B]$ with a reflective boundary at $x = A$.

2.2 Dynamics of Many Particles

Populations are made up of many individuals, not just one. For this reason, we need to extend our framework for the dynamics within a population to include many particles. Again, these particles could represent voters, fish, bacteria, or something else. The main goal of this Section is to introduce a framework for the dynamics of a population with many individuals, which includes births, deaths, and movement. Ultimately, we will derive the 1D FKPP equation, following similar methods as used in [61], and prove the associated population invasion speed. This equation will be used in Chapter 3 to model a bacteria population and in Chapter 4 to model a fish population.

2.2.1 Fisher-Kolmogorov-Petrovskii-Piscounov (FKPP) Equation

In the previous Section, we kept track of the location of the particle for all time. For many particles, this is difficult to do. Instead, we introduce a population function that tracks the location of all particles and when an event occurs, we change the population function instead of changing individual locations. Once we have introduced the population function, we will define 3 processes: birth, death, and movement. Each one of these processes represent an operation being applied to the population function. A birth requires adding a particle, death removing a particle, and movement results in removing one particle from a location and adding it to another location. These three processes will be contained in a master equation for the population dynamics. The rest of the derivation of the FKPP equation will be a thorough analysis of this master equation. To do this, we will use a variant of the Kramers-Moyal expansion [62, 63, 64], a Fourier space expansion, and a special case of the Liouville equation. Returning back to real space, we will be left with the 1D FKPP equation.

Consider a population of particles. At time t, let there be $N(t)$ particles in the system. Let the particles have locations $\mathbf{x} = x_1, x_2, \ldots, x_{N(t)}$ on the 1D interval $[-\pi, \pi)$. We use this finite interval as it means the inverse Fourier transform will be a Fourier series over countably many Fourier modes, rather than an integral.

- For births, assume each particle gives birth at rate r and the offspring is placed at the same location as the parent.

- For deaths, assume that the population has a carrying capacity K and that individuals die with rate $\frac{1}{K}\sum_j g(x_i - x_j)$ where g is a nonnegative, symmetric function for competition between individuals. We will allow g to tend to the delta function $r\delta(x-y)$ during the derivation as we are only interested in local competition. We also assume that K is large as we are interested in the large population limit.

- For movement, assume particles move from location x to location y with rate $d(x-y)$ where d is also a nonnegative, symmetric function. We will choose a d that corresponds to individuals moving according to Brownian motion on a microscopic level.

We begin the derivation with general functions g and d and introduce specific functions only when necessary. Then, define the population function $\phi(x, \mathbf{x}, t)$ as

$$\phi(x, \mathbf{x}, t) = \frac{1}{K} \sum_{i=1}^{N(t)} \delta(x - x_i).$$

We drop the $\mathbf{x}$ argument for the rest of the calculation.

We need to define the operators for the birth, death, and movement processes as they will determine how the population function changes when an event occurs. They are required to build the master equation for the system. When a birth occurs at location y, we add the offspring to location y. In terms of the population function ϕ, this is equivalent to adding a Dirac delta function at y. Similarly, when a death occurs at location y, we remove the Dirac delta function from location y in the population function. We define birth and death operators Δ_y^+ and Δ_y^- on an arbitrary functional $F[\phi(x,t)]$ as

$$\Delta_y^{\pm} F\left[\phi(x,t)\right] = F\left[\phi(x,t) \pm \frac{1}{K}\delta(x-y)\right].$$

We use an arbitrary functional here to define the operators but these operators will be applied to the probability state space functional during the analysis of the functional master equation. When an individual moves from location y_1 to location y_2, this is equivalent to subtracting a Dirac delta function at y_1 and adding one at y_2. Define the movement operator for movement from location y_1 to location y_2 as $\Delta_{y_1}^- \Delta_{y_2}^+$. On an arbitrary functional $F[\phi(x,t)]$, this is given by

$$\Delta_{y_1}^- \Delta_{y_2}^+ F\left[\phi(x,t)\right] = F\left[\phi(x,t) - \frac{1}{K}\delta(x-y_1) + \frac{1}{K}\delta(x-y_2)\right].$$

We have three operators for birth, death, and movement given by Δ_y^+, Δ_y^-, and $\Delta_{y_1}^- \Delta_{y_2}^+$ respectively.

In addition to the functional operators, we also need to know the rates at which these events occur to build the master equation. Define $\beta(x, \phi)$ to be the birth rate at location x when the system is in state ϕ. As each offspring is placed at the same location as the parent, this rate must be equal to the number of particles at location x multiplied by their individual birth rate r. Hence, the

birth rate is given by

$$\beta(x, \phi) = rK\phi(x, t). \tag{2.15}$$

Define $\gamma(x, \phi)$ to be the death rate at location x when the system is in state ϕ. The death rate is equal to the product of the number of particles at location x and the total competition experienced at that location from particles at other locations. This total competition is given by summing over the competition kernels for every other location. Hence, the death rate is given by

$$\gamma(x, \phi) = \phi(x) \sum_{i=1}^{N(t)} g(x - x_i).$$

Instead of only summing over the locations of the particles, we could integrate over the whole domain. This will be helpful for mathematical simplicity. In this way, we can rewrite the death rate as

$$\gamma(x, \phi) = K \int_{-\pi}^{\pi} \phi(x)\phi(y)g(x - y)dy. \tag{2.16}$$

This equivalence of definitions can be seen by substituting the definition for $\phi(y)$ in the integral. Finally, define the movement rate $\alpha(x, y, \phi)$ as the rate of an individual at location y moving to location x when the system is in state ϕ. This rate is equal to the product of the number of particles at location y and the rate $d(x - y)$ to move to location x. Hence, the movement rate is given by

$$\alpha(x, y, \phi) = K\phi(y)d(x - y). \tag{2.17}$$

We have now defined all three rates for birth, death, and movement. Using these rates and their equivalent operators, we can construct the functional master equation for our system. This master equation explains how the probability of finding our system in a given state develops over time in terms of births, deaths, and movements. The rest of this Section will be dedicated to analysing this master equation and deriving the 1D FKPP equation.

Let $P(\phi, t)$ be the probability of the finding the system in state ϕ at time t. For our system to be in state ϕ at time t, three different events could have taken place for this system to arrive at ϕ. The system could have been in state $\Delta_x^- \phi$

and then a birth occurred at location x, in state $\Delta_x^+\phi$ and a death occurred at location x, or in state $\Delta_x^-\Delta_y^+\phi$ and a particle moved from location y to location x. The three events are summarised in the master equation as

$$\frac{\partial}{\partial t}P(\phi,t) = \int_{-\pi}^{\pi} Q(\phi,x)P(\phi,t)dx, \tag{2.18}$$

where

$$Q(\phi,x) = (\Delta_x^- - 1)\beta(x,\phi) + (\Delta_x^+ - 1)\gamma(x,\phi) + \int_{-\pi}^{\pi}(\Delta_x^-\Delta_y^+ - 1)\alpha(x,y,\phi)dy. \tag{2.19}$$

The first term is for births, the second term for deaths, and the last term for movement. This is the functional master equation for our system. We will now carry out an extensive analysis of this equation, which will provide a framework for an analysis in Chapter 5.

We will begin by expanding the birth, death, and movement operators using a variation of the Kramers-Moyal expansion [62, 63, 64]. We will substitute this expansion into the master equation with the formulas for the birth, death, and movement rates, which will result in the master equation depending on ϕ and functional derivatives of ϕ. At this point, the derivation will move to Fourier space, as it will be easier to manage the real space convolutions as Fourier space products. In addition, using results from complex integration, the master equation simplifies significantly in Fourier space. We will then define explicitly the death and movement functions g and d and return to real space with the 1D FKPP equation.

We now begin our analysis of the master equation. Applying a variation of the Kramers-Moyal expansion to the birth, death, and movement operators will allow us to rewrite the operators in terms of functional derivatives using a Taylor expansion in K^{-1}, as we have assumed that K is large. This is given by

$$\Delta_x^{\pm} = 1 \pm \frac{1}{K}\frac{\delta}{\delta\phi(x)} + \frac{1}{2K^2}\frac{\delta^2}{\delta\phi(x)^2}, \tag{2.20}$$

which ignores higher order terms in K^{-1} and where $\delta/\delta\phi(x)$ is functional differ-

entiation, which is defined for an arbitrary functional $F[\phi]$ as

$$\frac{\delta F[\phi(x)]}{\delta\phi(y)} = \lim_{\epsilon\to 0}\frac{F[\phi+\epsilon\delta(x-y)]-F[\phi]}{\epsilon}.$$

This is the expansion for the birth and death operators. The movement operator is a product of the birth and death operators so the expansion is given by

$$\begin{aligned}\Delta_x^-\Delta_y^+ &= \left(1-\frac{1}{K}\frac{\delta}{\delta\phi(x)}+\frac{1}{2K^2}\frac{\delta^2}{\delta\phi(x)^2}\right)\left(1+\frac{1}{K}\frac{\delta}{\delta\phi(y)}+\frac{1}{2K^2}\frac{\delta^2}{\delta\phi(y)^2}\right)\\ &= 1+\frac{1}{K}\left(\frac{\delta}{\delta\phi(y)}-\frac{\delta}{\delta\phi(x)}\right)+\frac{1}{K^2}\left(\frac{1}{2}\frac{\delta^2}{\delta\phi(x)^2}+\frac{1}{2}\frac{\delta^2}{\delta\phi(y)^2}-\frac{\delta}{\delta\phi(x)}\frac{\delta}{\delta\phi(y)}\right).\end{aligned} \tag{2.21}$$

We now substitute the expansions for the operators $\Delta_x^{\pm}, \Delta_x^-\Delta_y^+$ in (2.20) and (2.21) into the equation for $Q(\phi,x)$ in (2.19). Expanding and simplifying gives

$$\begin{aligned}Q(\phi,x) = &\frac{1}{K}\frac{\delta}{\delta\phi(x)}\left(-\beta(x,\phi)+\gamma(x,\phi)-\int_{-\pi}^{\pi}\alpha(x,y,\phi)dy\right)\\ &+\frac{1}{2K^2}\frac{\delta^2}{\delta\phi(x)^2}\left(\gamma(x,\phi)+\beta(x,\phi)+\int_{-\pi}^{\pi}\alpha(x,y,\phi)dy\right)\\ &+\frac{1}{K}\int_{-\pi}^{\pi}\frac{\delta}{\delta\phi(y)}\alpha(x,y,\phi)dy+\frac{1}{2K^2}\int_{-\pi}^{\pi}\frac{\delta^2}{\delta\phi(y)^2}\alpha(x,y,\phi)dy\\ &-\frac{1}{K^2}\int_{-\pi}^{\pi}\frac{\delta}{\delta\phi(x)}\frac{\delta}{\delta\phi(y)}\alpha(x,y,\phi)dy.\end{aligned}$$

We now also substitute the equations for the birth, death, and movement rates in (2.15), (2.16), and (2.17) into this equation giving

$$\begin{aligned}&Q(\phi,x) =\\ &\frac{\delta}{\delta\phi(x)}\left(-r\phi(x,t)+\int_{-\pi}^{\pi}\phi(x)\phi(y)g(x-y)dy-\int_{-\pi}^{\pi}\phi(y)d(x-y)dy\right)\\ &+\frac{1}{2K}\frac{\delta^2}{\delta\phi(x)^2}\left(\int_{-\pi}^{\pi}\phi(x)\phi(y)g(x-y)dy+r\phi(x,t)+\int_{-\pi}^{\pi}\phi(y)d(x-y)dy\right)\\ &+\int_{-\pi}^{\pi}\frac{\delta}{\delta\phi(y)}\phi(y)d(x-y)dy+\frac{1}{2K}\int_{-\pi}^{\pi}\frac{\delta^2}{\delta\phi(y)^2}\phi(y)d(x-y)dy\\ &-\frac{1}{K}\int_{-\pi}^{\pi}\frac{\delta}{\delta\phi(x)}\frac{\delta}{\delta\phi(y)}\phi(y)d(x-y)dy.\end{aligned}$$

We can now let $K \to \infty$ as we are only interested in the large population dynamics. This gives

$$\begin{aligned}
&Q(\phi, x) = \\
&\frac{\delta}{\delta\phi(x)}\left(-r\phi(x,t) + \int_{-\pi}^{\pi}\phi(x)\phi(y)g(x-y)dy - \int_{-\pi}^{\pi}\phi(y)d(x-y)dy\right) \\
&+ \int_{-\pi}^{\pi}\frac{\delta}{\delta\phi(y)}\phi(y)d(x-y)dy,
\end{aligned}$$

and substituting this equation for $Q(\phi, x)$ back into the master equation (2.18) gives

$$\begin{aligned}
&\frac{\partial}{\partial t}P(\phi,t) = \\
&\int_{-\pi}^{\pi}\left[\frac{\delta}{\delta\phi(x)}\left(-r\phi(x,t) + \int_{-\pi}^{\pi}\phi(x)\phi(y)g(x-y)dy - \int_{-\pi}^{\pi}\phi(y)d(x-y)dy\right)\right. \\
&\left.+ \int_{-\pi}^{\pi}\frac{\delta}{\delta\phi(y)}\phi(y)d(x-y)dy\right]P(\phi,t)dx.
\end{aligned} \tag{2.22}$$

The master equation now contains convolutions. To make these convolutions easier to handle, we move to Fourier space where they become products. Define the Fourier space transforms of ϕ, g, d as

$$\begin{aligned}
\phi_n(t) &= \frac{1}{2\pi}\int_{-\pi}^{\pi}\phi(x,t)e^{-inx}dx \\
g_k &= \frac{1}{2\pi}\int_{-\pi}^{\pi}g(x)e^{-ikx}dx \\
d_k &= \frac{1}{2\pi}\int_{-\pi}^{\pi}d(x)e^{-ikx}dx,
\end{aligned}$$

and the inverse Fourier transforms as

$$\begin{aligned}
\phi(x,t) &= \sum_n \phi_n(t)e^{inx} \\
g(x-y) &= \sum_k g_k e^{ik(x-y)} \\
d(x-y) &= \sum_k d_k e^{ik(x-y)},
\end{aligned} \tag{2.23}$$

as we are on the finite interval $[-\pi, \pi)$. Using these Fourier space expansions, the function derivative for ϕ can be rewritten in terms of the Fourier modes ϕ_n as

$$\frac{\delta}{\delta\phi(x)} = \sum_n \frac{\delta\phi_n}{\delta\phi}\frac{\delta}{\delta\phi_n} = \frac{1}{2\pi}\sum_n \frac{\delta}{\delta\phi_n}e^{-inx}.$$

In Fourier space, we can now substitute the inverse Fourier expansions in (2.23) into the functional master equation in (2.22). Making this substitution and simplifying gives

$$\begin{aligned}\frac{\partial}{\partial t}P(\phi,t) = &-\sum_{p,n}\frac{\delta}{\delta\phi_p}P(\phi,t)\frac{1}{2\pi}r\phi_n(t)\int_{-\pi}^{\pi}e^{i(n-p)x}dx \\ &+\sum_{p,n,m,k}\frac{\delta}{\delta\phi_p}P(\phi,t)\frac{1}{2\pi}\phi_n(t)\phi_m(t)g_k\int_{-\pi}^{\pi}e^{i(n+k-p)x}dx\int_{-\pi}^{\pi}e^{i(m-k)y}dy \\ &-\sum_{p,n,k}\frac{\delta}{\delta\phi_p}P(\phi,t)\frac{1}{2\pi}\phi_n(t)d_k\int_{-\pi}^{\pi}e^{i(k-p)x}dx\int_{-\pi}^{\pi}e^{i(n-k)y}dy \\ &+\sum_{p,n,k}\frac{\delta}{\delta\phi_p}P(\phi,t)\frac{1}{2\pi}\phi_n(t)d_k\int_{-\pi}^{\pi}e^{ikx}dx\int_{-\pi}^{\pi}e^{i(n-p-k)y}dy.\end{aligned}$$

The Cauchy Integral Theorem [66] tells us that these integrals will all be equal to zero unless the exponents in the integrands are themselves zero as the integrands have no poles within the unit circle. When the exponents are equal to zero, the integrals are equal to 2π. Hence, we require the exponents to be equal to zero and we gather conditions for the sum variables. This gives

$$\frac{\partial}{\partial t}P(\phi,t) = \sum_p \frac{\delta}{\delta\phi_p}P(\phi,t)R(\phi_p), \tag{2.24}$$

where

$$R(\phi_p) = -r\phi_p(t) + 2\pi\sum_m \phi_{p-m}(t)\phi_m(t)g_m + 2\pi\phi_p(t)(d_0 - d_p).$$

The functional master equation for our system is now in the form of the Liouville equation [60], which is a special case of the forward Fokker-Planck equation (2.5)

when $b(x,t) = 0$. The master equation (2.24) has solutions ϕ_p when

$$\frac{d}{dt}\phi_p = r\phi_p - 2\pi \sum_m g_m \phi_{p-m}\phi_m + 2\pi(d_p - d_0)\phi_p, \tag{2.25}$$

which is a first-order ordinary differential equation for the Fourier modes ϕ_p which we have recovered from the functional master equation. For the rest of this derivation of the 1D FKPP equation, we will focus on (2.25). We only need to define functions d, g and return to real space. For movement, we have assumed that the particles are moving according to Brownian motion with diffusion coefficient D on a microscopic level. To model this here we assume that individuals remain static at some location x and then move to location y with rate $d(x-y)$. In order to resolve the difference between the microscopic Brownian motion we want to model and the framework we are using here, we assume that individuals move at random times that are exponentially distributed with rate γ. The distance traveled is a normal random variable with mean zero and variance D/γ. In the limit $\gamma \to \infty$, the movement of the individuals converges to Brownian motion with diffusion coefficient D, which is the movement we want to model. Hence, we define the movement rate $d(x-y)$ to move from location x to location y as

$$d(x-y) = \frac{\gamma}{\sqrt{4\pi D/\gamma}} \exp\left(\frac{-\gamma(x-y)^2}{4D}\right).$$

This movement rate has Fourier modes given by

$$\begin{aligned} d_k &= \frac{1}{2\pi}\int_{-\pi}^{\pi} d(x)e^{-ikx}dx = \frac{\gamma}{2\pi\sqrt{4\pi D/\gamma}}\int_{-\pi}^{\pi} \exp\left(\frac{-\gamma x^2}{4D} - ikx\right)dx \\ &\approx \frac{\gamma}{2\pi\sqrt{4\pi D/\gamma}}\int_{-\infty}^{\infty} \exp\left(\frac{-\gamma x^2}{4D} - ikx\right)dx \\ &= \frac{\gamma}{2\pi\sqrt{4\pi D/\gamma}} 2\sqrt{\frac{\pi D}{\gamma}} \exp\left(-\frac{D}{\gamma}k^2\right) = \frac{\gamma}{2\pi}\exp\left(-\frac{D}{\gamma}k^2\right), \end{aligned}$$

where the approximation follows as we are considering large γ so the exponential has a very sharp peak at zero. Hence, the large tail error is small and we can shift domains from $[-\pi, \pi)$ to $(-\infty, \infty)$. Considering the movement term in (2.25), we see $d_p - d_0 = \frac{\gamma}{2\pi}(e^{-\frac{D}{\gamma}p^2} - 1) \approx -\frac{D}{2\pi}p^2$ as we only need to consider small $1/\gamma$ as

we are only interested in the case when $\gamma \to \infty$. Substituting these modes into (2.25) gives

$$\frac{d}{dt}\phi_p = r\phi_p - 2\pi \sum_m g_m \phi_m \phi_{p-m} - Dp^2 \phi_p. \tag{2.26}$$

We now return to real space. Note that the Fourier modes of the product of two arbitrary functions f and g are given by

$$\begin{aligned}\mathcal{F}_k[f(x)g(x)] &= \frac{1}{2\pi}\int_{-\pi}^{\pi} f(x)g(x)e^{-ikx}dx = \frac{1}{2\pi}\int_{-\pi}^{\pi}\sum_n f_n e^{inx}\sum_m g_m e^{imx}e^{-ikx}dx \\ &= \frac{1}{2\pi}\sum_{n,m} f_n g_m \int_{-\pi}^{\pi} e^{ix(n+m-k)}dx = \sum_n f_n g_{k-n},\end{aligned}$$

where the last equality holds because, according to the Cauchy Integral Theorem [66], this integral is equal to zero when the exponent is not zero as the integrand has no poles within the unit circle. When the exponent is zero, the integral is equal to 2π. The inverse Fourier transform is given by

$$\begin{aligned}\mathcal{F}^{-1}\left[\sum_n f_n g_{k-n}\right](x) &= \sum_k e^{ikx}\sum_n f_n g_{k-n} = \sum_k e^{inx}e^{i(k-n)x}\sum_n f_n g_{k-n} \\ &= \sum_n f_n e^{inx}\sum_k e^{i(k-n)x} g_{k-n} = f(x)g(x).\end{aligned} \tag{2.27}$$

Also note that the Fourier modes of the convolution of two arbitrary functions f and g are given by

$$\begin{aligned}&\mathcal{F}_k\left[\int_{-\pi}^{\pi} f(x-y)g(y)dy\right] = \frac{1}{2\pi}\int_{-\pi}^{\pi}\int_{-\pi}^{\pi} f(x-y)g(y)dy e^{-ikx}dx \\ &= \frac{1}{2\pi}\int_{-\pi}^{\pi}\int_{-\pi}^{\pi}\sum_n f_n e^{in(x-y)}\sum_m g_m e^{imy}dy e^{-ikx}dx \\ &= \frac{1}{2\pi}\sum_{n,m} f_n g_m \int_{-\pi}^{\pi} e^{ix(n-k)}dx \int_{-\pi}^{\pi} e^{iy(-n+m)}dydx = 2\pi f_k g_k.\end{aligned}$$

The inverse Fourier transform is given by

$$\begin{aligned}\mathcal{F}^{-1}[2\pi f_k g_k](x) &= \sum_k e^{ikx} 2\pi f_k g_k = \sum_k e^{ikx} \int_{-\pi}^{\pi} f_k g_k dy \\ &= \int_{-\pi}^{\pi} \sum_k f_k e^{ik(x-y)} g_k e^{iky} dy = \int_{-\pi}^{\pi} f(x-y)g(y)dy.\end{aligned} \tag{2.28}$$

From these results, we can calculate the inverse Fourier transform of (2.26). Recall the inverse Fourier transform $\phi(x,t) = \sum_n \phi_n(t)e^{inx}$ from (2.23). Differentiating with respect to time and substituting (2.26) gives

$$\begin{aligned}&\frac{\partial}{\partial t}\phi(x,t) = \sum_n e^{inx}\frac{d}{dt}\phi_n(t) = \sum_n e^{inx}\left(r\phi_n - 2\pi\sum_m g_m\phi_m\phi_{n-m} - Dn^2\phi_n\right) \\ &= r\sum_n \phi_n e^{inx} - \sum_n e^{inx}\sum_m 2\pi g_m\phi_m\phi_{n-m} + D\frac{d^2}{dx^2}\sum_n \phi_n e^{inx},\end{aligned} \tag{2.29}$$

noting in the third term that

$$\frac{d^2}{dx^2}e^{inx} = -n^2 e^{inx}.$$

Now, consider the second term in the last line of (2.29). Let $f_m = 2\pi g_m\phi_m$. Then, this term becomes

$$\sum_n e^{inx}\sum_m 2\pi g_m\phi_m\phi_{n-m} = \sum_n e^{inx}\sum_m f_m\phi_{n-m} = f(x)\phi(x),$$

using the result from (2.27). From considering the Fourier modes of $f(x)$ given by $f_m = 2\pi g_m\phi_m$, we see that

$$f(x) = \int_{-\pi}^{\pi} g(x-y)\phi(y)dy,$$

using the result from (2.28), so the inverse Fourier transform of the second term in the last line of (2.29) is given by

$$\mathcal{F}^{-1}\left[\sum_m 2\pi g_m\phi_m\phi_{n-m}\right] = \phi(x)\int_{-\pi}^{\pi} g(x-y)\phi(y)dy.$$

Hence, substituting the definition for $\phi(x,t)$ in (2.29) gives

$$\frac{\partial}{\partial t}\phi(x,t) = r\phi(x,t) - \int_{-\pi}^{\pi} g(x-y)\phi(y)dy\phi(x) + D\frac{d^2}{dx^2}\phi(x,t).$$

Finally, we let $g(x-y)$ tend to the delta function $r\delta(x-y)$ as we are only interested in local competition. This gives

$$\frac{\partial}{\partial t}\phi(x,t) = r\phi(x,t)\left(1-\phi(x,t)\right) + D\frac{d^2}{dx^2}\phi(x,t),$$

which is the 1D FKPP equation. The three terms show the effects of the birth, death, and movement processes on the population function ϕ. In Chapter 3, we will use the nondimensionalised FKPP equation extended to two dimensions given by $\phi_t = \phi_{xx} + \phi_{yy} + \phi(1-\phi)$ to model a bacteria population. In Chapter 4, we will use the 1D FKPP equation to model a fish population.

Note that when searching for travelling wave solutions to the nondimensionalised, linearised 1D FKPP equation $\phi_t = \phi_{xx} + \phi$ of the form $\phi(x,t) = \psi(x-ct)$ for invasion speed c, we have solutions that solve

$$\psi'' + c\psi' + \psi = 0,$$

which has solutions of the form

$$\psi(x-ct) = A_1 e^{\frac{-c+\sqrt{c^2-4}}{2}(x-ct)} + A_2 e^{\frac{-c-\sqrt{c^2-4}}{2}(x-ct)},$$

for constants A_1, A_2. Hence,

$$\psi(x-2t) = e^{-(x-2t)} \tag{2.30}$$

is a travelling wave solution to the nondimensionalised, linearised 1D FKPP equation. We will use this solution to find solutions for the linearised 2D FKPP equation in Chapter 3.

2.2.2 FKPP Invasion Speed Derivation

The FKPP equation is one of the standard equations used to model biological invasions. A key feature of a biological invasion is the speed of invasion. Under-

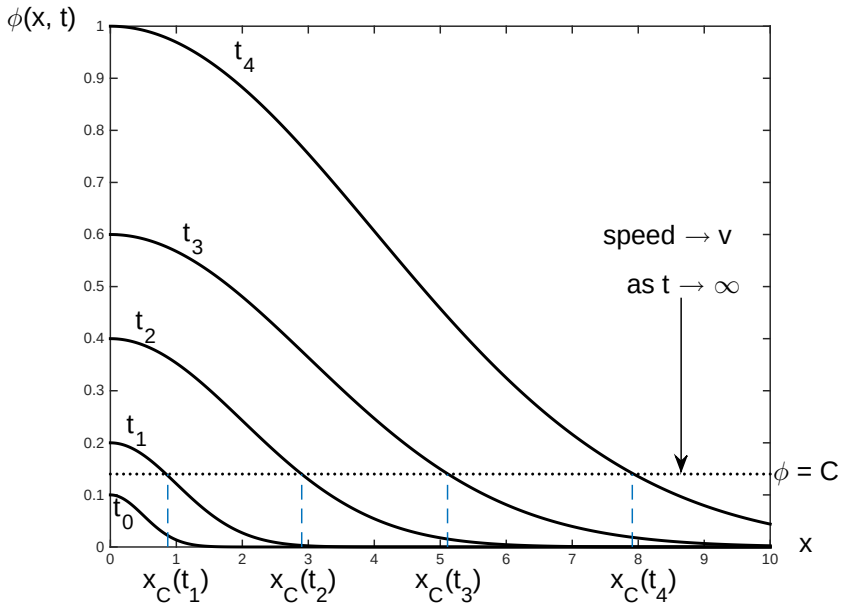

Figure 2-1: An invading front (solid lines) at various times. The front location is determined by the intersection of the population front with the line $\phi(x_C(t), t) = C$ (dotted line). These locations are labelled as the $x_C(t)$ (dashed lines)

.

standing how quickly a population will invade into a new territory is crucial in mathematical biology. This invasion speed will also be used in Chapters 3 and 4 in this thesis. In this Section, we will recap the derivation of the equation for the invasion speed of the FKPP equation using [21] . We will do this by using a Fourier space argument and results from complex integration to derive a dispersion relation for the population. The population invasion speed will then be determined from the dispersion relation.

We begin by defining the population invasion speed. The FKPP equation creates a pulled front, which means the dynamics of the equation, including the invasion speed, are determined by the low density population ahead of the front. In terms of the biological dynamics of a population, this means that as the population moves into new, hospitable environments, only a few initial 'seed' individuals are needed for the population in this new area to grow to large, sustainable levels. For this reason, we only need to consider the linearised 1D FKPP equation, given by

$$\frac{\partial}{\partial t}\phi(x,t) = D\frac{\partial^2}{\partial x^2}\phi(x,t) + r\phi(x,t). \tag{2.31}$$

All populations that evolve according to this equation will grow unbounded and so we can calculate the invasion speed for any population that has positive initial conditions. In addition, populations developing according to the linearised 1D FKPP equation will invade both to the left and to the right. Without loss of generality, we consider populations invading to the right. For some positive constant C, the population invasion speed v^* is defined as the speed of the positions $x_C(t)$ at which $\phi(x,t)$ reaches the value C, i.e. the asymptotic speed of the points $x_C(t)$ that satisfy $\phi(x_C(t),t) = C$, which is given by $v^* = \lim_{t\to\infty} \frac{dx_C}{dt}$. This definition is shown in Figure 2-1. Note that previously we were working on the domain $[-\pi, \pi)$ but now we consider the domain $(-\infty, \infty)$, as we require an infinite domain to define the asymptotic invasion speed.

In order to calculate this invasion speed, we move to Fourier space in order to use some results from complex integration. We define the inverse Fourier transform for ϕ as

$$\phi(x,t) = \frac{1}{2\pi}\int_{-\infty}^{\infty} \phi_k(t) e^{ikx} dk, \tag{2.32}$$

for Fourier modes $\phi_k(t)$. We also give an ansatz for how the Fourier modes depend on the Fourier mode number given by $\phi_k(t) = \phi_k \exp(-i\omega(k)t)$ where $\omega(k)$ is the dispersion relation for the population. Substituting this ansatz into (2.32) gives

$$\phi(x,t) = \frac{1}{2\pi}\int_{-\infty}^{\infty} \phi_n e^{ikx - i\omega(k)t} dk.$$

The results that we would like to use from complex integration depend on the population front neither growing or decaying in time. Given that the population ahead of the front is growing, we need to view the population through a moving frame that keeps the population front constant. We have assumed the population has invasion speed v^* so we will consider the moving reference frame $\zeta = x - v^*t$. Rewriting (2.32) with this moving reference frame and then using [65] to deform the integral onto $(-\infty + i\beta, \infty + i\beta)$ gives

$$\phi(\zeta,t) = \frac{1}{2\pi}\int_{-\infty+i\beta}^{\infty+i\beta} \phi_k e^{ik\zeta} e^{-i[\omega(k) - v^*k]t} dk, \tag{2.33}$$

where β is still undefined. The next part of this derivation requires the calculation of two formulas for the population invasion speed v^*. Both formulas are derived

considering ϕ as $t \to \infty$. The first equation comes from there being no maximum for the integral exponents and second equation comes from the requirement that ϕ should neither grow nor decay in time in our moving reference frame.

Now, for the first equation, let $t \to \infty$. The largest contribution to (2.33) occurs in the complex plane where the coefficient of t is largest. We define this coefficient as $G(k) = \omega(k) - v^*k$. We want to find the point in the complex plane where this coefficient is largest. This point will be where $G'(k) = 0$. However, this point will not be a local maximum according to the maximum modulus principle [67] so it cannot occur at a boundary. Hence, it must be a saddlepoint. Define this saddlepoint in the complex plane to be k^* so $G'(k^*) = 0$. We set $\beta = \text{Im}(k^*)$ in (2.33). From the definition of $G(k)$, it then follows that $\omega'(k^*) - v^* = 0$ so

$$v^* = \omega'(k^*). \tag{2.34}$$

This is the first equation for v^*.

For the second equation, again let $t \to \infty$. We are viewing ϕ through a moving reference frame so that the population front is not growing or decaying in time. For this to be the case, (2.33) must be independent of time everywhere, including at the saddlepoint k^*. Hence, we must have $\text{Im}(G(k^*)) = \text{Im}(\omega(k^*) - v^*k^*) = 0$ and so

$$v^* = \frac{\text{Im}(\omega(k^*))}{\text{Im}(k^*)}. \tag{2.35}$$

This is the second equation for v^*.

We now have two equations for the population invasion speed v^* in terms of $\omega(k^*)$. To determine v^*, we first calculate $\omega(k^*)$ for the FKPP equation. We look for solutions of the form $\phi(x,t) \propto e^{ikx - i\omega(k)t}$. Substituting this into (2.31) gives

$$\omega(k) = i(r - Dk^2). \tag{2.36}$$

We now have the equation for the dispersion relation $\omega(k)$ for the linearised FKPP equation. Substituting (2.36) into (2.34) gives

$$v^* = \omega'(k^*) = -2iDk^*.$$

But v^* is real so the right hand side is real. Hence, it must be that k^* is purely

imaginary so $k^* = i\beta$ and

$$v^* = \omega'(i\beta) = 2D\beta. \tag{2.37}$$

Substituting (2.36) into (2.35) gives

$$v^* = \frac{\mathrm{Im}(\omega(i\beta))}{\mathrm{Im}(i\beta)} = \frac{(r + D\beta^2)}{\beta}.$$

Setting these two equations equal to each other and solving for β gives

$$\beta = \pm\sqrt{\frac{r}{D}}.$$

Using the positive value for β in (2.37), as we are interested in populations invading to the right, gives

$$v^* = 2\sqrt{rD}. \tag{2.38}$$

This is the equation for the population invasion speed for the FKPP equation, which depends on both the growth rate r and diffusion coefficient D. We will use this result in both Chapters 3 and 4.

Chapter 3

Invasions and Reactive Boundaries

When a population enters a new territory, a common question to ask is 'how is the surrounding environment affected by this new population?' However, it is equally important to understand how the population is affected by the environment. There are many examples of ways the environment can influence local dynamics. They include changing the properties of fluids in porous media [68, 69], physiologically altering biofilms attached to solid surfaces [70, 71], and increasing diffusion along roadsides [72, 73].

The environment can have any number of different effects on the populations interacting with it. When considering the introduction of a new population, the environment can influence the long term genetic diversity [74, 75]. This was confirmed by Möbius et. al. in their work on bacteriophage T7 moving in an environment of E. coli [36]. They found that a heterogenous environment significantly affects the genetic diversity of a population. In particular, the experimental domain is a patch of two types of E. coli. One type is T7-resistant and the other is not. When it reaches the non-resistant E. coli, the T7 "infects bacterial cells and lyses them, releasing a large number of new phage particles which undergo passive dispersal and can infect nearby cells, a cycle of growth and replication that leads to an advancing population front" [36]. The non-resistant E. coli provides a region of good growth conditions for the T7. The T7-resistant E. coli does not. When the T7 enters this hostile region, it does not release a large number of new particles. In this region, which acts as an obstacle for the T7, the growth

conditions are very poor. The results show that the obstacle created a kink in the front of T7 near the boundary with the obstacle and that there was a significant reduction in speed near the boundary. A constant speed model was suggested to predict these results but it did not accurately reflect the shape of the front after the kink had formed in the population. The experimental results lagged behind the constant speed model significantly. Möbius et. al. then considered the 2D FKPP equation with a location-dependent growth rate to determine the effect of the obstacles on the population front. This model agrees qualitatively with the experimental results. The lag is seen in the model in addition to the shape of the front changing near the boundary and a slow down of the front near the widest point of the obstacle.

Motivated by this work, we consider in this Chapter a population invading a 2D environment with individuals that give birth, die and move. The simplest model that captures these dynamics is given by the 2D FKPP equation

$$u_t = u_{xx} + u_{yy} + u(1-u), \tag{3.1}$$

where we have set $r = D = 1$, which is possible by rescaling time by $t' = rt$ and space by $x' = y' = \sqrt{r/D}$ and then rewriting the 2D FKPP equation in terms of t', x', y'. In order to model the obstacles, we choose environments that have at least one boundary, which will simulate the obstacle. Hence, for the environments we consider a corridor of finite width $L > 0$ given by $C_L = \{(x, y) : x \in \mathbb{R}, 0 \leq y \leq L\}$ and a corridor of infinite width given by $C_\infty = \{(x, y) : x \in \mathbb{R}, y \geq 0\}$. We introduce a mixed or reactive boundary on the $y = 0$ boundary as it accurately reflects the experimental dynamics of the T7 bacteriophage near the resistant E. coli obstacle. A mixed boundary means that some of the individuals can pass through the boundary while others are reflected back. When considering the bacteriophage example, a mixed boundary is appropriate as each E. coli cell on the border of the T7-resistant region can only be infected once. Once a particular cell has been infected, the T7 can no longer cross the boundary at this point. Hence, it is a mixed boundary. The mixed boundary condition is given by

$$u_y = \alpha u \text{ on } y = 0, \tag{3.2}$$

where $\alpha \geq 0$ is some reaction rate. When α is large, the boundary is very

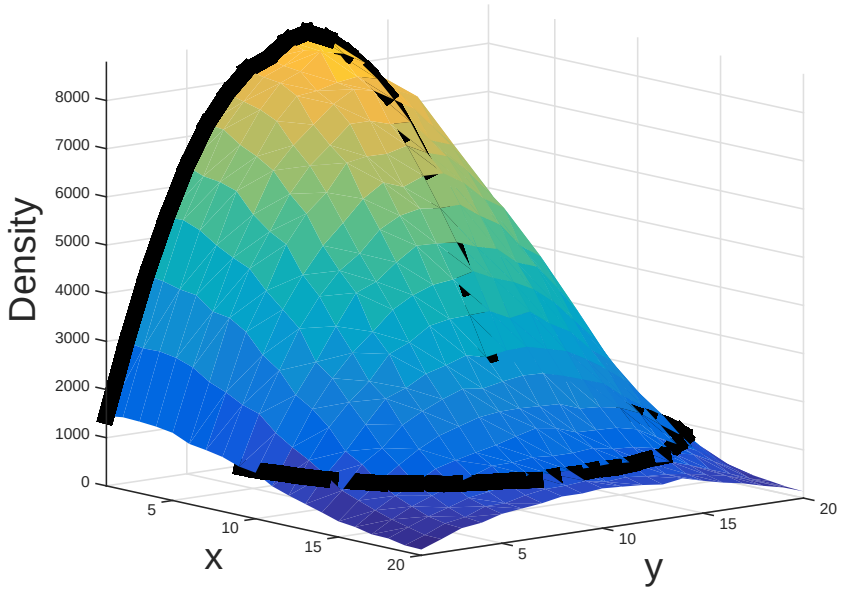

Figure 3-1: The two regions of the population that we explore in this Chapter are shown in thick black lines. We are concerned with the low density dynamics ahead of the front and the high density stable state behind the front.

hostile and nearly absorbing. When α is small, the boundary is barely hostile and nearly reflective. The reaction rate α is a measure of how hostile the obstacle in the environment is. Möbius et. al. used the 2D FKPP equation to model the influence of the change in growth rate in the resistant and non-resistant regions. Here, we are modelling the influence of the strength of the hostile boundaries on the population. We model this mixed boundary according to [76]. When we consider C_L, we also introduce a mixed boundary condition $u_y = -\beta u$ on $y = L$ for reaction rate $\beta \geq 0$. The negative sign is due to the change of orientation of the $y = L$ boundary compared to the $y = 0$ boundary. This second mixed boundary allows us to consider the effects two obstacles could have on a population. Note that when $\beta = 0$, the boundary at $y = L$ is reflective, and as $\beta \to \infty$, the condition tends to an absorbing boundary. Hence, we can perform the following calculations with general β and then set $\beta = 0, \beta \to \infty$ when we want the results for a reflective or absorbing boundary respectively.

The dynamics of the population change as the density of the population changes. The dynamics of the population in the low density region where the population is unstable are analysed in Section 3.1. We linearise the 2D FKPP equation to find results on the speed of the population and the corridor widths

that can support populations with different speeds. In Section 3.2, we study the dynamics when the population density is high and stable. There we show the conditions required for the survival and stability of the population. These two regimes are shown in Figure 3-1.

3.1 Ahead of the Front

In this Section, we are interested in determining how a hostile boundary affects the shape of the population invasion ahead of the front. The population density ahead of the front is very small so we can assume $u(x, y, t) \ll 1$. With this assumption, we can linearise (3.1). The linearised 2D FKPP equation is given by

$$u_t = u_{xx} + u_{yy} + u. \tag{3.3}$$

We now seek to find solutions to (3.3). Consider a separable solution given by $u(x, y, t) = \exp(-(x - ct))v(y)$ for some function $v(y)$ and for invasion speed c. We assume the solution has this form as $u(x, t) = \exp(-(x - ct))$ is a traveling wave solution to the 1D FKPP equation, as shown in the technical introduction in (2.30). Substituting this solution into (3.3) gives

$$v_{yy} + (2 - c)v = 0, \tag{3.4}$$

a second order differential equation for the function $v(y)$ which gives the dependence on the second spatial coordinate. In terms of v, the boundary condition (3.2) is given by

$$v_y = \alpha v. \tag{3.5}$$

We now focus on finding solutions of (3.4) and (3.5). In the absence of a mixed boundary, the population would invade at speed $c = 2$, which we calculated in the technical introduction in (2.38). We assume that, with a hostile boundary, the invasion will be no faster than an invasion with no hostile boundary so $c \leq 2$. We define $p = \sqrt{2 - c}$ to simplify our notation. Note that when the population has invasion speed $c = 2, p = 0$ and when $c = 0, p = \sqrt{2}$. The solution to (3.4)

and (3.5) is then given by

$$v(y) = A\left(\cos(py) + \frac{\alpha}{p}\sin(py)\right), \tag{3.6}$$

for some undetermined constant A. We now consider this solution in C_L with a varying reaction rate β at $y = L$ and in C_∞.

3.1.1 C_L

We now consider the solution (3.6) for $v(y)$ in the domain C_L with the mixed boundary condition

$$v_y(L) = -\beta v, \tag{3.7}$$

for reaction rate $\beta \geq 0$. Applying (3.7) to (3.6) gives

$$(p^2 - \alpha\beta)\tan(pL) = p(\alpha + \beta). \tag{3.8}$$

This equation provides a condition that α, β, p, L must satisfy. This equation is shown in Figure 3-2. For a given α, β, L, (3.8) has a countable number of solutions for p. The values we are interested in are the values in $[0, \sqrt{2}]$ as they correspond to a nonnegative invasion speed c.

We can determine the relationship between L, α, and β when the population front has speed $c = 0$ by setting $p = \sqrt{2}$ which gives

$$(2 - \alpha\beta)\tan(\sqrt{2}L) = \sqrt{2}(\alpha + \beta). \tag{3.9}$$

Setting $\beta = 0$ gives $\sqrt{2}\tan(\sqrt{2}L) = \alpha$ for a reflective boundary at $y = L$ and letting $\beta \to \infty$ gives $-\alpha\tan(\sqrt{2}L) = \sqrt{2}$ for an absorbing boundary at $y = L$. For given α, β and the mixed boundary condition (3.7), the corridor width $L^m_{\alpha,\beta}$ that results in a population with invasion speed zero is given by

$$L^m_{\alpha,\beta} = \begin{cases} \frac{1}{\sqrt{2}}\tan^{-1}\left(\frac{\sqrt{2}(\alpha+\beta)}{2-\alpha\beta}\right) & \text{for } \alpha\beta < 2 \\ \frac{1}{\sqrt{2}}\left[\pi + \tan^{-1}\left(\frac{\sqrt{2}(\alpha+\beta)}{2-\alpha\beta}\right)\right] & \text{for } \alpha\beta > 2. \end{cases}$$

There are cases here because we need the smallest positive root for $\tan(\sqrt{2}L) =$

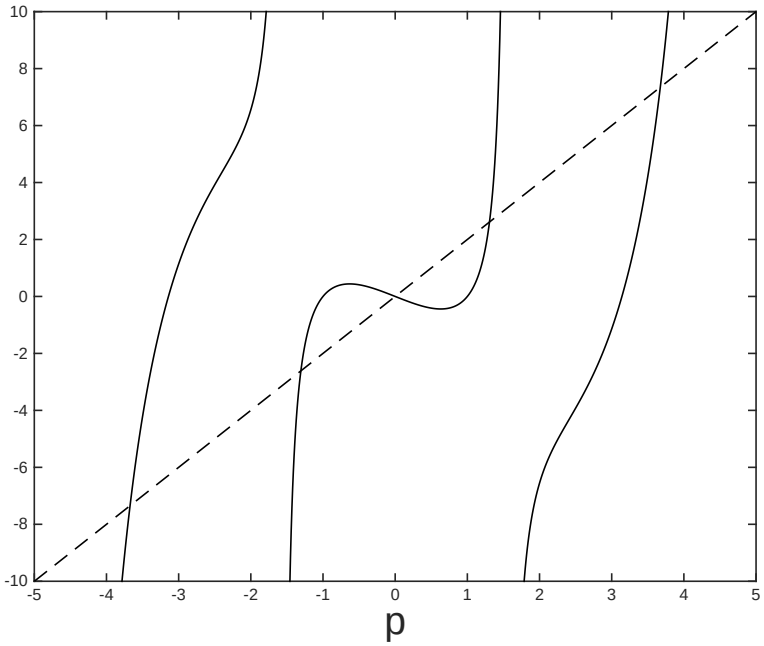

Figure 3-2: The equation $(p^2 - \alpha\beta)\tan(pL) = p(\alpha + \beta)$. The left hand side is shown in the solid line and the right hand side in the dashed line. $\alpha = \beta = L = 1$

$\sqrt{2}(\alpha + \beta)/(2 - \alpha\beta)$. Letting $\alpha \to \infty$ gives the critical corridor width

$$L^m_{\infty,\beta} = \frac{1}{\sqrt{2}}\left[\pi + \tan^{-1}\left(-\frac{\sqrt{2}}{\beta}\right)\right].$$

This value of $L^m_{\infty,\beta}$ is critical in the sense that if $L > L^m_{\infty,\beta}$, the population will invade forward for any value of α. If $L < L^m_{\infty,\beta}$, the population will invade forward if α is small enough but it will not invade forward if α is large enough. This relationship is shown in Figure 3-3. When $\beta = 0$ and when $\beta \to \infty$, the corridor width $L^m_{\alpha,0}, L^m_{\alpha,\infty}$ that results in a population with invasion speed zero is given respectively by

$$\begin{aligned} L^m_{\alpha,0} =& \frac{1}{\sqrt{2}}\tan^{-1}\left(\frac{\alpha}{\sqrt{2}}\right) \\ L^m_{\alpha,\infty} =& \frac{1}{\sqrt{2}}\left[\pi + \tan^{-1}\left(-\frac{\sqrt{2}}{\alpha}\right)\right], \end{aligned}$$

and letting $\alpha \to \infty$ gives the critical corridor widths $L^m_{\infty,0} = \pi/(2\sqrt{2}), L^m_{\infty,\infty} = \pi/\sqrt{2}$.

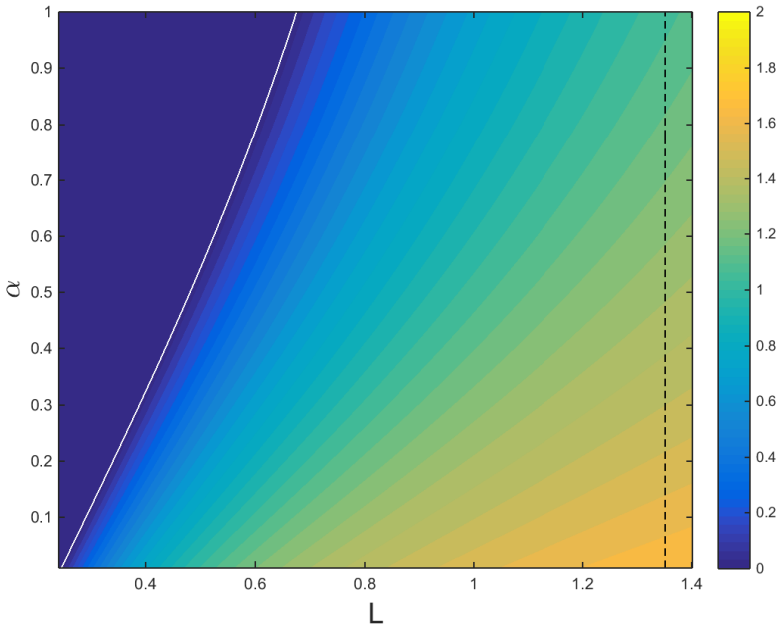

Figure 3-3: The relationship between reaction rate α, corridor width L, and invasion speed c. The white line shows the curve where the invasion has speed zero, which comes from equation (3.9). The dashed black line shows the critical corridor width $L^m_{\infty,\beta}$, above which the invasion always has a positive speed, for any value of α. The colour bar shows the speed c.

If $\alpha = \beta$, then the corridor width L_α^m is then

$$L_\alpha^m = \begin{cases} \frac{1}{\sqrt{2}} \tan^{-1}\left(\frac{2\sqrt{2}\alpha}{2-\alpha^2}\right) & \text{for } \alpha^2 < 2 \\ \frac{1}{\sqrt{2}}\left[\pi + \tan^{-1}\left(\frac{2\sqrt{2}\alpha}{2-\alpha^2}\right)\right] & \text{for } \alpha^2 > 2. \end{cases}$$

Letting $\alpha \to \infty$ gives $L_\infty^m = \pi/\sqrt{2}$.

As an aside, if $\alpha = \beta = 0$, we return to (3.6) to see that the solution is now

$$v(y) = A\cos(py).$$

Applying the reflective boundary condition $v_y(L) = 0$ when $\beta = 0$ at $y = L$ gives that

$$pL = \pi n \text{ for } n \in \{0, 1, \dots\}.$$

Recall that $p = \sqrt{2 - c}$ from (3.6). It then follows that the relationship between the population invasion speed c and the corridor width L is given by

$$c = 2 - \frac{n^2\pi^2}{L^2} \to 2 \text{ as } L \to \infty,$$

which agrees with the invasion speed for the 1D FKPP equation we calculated in the technical introduction in (2.38) with $r = D = 1$.

3.1.2 C_∞

We now consider the population front in the domain C_∞. As there is only one boundary, we must impose the second boundary by considering the population front as $y \to \infty$. We try to set $v(y) \to 1$ in (3.6) but we find there are no solutions. Far away from the mixed boundary at $y = 0$, the population should tend to the solution of the 1D FKPP equation with invasion speed $c = 2$ as the effects of the hostile boundary will be negligible infinitely far away from the boundary. We return to (3.4) with this speed requirement and see that it is now given by

$$v_{yy} = 0,$$

and the mixed boundary condition (3.5) at $y = 0$ gives

$$v(y) = v_0(1 + \alpha y),$$

for some constant v_0. The solution to (3.3) with boundary condition (3.2) is now explicitly given by

$$u(x, y, t) = u_0 \exp(-(x - 2t))(1 + \alpha y),$$

for some constant u_0. From this equation, we can study the behaviour of the population ahead of the front in terms of the level sets $u(x, y, t) = K$ for some constant $0 < K \ll 1$, as we are only considering ahead of the population front. The curves for these level sets are then given by

$$y = \frac{1}{\alpha}\left(\frac{K}{u_0}\exp(x - 2t) - 1\right),$$

with gradient

$$\frac{dy}{dx} = \frac{1}{\alpha}\frac{K}{u_0}\exp(x - 2t).$$

Note that when $y = 0$

$$\exp(x - 2t) = \frac{u_0}{K},$$

so the gradient at $y = 0$ is $dy/dx = 1/\alpha$, which is interesting because it is independent of the level set chosen. This effect is shown in Figure 3-4. The curvature in the level set near the boundary is more significant for larger α.

3.2 Behind the Front

3.2.1 Survival

We consider the survival of the population behind the front. In this region, there is no variation in the population density in the x direction as the invading front has passed and the population has reached a steady state so the population density does not change with time. Hence, the population far behind the front is now independent of both x and t so we write $u(x, y, t) = w(y)$. The 2D

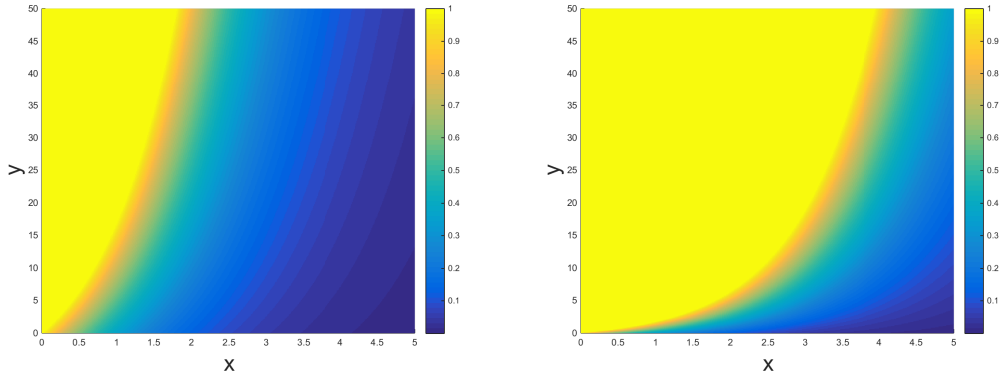

(a) (b)

Figure 3-4: The solution $u(x, y, t) = u_0 \exp(-(x - 2t))(1 + \alpha y)$ to the linearised FKPP equation $u_t = u_{xx} + u_{yy} + u$ in the domain C_∞ with $u_0 = K = 1, t = 1$. The colour bar goes from zero to one as we are considering the population ahead of the front. The colour bar shows the value of the population density $u(x, y, t)$. (a) $\alpha = 0.1$ (b) $\alpha = 1$.

nondimensionalised FKPP equation (3.1) is now

$$w_{yy} = w(w - 1). \tag{3.10}$$

The boundary condition behind the front remains the same and is given by

$$w_y = \alpha w \text{ on } y = 0.$$

We note that $w(y) = 0$ everywhere is a solution behind the front so it is possible that the population dies out. To analyse these equations, we define $z = w_y$ so that we have

$$w_y = z, \quad z_y = w(w - 1).$$

This system of differential equations has steady states at $(0, 0)$ and $(1, 0)$ and a Jacobian matrix given by

$$J = \begin{pmatrix} 0 & 1 \\ 2w - 1 & 0 \end{pmatrix},$$

which has eigenvalues $\pm\sqrt{2w - 1}$ so that $(0, 0)$ is a centre and $(1, 0)$ is a saddle-point. We can also express these dynamics as a two-dimensional Hamiltonian

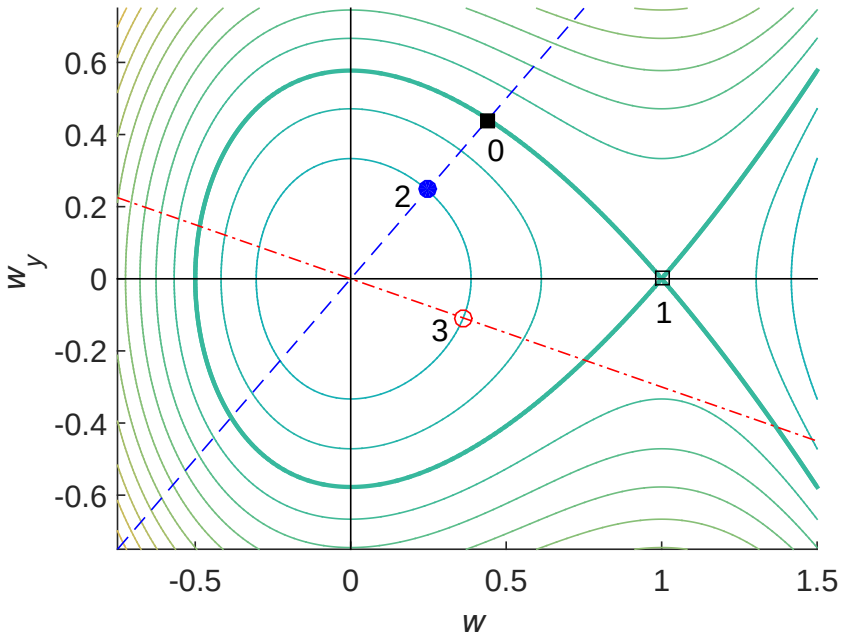

Figure 3-5: The phase plane produced by the equations $w_y = z, z_y = w(w-1)$. The solid lines show trajectories in the phase plane, the dashed blue line shows the boundary condition $w_y = \alpha w$ when $y = 0$, the dot dashed red line shows the mixed boundary condition $w_y = -\beta w$ when $y = L$, and the thick solid line shows the boundary condition for C_∞ where $w(y) \to 1$ as $y \to \infty$. Points $(w_0, z_0), \ldots, (w_3, z_3)$ are indicated by the labels $0, 1, 2, 3$.

system, given by

$$\begin{aligned} w_y &= z = \frac{\partial H}{\partial z} \\ z_y &= w(w-1) = -\frac{\partial H}{\partial w}. \end{aligned} \tag{3.11}$$

where the Hamiltonian $H(w, z)$ is given by

$$H(w, z) = \frac{1}{2}z^2 + \left(\frac{1}{2}w^2 - \frac{1}{3}w^3\right). \tag{3.12}$$

The phase plane is shown in Figure 3-5. In C_∞, there is a unique trajectory that corresponds to the boundary conditions $z = w_y = \alpha w$ on $y = 0$, which is shown in the dashed blue line, and $w \to 1$ as $y \to \infty$, which is shown by the thick solid line, and when $w, z > 0$ for all $y \geq 0$. This trajectory starts at the point

(w_0, z_0), where the line $z = w_y = \alpha w$ and the stable manifold intersect when $w, z > 0$, and follows the stable manifold to the point $(w_1, z_1) = (1, 0)$ as $y \to \infty$. We can find an analytic expression for this curve by solving (3.10), which gives

$$w(y) = 1 - \frac{3}{2}\text{sech}^2\left(\frac{(y + y_0)}{2}\right), \tag{3.13}$$

for an undetermined constant y_0. The equation in (3.13) clearly satisfies the boundary condition $w \to 1$ as $y \to \infty$. We can determine y_0 implicitly from the boundary condition $w_y = \alpha w$ on $y = 0$ using

$$\frac{3}{2}\tanh\left(\frac{y_0}{2}\right) = \alpha\left[\cosh^2\left(\frac{y_0}{2}\right) - \frac{3}{2}\right]. \tag{3.14}$$

Since the left-hand-side of (3.14) increases monotonically from zero and asymptotically approaches $3/2$ as y_0 increases to infinity, and the right-hand side increases monotonically from $-\alpha/2$ at $y_0 = 0$ to very large positive values as y_0 increases, it is clear that for any fixed $\alpha > 0$, the equation (3.14) has a unique positive solution for y_0. Since the left-hand-side is always positive, we have that y_0 always satisfies

$$y_0 \geq 2\text{cosh}^{-1}\left(\sqrt{\frac{3}{2}}\right) > 0.$$

In C_L, the phase plane trajectories can start anywhere on the line $z = w_y = \alpha w$. The starting point is determined by the finite width L, for example at $(w_2, z_2 = \alpha w_2)$, which provides a constraint on the contour. The trajectory ends on the line $z = w_y = -\beta w$, at the point $(w_3, z_3 = -\beta w_3)$.

The finite width constraint can be expressed through the requirement that the contour containing the trajectory must correspond to a value of H that satisfies the following constraint. Firstly, recall that $w_y = z$ from (3.11) and using (3.12), we have

$$w_y = z = (2H(w_2, \alpha w_2) + 2w^3/3 - w^2)^{1/2}.$$

Then, the requirement is

$$\begin{aligned} L &= \int_0^L dy = \int_\gamma \frac{dy}{dw} dw \\ &= \int_\gamma \frac{1}{w_y} dw \\ &= \int_\gamma \frac{1}{(2H(w_2, \alpha w_2) + 2w^3/3 - w^2)^{1/2}} dw \end{aligned} \tag{3.15}$$

which follows from the Hamiltonian (3.12), starting from the initial condition (w_2, z_2) and setting $H = H(w_2, z_2)$ which is determined by the initial condition, and integrating along the trajectory γ starting at the point (w_2, z_2) and ending at (w_3, z_3). For a specified finite value of L, the constraint (3.15) selects a trajectory in the phase plane that satisfies both this constraint and the required boundary conditions, showing that a unique, positive solution exists for any positive L.

3.2.2 Stability

To determine the stability of the population solutions behind the front, we return to the full dynamics. Behind the front, as the population front has already passed, there is no longer any variation in the x direction. Hence, we aim to analyse the 1D FKPP equation given by

$$u_t = u_{yy} + u(1 - u), \tag{3.16}$$

with boundary condition

$$u_y = \alpha u \quad \text{when } y = 0.$$

We note that $u = 0$ everywhere is a solution to these equations as the population can die out for large reaction rates α, β. We are interested in determining when the solution $u = 0$ is stable and unstable. As we are considering small population sizes around $u = 0$, we can linearise (3.16) to get

$$u_t = u_{yy} + u.$$

We begin with the ansatz $u(y,t) = e^{\sigma t}v(y)$. We choose this ansatz because we want to determine when the solution grows or decays in time, without any information about the dependence on the spatial y direction. Substituting this ansatz into the linear FKPP equation gives

$$v''(y) = (\sigma - 1)v(y),$$

with boundary condition

$$v_y = \alpha v \quad \text{when } y = 0.$$

Define $q = \sqrt{1-\sigma}$ to simplify notation. Solutions for v have the form

$$v(y) = A\cos(qy) + B\sin(qy),$$

and substituting the boundary condition gives

$$v(y) = A\left(\cos(qy) + \frac{\alpha}{q}\sin(qy)\right), \tag{3.17}$$

for some constant A. In C_L, applying the mixed boundary condition $v_y = -\beta v$ on $y = L$ to (3.17) gives

$$\tan(qL) = \frac{\alpha+\beta}{q - \frac{\alpha\beta}{q}}.$$

We want to know when the solution changes from growing in time to decaying in time. This occurs at $\sigma = 0$, which gives $q = 1$ and so

$$\tan(L) = \frac{\alpha+\beta}{1-\alpha\beta}.$$

This gives us a condition behind the front when the zero steady state transitions between stable and unstable. When $\alpha > (\tan(L) - \beta)/(1 + \beta\tan(L)$, the zero state is stable and the population solution decays to zero. Otherwise, the zero state is unstable and the population grows away from the zero state. Using the Poincare-Bendixson Theorem [77], we know that in the absence of any limit cycles, the population must tend to the positive steady state.

This condition is shown in Figure 3-6. In addition, when $L > \pi + \tan^{-1}(-1/\beta)$,

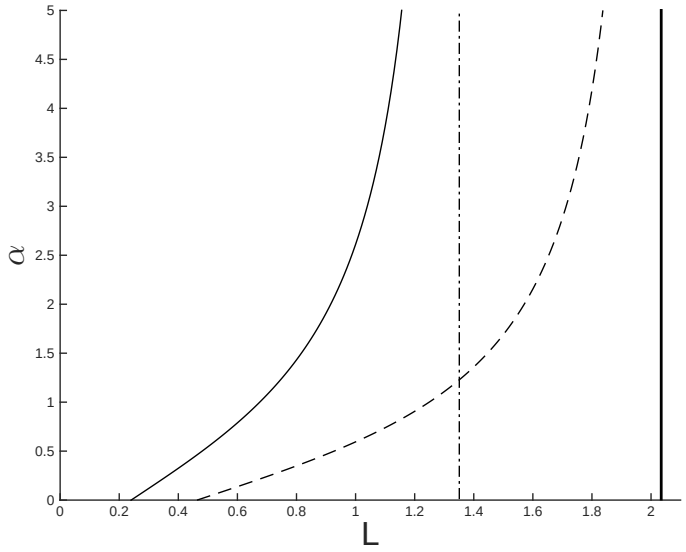

Figure 3-6: The conditions for the population having a zero invasion speed determined by the dynamics ahead of the front, given by $\alpha = (2\tan(\sqrt{2}L) - \sqrt{2}\beta)/(\sqrt{2}+\beta\tan(\sqrt{2}L))$ in the solid line, and for the population having a nonzero stable steady state behind the front, given by $\alpha = (\tan(L) - \beta)/(\beta\tan(L)+1)$ in the dashed dotted line, as functions of reaction rate α and corridor width L when there is a mixed boundary at $y = L$. The dashed line shows the critical corridor width $L^m_{\infty,\beta} = (\pi + \tan^{-1}(-\sqrt{2}/\beta))/\sqrt{2}$ such that, for $L > L^m_{\infty,\beta}$, the population will always have a positive invasion speed according to the dynamics ahead of the front. We also see that, when $L > \pi + \tan^{-1}(-1/\beta)$, shown in the thick solid line, the population will always have a stable nonzero steady state regardless of the value of α. $\beta = 1/2$.

the population will always have a stable nonzero steady state behind the front, for any value of α. When $\beta = 0$, this condition is $\tan(L) = \alpha$ for a reflective boundary and when $\beta \to \infty$, this condition is $\tan(L) = -\frac{1}{\alpha}$ for an absorbing boundary.

As we can see from these figures, as α increases from zero, the non-zero steady state behind the front becomes unstable before the population invasion speed determined ahead of the front can reach zero. This suggests that the population invasion collapses before it reaches zero invasion speed predicted by the theory ahead of the front. In addition, as the FKPP equation is a pulled front, the invasion speed is determined by the dynamics ahead of the front. We now see that this is not the case for the 2D FKPP with hostile boundaries as the invasion speed is significantly determined by the dynamics behind the front.

3.3 Simulations

We have analysed the 2D FKPP equation both ahead of and behind the population front and found conditions for when the population is predicted to collapse and when the population is predicted to have speed zero. To explore the applicability of these conditions, we simulate both individual based models and population based models. The individual based models are stochastic as they include significant randomness in the birth, death, movement, and absorption processes. The population based models of the 2D FKPP equation are deterministic and provide the large population limit of the individual based, stochastic simulations. In this Section, we simulate stochastic models ahead of and behind the front and we simulate a deterministic model of the 2D FKPP equation.

3.3.1 Stochastic Models

Consider the domain $R_L = \{(x, y) : 0 \leq x \leq 1, 0 \leq y \leq L\}$, a rectangle with length 1 in the x direction and length L in the y direction. We divide this rectangle into a 20 by 20 grid. Let $N_{i,j}(t)$ by the number of individuals in the (i, j) square at time t. Each square has carrying capacity K. Individuals at location (i, j) in the domain are born with rate r and die with rate $rN_{i,j}(t)/K$. When a patch is at carrying capacity, the birth and death rates are equal. Individuals

(a)

(b)

(c)

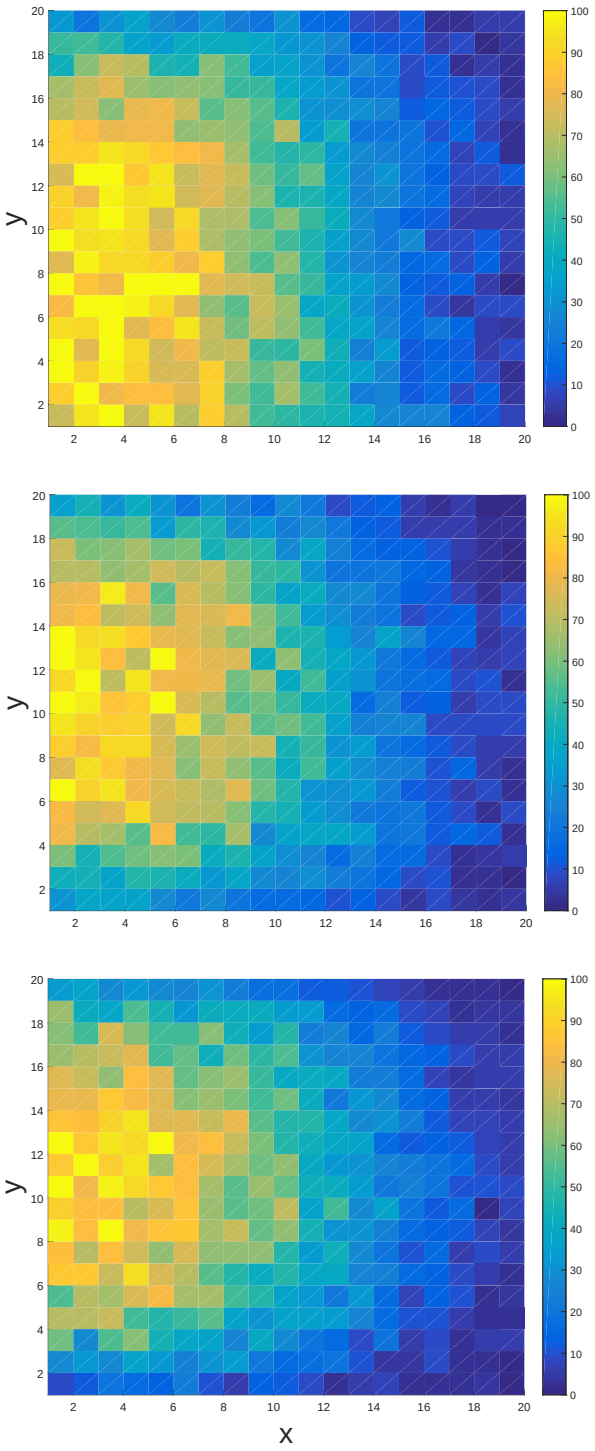

Figure 3-7: The stochastic simulations of the absorbing boundary at $y = L$ ahead of the front. We set $r = D = L = 1, K = 100$ and increment each run for 100 time steps. The colour bar shows the number of individuals in each square. (a) $\alpha = 0$, (b) $\alpha = 0.5$, (c) $\alpha = 1$.

move to neighbouring squares with rate D. In the y direction, we impose the discrete space equivalent of the mixed boundary condition (3.2) at $y = 0$. This is done by taking an individual that jumps to position $(i, -1)$ and removing it from the system with probability αh, where $h = L/20$, the length of a square in the y direction, and otherwise placing it at the position $(i, 1)$, which follows the method of [76]. The initial condition for the stochastic simulations ahead of the front is the left half of R_L set to carrying capacity and everywhere else empty. In the x direction, we impose reflective boundary conditions. This is to simulate the population invading through the domain from left to right.

We now consider the different cases for the boundary at $y = L$. When there is an absorbing boundary at $y = L$, we remove all individuals that jump to position $(i, 21)$. As we increase the reaction rate α, the population front creates a corridor within R_L away from the boundaries. These effects are shown in Figure 3-7. When there is a reflective boundary at $y = L$, we place all individuals that jump to position $(i, 21)$ in position $(i, 19)$. The stochastic invasion reaches carrying capacity along the line $y = L$ in the simulations. These effects are shown in Figure 3-8. When there is a mixed boundary also at $y = L$, we see the effects of the hostile boundaries on both boundaries. These effects are shown in Figure 3-9. The mixed boundary is introduced by taking an individual that jumps to position $(i, 21)$ and removing it from the system with probability βh where $h = L/20$ and otherwise placing it at the position $(i, 19)$. In these figures, we see the various ways the population invasion can develop as a function of the reaction rate α.

Behind the front, we impose periodic boundary conditions in the x direction to simulate the fact that we are behind the front so there is no dependence on the x location. The initial condition for this model is the whole domain R_L set to carrying capacity. This is to simulate the population invasion front already passing and now we are at a steady state behind the front.

The results behind the front vary depending on the boundary condition at $y = L$. For an absorbing boundary, we see the population behind the front creates a corridor as α increases. This is shown in Figure 3-10. Similar results for a reflective and mixed boundary are shown in Figures 3-11 and 3-12 respectively.

(a)

(b)

(c)

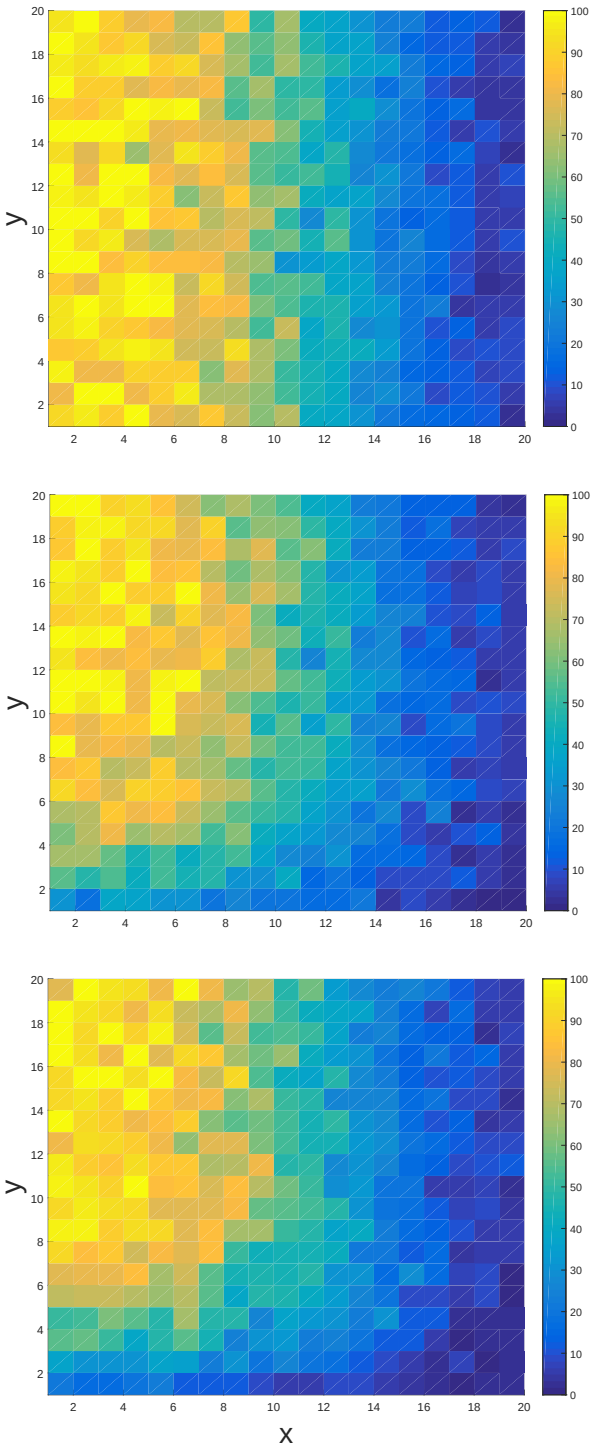

Figure 3-8: The stochastic simulations of the reflective boundary at $y = L$ ahead of the front. We set $r = D = L = 1, K = 100$ and increment each run for 100 time steps. The colour bar shows the number of individuals in each square.(a) $\alpha = 0$, (b) $\alpha = 0.5$, (c) $\alpha = 1$.

(a)

(b)

(c)

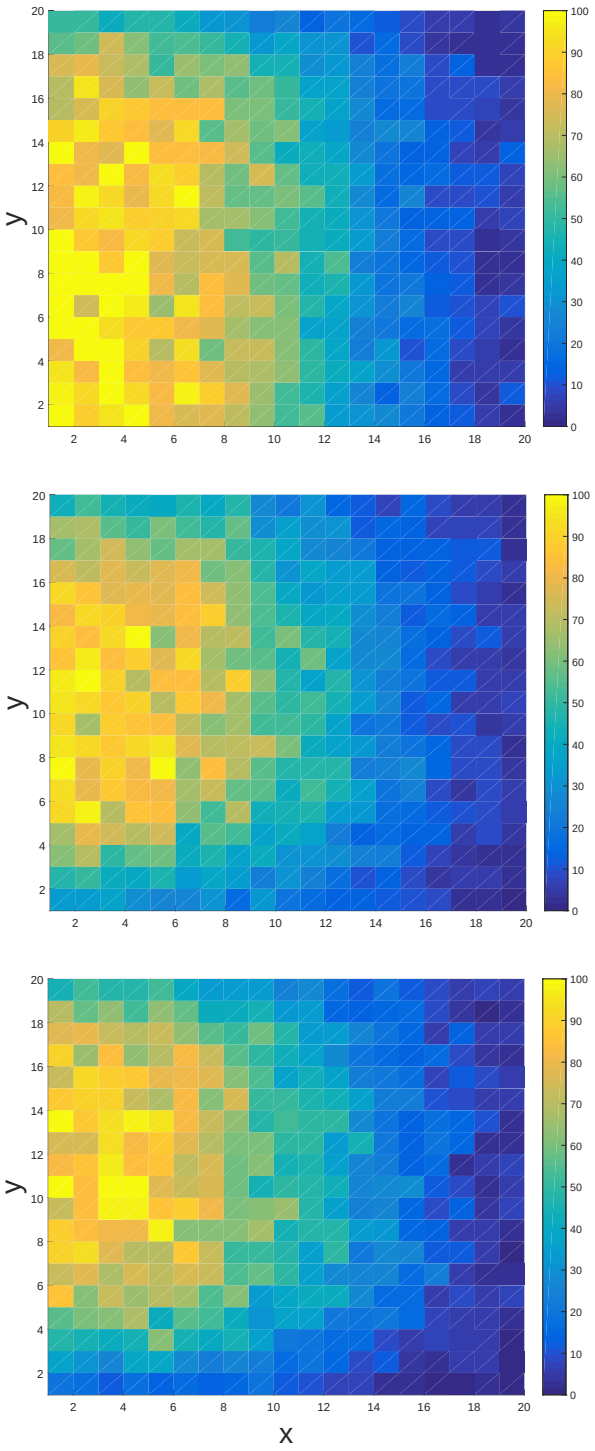

Figure 3-9: The stochastic simulations of the mixed boundary at $y = L$ ahead of the front. We set $\beta = 10, r = D = L = 1, K = 100$ and increment each run for 100 time steps. The colour bar shows the number of individuals in each square. (a) $\alpha = 0$, (b) $\alpha = 0.5$, (c) $\alpha = 1$.

(a)

(b)

(c)

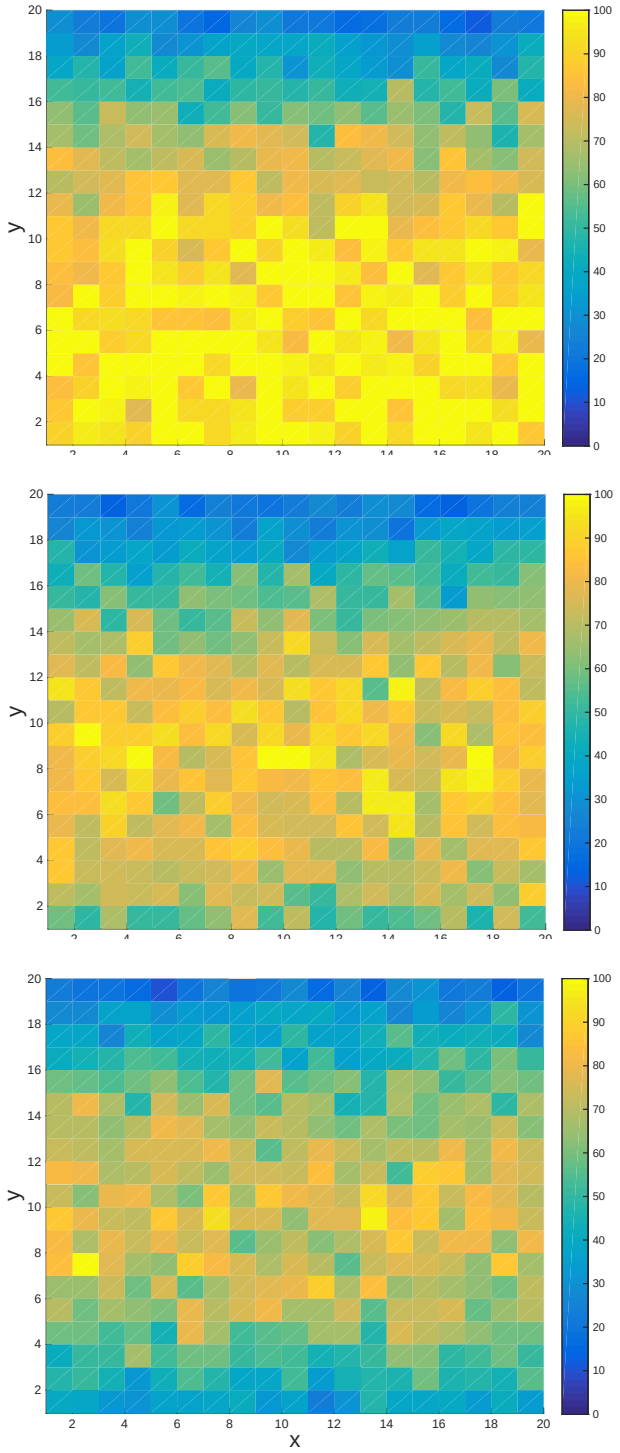

Figure 3-10: The stochastic simulations of the absorbing boundary at $y = L$ behind the front. We set $r = D = L = 1, K = 100$ and increment each run for 300 time steps. The colour bar shows the number of individuals in each square.(a) $\alpha = 0$, (b) $\alpha = 0.1$, (c) $\alpha = 0.25$.

(a)

(b)

(c)

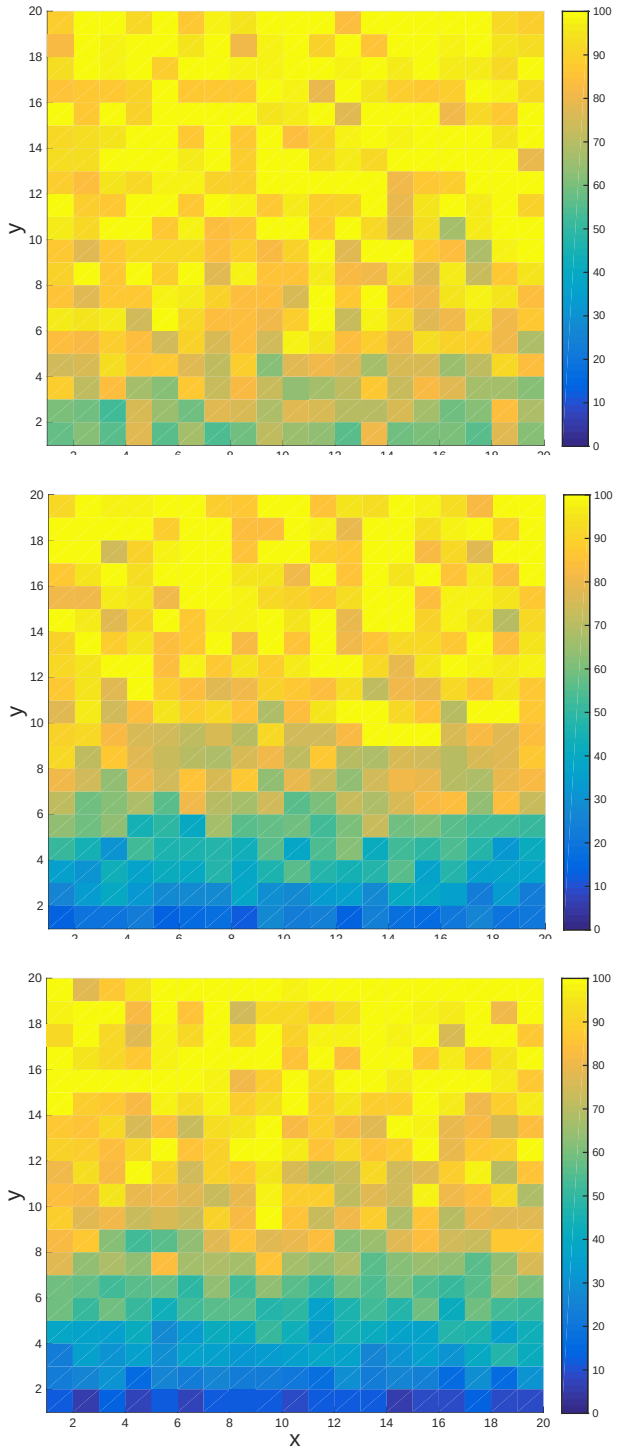

Figure 3-11: The stochastic simulations of the reflective boundary at $y = L$ behind the front. We set $r = D = L = 1, K = 100$ and increment each run for 300 time steps. The colour bar shows the number of individuals in each square.(a) $\alpha = 0.1$, (b) $\alpha = 0.5$, (c) $\alpha = 1$.

(a)

(b)

(c)

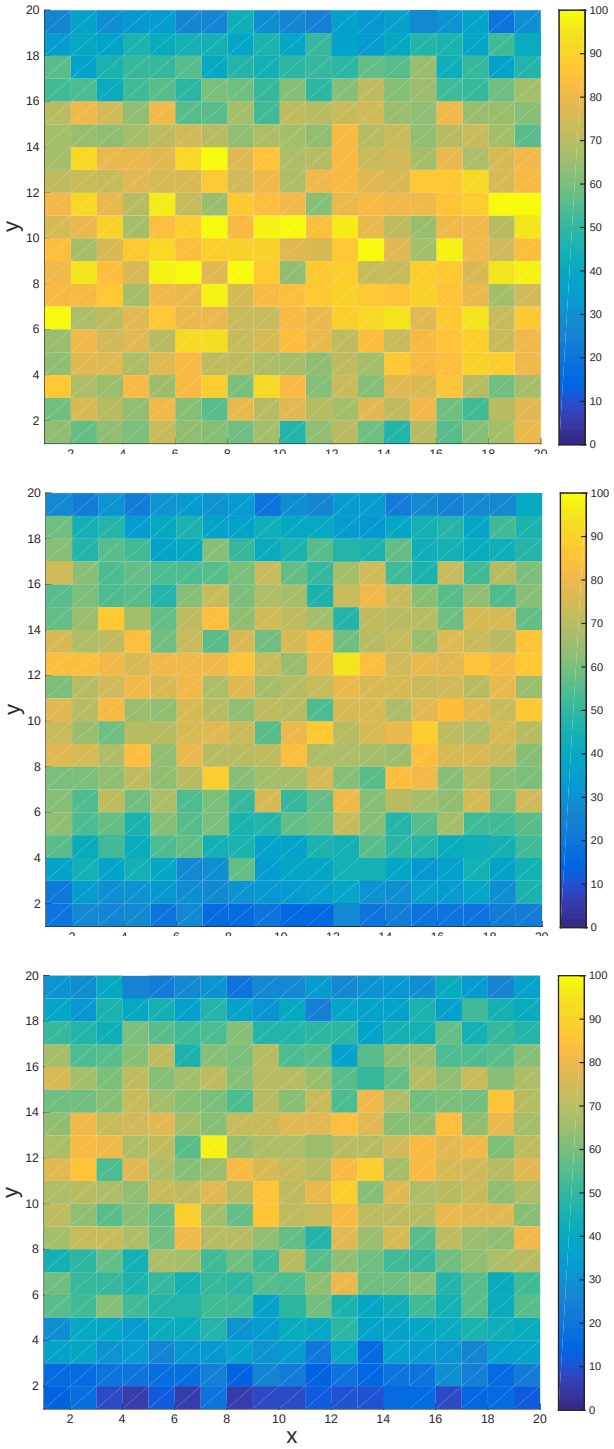

Figure 3-12: The stochastic simulations of the mixed boundary at $y = L$ behind the front. We set $r = D = L = 1, K = 100$ and increment each run for 300 time steps. The colour bar shows the number of individuals in each square.(a) $\alpha = 0.1$, (b) $\alpha = 0.5$, (c) $\alpha = 1$.

3.3.2 Deterministic Model

The conditions for collapse and reaching speed zero have been predicted from analysing the 2D FKPP equation. Here we confirm these results by simulating the population invasion and measuring the invasion speed for different parameter values. We use the two step Adams-Bashforth method [78] to model the 2D FKPP equation and we calculate the invasion speed by tracking the location of level sets as the population progresses through the environment.

The results for various reaction rates α and corridor widths $L = 0.5, 1.5, 2.5$ with a reflective boundary at $y = L$ are shown in Figures 3-13, 3-14, and 3-15 respectively. In Figure 3-13, we see that the invasion speed we measure dips sharply away from the speeds predicted by the theory ahead of the front. The speeds quickly decay reaching zero at the black square, which is at the location of predicted parameter values for collapse behind the front. We see that even for α values before collapse, there is a significant difference between the theory and observed results. We are happy with this divergence between the theory and observed results because we predicted the critical corridor width in Section 3.1.1. This figure confirms our prediction that the population collapses with this corridor width at the black square. In both Figures 3-14 and 3-15, the observed results agree with the predicted theory, despite both displaying speeds that are slower than the theory predicts.

3.4 Conclusion

In this Chapter, we have explored the 2D FKPP equation $u_t = u_{xx} + u_{yy} + u(1-u)$ on a corridor with finite width C_L with the mixed boundary conditions $u_y = \alpha u$ on $y = 0$ and $u_y = -\beta u$ on $y = L$ and on a corridor with infinite width C_∞ with only the $y = 0$ mixed boundary for reaction rates α, β. Ahead of the front on C_L, we found an equation relating the reaction rates, the width of the corridor, and the speed of the population. From this equation, we can determine when we expect the population to have speed zero for given values of α, β, L. For C_∞, the second boundary condition came from the requirement that the population is unaffected by the boundary very far away. This allowed us to derive an explicit equation for the population ahead of the front. From this, it

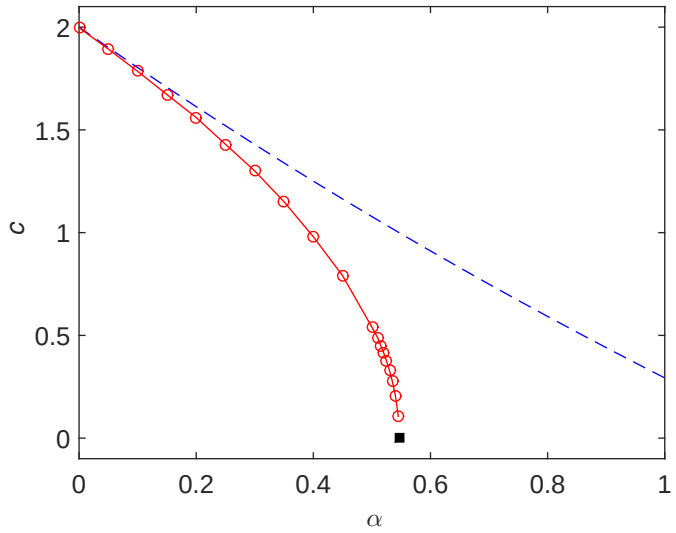

Figure 3-13: A comparison between the simulations of the 2D FKPP equation (red solid line) and predicted, low density theory ahead of the front (blue dashed line) for the population invasion speed. We vary the reaction rate α for the boundary at $y = 0$. There is a reflective boundary at $y = L$. $L = 0.5$

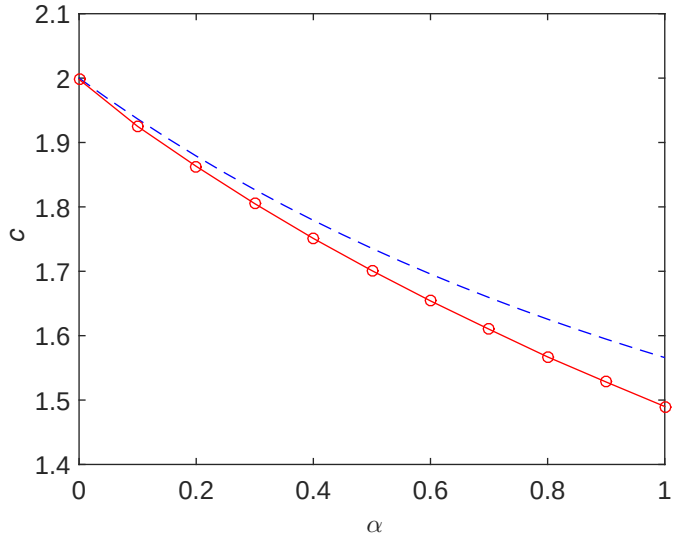

Figure 3-14: A comparison between the simulations of the 2D FKPP equation (red solid line) and predicted, low density theory ahead of the front (blue dashed line) for the population invasion speed. We vary the reaction rate α for the boundary at $y = 0$. There is a reflective boundary at $y = L$. $L = 1.5$

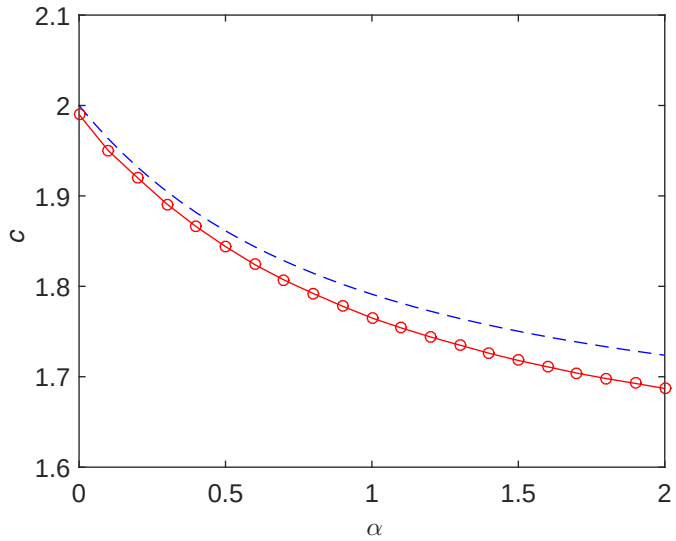

Figure 3-15: A comparison between the simulations of the 2D FKPP equation (red solid line) and predicted, low density theory ahead of the front (blue dashed line) for the population invasion speed. We vary the reaction rate α for the boundary at $y = 0$. There is a reflective boundary at $y = L$. $L = 2.5$

can be shown that the level sets ahead of the front meet the $y = 0$ boundary with constant gradient, independent of the level set chosen. The next Section of this Chapter analysed the survival and stability of the population behind the front. Using a phase plane argument, we showed that a positive solution exists for any positive L. For the stability, we again found an equation relating the reaction rates and the corridor width for when the zero steady state becomes unstable. Comparing this equation with the equation for when the population ahead of the front reaches speed zero showed that, as the reaction rates increase, the population behind the front becomes unstable before the population ahead of the front reaches speed zero. This was confirmed by deterministic simulations.

Returning to the work by Möbius et. al. [36], we see that our results agree. They found that as the T7 invades past the T7-resistant region of E. coli, a kink is formed in the population invading front. We found this same kink occurring in the invading front in C_∞, shown in Figure 3-4. Our research here explores new areas of this population invasion as well. For example, if we were to run an experiment with a T7 invasion on a corridor of width L with two T7-resistant regions on either side, our results predict when this invasion will have speed

zero. It is not when the population ahead of the front achieves speed zero but when the population zero state behind the front becomes stable. This point is determined by the reaction rates on either boundary and the width of the corridor. As our work looks at mixed boundaries with varying reaction rates, it is biologically significant as it can be applied to situations where the effectiveness of the boundary is not constant, such as drug treatment.

Chapter 4

Invasions and Intraspecies Conflict

Interactions between populations can have either positive, negative, or neutral benefits for the populations involved. Positive interactions include mutualism, when both individuals benefit mutually, and commensalism, when one individual benefits and the other neither benefits or is harmed. Examples of these positive interactions include marine communities buffering one another in physically stressful habitats [79], plants adjusting their environment to make it more suitable for themselves [80], and ants drinking the honeydew produced by homoptera resulting in the homoptera feeding more and producing more honeydew [81].

These positive interactions between populations can have significant effects on the development of the populations involved. These effects include the creation of species-rich communities supported by a single resource [82], the evolution of phenotypes in an opportunistic pathogen for rapid adaptation [83], and even the introduction of stable population equilibrium that would not exist otherwise [84].

One of the possible resulting effects of positive interactions between populations is both populations invading faster together. This has been seen experimentally in microbial parasites [85] and in invasive succulents [86]. Elliott and Cornell theoretically showed that a mutualistic relationship between phenotypes can result in a faster range expansion than if only one phenotype was present in the population, for both deterministic and stochastic models [87, 88].

In this Chapter, we consider whether antagonistic interactions between individuals can also influence the speed of invasion of a population. This question is

important because it means that we must give significant consideration to how we alter biological systems as it may have consequences that are severely detrimental to local conservation efforts. With this in mind, we discuss the particularly invasive Trinidadian guppy *Poecilia Reticulata* which is introduced to control the mosquito population [90, 91]. The reproduction of the guppy, an interaction between individual male and female guppies, has been well studied. The sexual responsiveness of female guppies varies with the colour of the male guppies [92] while sexual harassment from male guppies alters the ways female guppies interact with other females [94, 96, 97]. In order to minimise the amount of sexual harassment they receive, female guppies associate with female guppies that are more sexually attractive than themselves [95]. However, when female guppies are distracted by the possibility of predation, the male guppies try to mate sneakily [93], and this again changes the dynamics of social groups [98]. Their reproduction can be considered sexual coercion or sexual conflict, which is not mutualistic [99], because the female guppies are highly selective in their choice of mate and they are willing to reproduce for very short periods of time while the male guppies experience significant competition from other male guppies so they choose to harass female guppies as much as possible. This, in turn, leads to significant evolutionary consequences in the species [100].

The aim of this Chapter is to determine if sexual conflict between male and female guppies might result in a faster speed for the invading population. When the guppies are introduced into new rivers and streams, even in very small numbers, they are very successful at reproducing and establishing a population [89]. These dynamics of a population density $u(x,t)$ at location x and time t growing from an unstable state $u = 0$ to a stable state $u = 1$ can be effectively modelled by the 1D FKPP equation, which is appropriate here as we model the relatively narrow streams and rivers the guppies live in. It is also appropriate to consider the 1D FKPP equation as a starting point as we determine whether this link between sexual conflict and invasion speed exists. With guppy diffusion coefficient D and growth rate r, the FKPP equation is given by

$$u_t = Du_{xx} + ru(1-u).$$

In (2.38), we calculated the invasion speed $v = 2\sqrt{rD}$, which is determined by

the low-density, linearised region of the population ahead of the front. However, sexual conflict is a nonlinear, second order interaction as it requires two individuals to interact with each other. The calculation of these second order terms is given in Appendix B. Hence, the linearised calculation of the population invasion speed v is unaffected by the nonlinear sexual conflict in the population.

In the rest of this Chapter, we show that sexual conflict between guppies changes the effective diffusion coefficient of the population, which in turn changes the invasion speed. The individual interaction between guppies induces a diffusion coefficient that can be orders of magnitude larger than that of a population without sexual conflict. In Section 4.1, we introduce a framework for the movement of one fish and how this movement can be used to calculate the diffusion coefficient of the fish. This framework is then extended to two fish in Section 4.2 with the addition of sexual conflict. We show how this pairwise interaction can influence the diffusion coefficient of the pair. Finally, in Section 4.3, we explore these results as they apply to a population of many male and female fish.

4.1 One Fish

The movement of fish has been studied mathematically in great detail. This research includes individual-based models and advection-diffusion equations [101], simulations of a spatially heterogeneous environment due to a habitat index [102], an advection-diffusion-reaction model structured by size [103], a spatial model for the effect of climate on recruitment of tuna [104], and a habitat-based advection-diffusion-reaction model used to design tag-recapture experiments [105].

In this Section, we introduce a highly simplified model of motion for an individual fish in order to calculate the diffusion coefficient. This motion takes the form of 'run and tumble' dynamics, which has been mathematically analysed in [106] and is usually applied to bacterial motion [107, 108, 109]. It can be applied here to fish as their observed movement also contains short runs followed by pauses and a run in a possibly different direction. Using the mean square displacement of the fish over long times, we calculate the diffusion coefficient of the fish from these 'run and tumble' dynamics. Finally, with the diffusion coefficient, we state a stochastic differential equation for the location of the fish over long times.

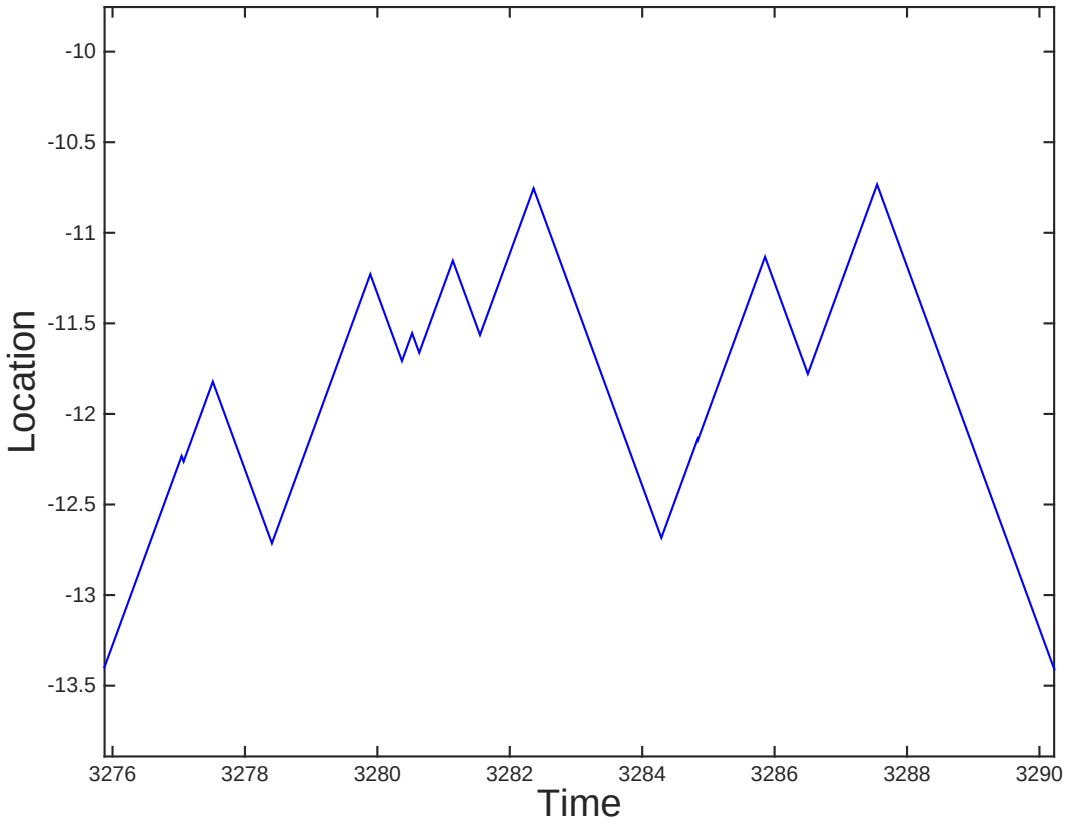

Figure 4-1: The 'run and tumble' movements of a single fish with constant speed $v = 1$ and mean time for a tumble $T = 1$.

Consider a point particle moving in a homogeneous 1D environment. We model the fish as point particles because we are only interested in the location of the fish and because they are small compared to the size of their environment. Assume the fish swims with constant speed v in the same direction for an exponentially distributed amount of time with mean T (a run). This run is exponentially distributed for its memorylessness property. We make a simplifying assumption here that the previous location of the fish does not influence future movement although this may not be true in practice. Then the fish forgets the direction it is swimming in and chooses a new direction, left or right, uniformly at random (a tumble). These are the 'run and tumble' dynamics, which are shown in Figure 4-1.

In order to calculate the macro diffusion coefficient corresponding to this movement, we use the mean square displacement of the fish. At time t, let the fish have location $X(t)$ with $X(0) = 0$. The mean square displacement is then

defined by $Q(t) = \mathbb{E}[X(t)^2]$. To analyse $Q(t)$ and derive the diffusion coefficient, we begin by conditioning on the first tumble event giving

$$\begin{aligned} Q(t) = &\mathbb{P}[\text{no tumble in } [0,t]]\mathbb{E}[X(t)^2|\text{no tumble in } [0,t]] \\ &+ \mathbb{P}[\text{tumble in } [0,t]]\mathbb{E}[X(t)^2|\text{tumble in } [0,t]], \end{aligned}$$

and using standard properties of exponential distributions gives

$$Q(t) = e^{-t/T}Q_0(t) + \int_0^t \frac{1}{T} e^{-\tau/T} Q_1(t|\tau)\, d\tau\,, \tag{4.1}$$

where $Q_0(t) = (vt)^2$ is the mean square displacement in the case that there are no tumble events (therefore simply the square of the displacement with constant speed v), and $Q_1(t|\tau)$ is the mean square displacement at time t given that the first tumble event was at time τ. Since this is the first tumble and the displacement after the tumble is independent of any previous movement, again from the memoryless property of the movement, we have the relationship $Q_1(t|\tau) = Q_0(\tau) + Q(t-\tau)$. Substituting this relationship into (4.1) gives

$$Q(t) = e^{-t/T}Q_0(t) + \int_0^t \frac{1}{T} e^{-\tau/T} \Big(Q_0(\tau) + Q(t-\tau) \Big)\, d\tau\,.$$

The second term of the integral contains a convolution in τ. We can solve this equation for $Q(t)$ using Laplace transforms, as convolutions in real space become products. Define $\mathcal{Q}(s) = \int_0^\infty e^{-st} Q(t)\, dt$ to be the Laplace transform of $Q(t)$. Then, taking the Laplace transform of the above equation gives

$$\mathcal{Q}(s) = \frac{2}{s}\left(\frac{v}{s+1/T}\right)^2 + \frac{1}{Ts+1}\mathcal{Q}(s) \;\Rightarrow\; \mathcal{Q}(s) = \frac{2v^2}{s^2(s+1/T)}\,,$$

and inverting the transform yields

$$Q(t) = 2v^2T\left(t - T + Te^{-t/T}\right). \tag{4.2}$$

This is the equation for the mean square displacement of a fish moving according to 'run and tumble' dynamics, swimming with constant speed v for an exponentially distributed amount of time with mean T.

We can now use this equation for the mean square displacement to determine

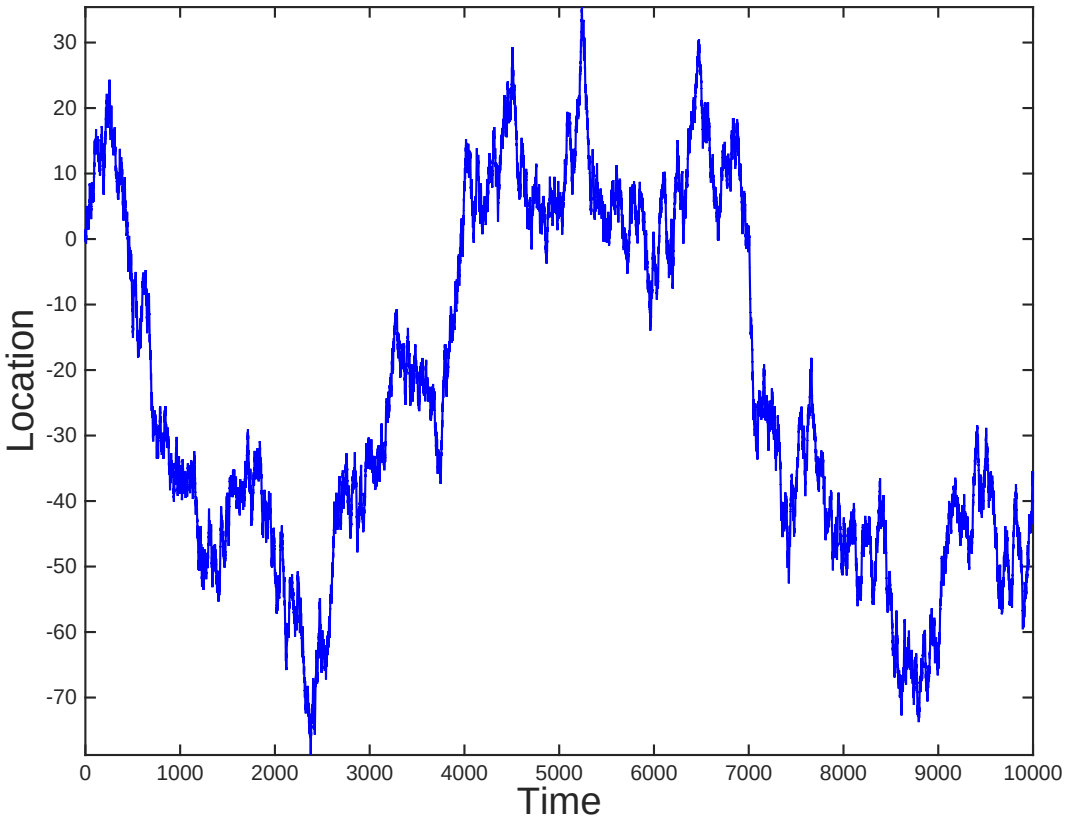

Figure 4-2: The large time diffusive movement of a single fish with constant speed $v = 1$ and mean time for a tumble $T = 1$.

the diffusion coefficient for the fish. For large times t, we note that

$$\lim_{t\to\infty} \frac{Q(t)}{t} = 2v^2T,$$

so the mean square displacement grows linearly in time. This is characteristic of a diffusion process [110, 111]. Hence, for large times t, the movement of the fish is diffusive and the diffusion coefficient is given by $D = v^2T$, half the coefficient of the large time approximation for $Q(t)$. This large time diffusive movement is shown in Figure 4-2.

We have now derived the diffusion coefficient for the movement of an individual fish. This diffusion coefficient can also be used to derive a stochastic differential equation for the location of the fish over long time periods. This is useful as it provides a description of the movement of the fish using the diffusion coefficient D over long time periods without explicitly needing the short time

parameters v and T. Let $p(x,t)$ be the probability that the fish is at location x at time t. Then, for large time t and for diffusion coefficient D, $p(x,t)$ satisfies the forward Fokker-Planck equation in the technical introduction in Section 2.1.2 given by

$$\frac{\partial p}{\partial t} = D\frac{\partial^2 p}{\partial x^2},$$

where $a(x,t) = 0$ and $b(x,t) = \sqrt{2D}$, as there is only diffusion and no drift in the movement of the fish. According to Itô's formula in the technical introduction 2.1.2, the stochastic differential equation for the location of the fish is given by

$$\frac{dX}{dt} = \sqrt{2D}\eta_X(t)\,, \tag{4.3}$$

where $\eta_X(t)$ is Gaussian white noise with mean zero and unit variance.

This stochastic differential equation provides the framework for the movement of one fish with diffusion coefficient $D = v^2T$. Considering a second fish will now allow us to introduce sexual conflict and determine the effect it has on the diffusion coefficient of the two fish as a pair.

4.2 Two Fish

In this Section, we extend the movement framework for one fish to include two fish, one male and one female, with the goal of introducing sexual conflict between the fish and determining whether this conflict can affect the diffusion coefficient of the pair of fish. This effect is not unique to sexual conflict. It will manifest for any collective motion arising from a coupled interaction. For two fish, we assume that, in the absence of interaction, the two fish will move according to the large time stochastic differential equation (4.3) calculated for one fish. In addition to this, we add response functions that represent the sexual conflict between the two fish. In particular, a conflict that results in the male tending to swim towards the female and the female tending to swim away from the male. These tendencies are well supported by empirical studies [97, 112]. Once the sexual conflict is introduced, we note that the movement of the pair of fish is very similar to the 'run and tumble' movement of the individual fish. This similarity will allow us to calculate the diffusion coefficient of the pair by

using the same large time diffusive movement argument and hence determine how sexual conflict influences the diffusion coefficient for a pair of fish.

Consider a male and female fish swimming in a homogeneous 1D environment with locations $X(t)$ and $Y(t)$ respectively at time t. In the absence of interaction we assume the fish move according to the stochastic differential equation (4.3) with individual diffusion coefficient D. We assume that the two fish have the same diffusion coefficient for mathematical simplicity here. As the female fish is usually larger than the male fish, it is very possible that the diffusion rates are different. This is an assumption that we can relax with the support of biological data. In addition, we add response functions v_X, v_Y due to the sexual conflict between the fish. We assume these response functions are only dependent on the locations of the two fish. The dynamics are given by

$$\begin{aligned} \frac{dX}{dt} =& v_X(X,Y) + \sqrt{2D}\eta_X(t)\,, \\ \frac{dY}{dt} =& v_Y(X,Y) + \sqrt{2D}\eta_Y(t)\,, \end{aligned} \tag{4.4}$$

where $\eta_X\,, \eta_Y$ are independent Gaussian white noise terms with mean zero and unit variance, as defined in the technical introduction in Section 2.1.1.

In order to further analyse these SDEs, we need to make assumptions about v_X, v_Y so that they accurately reflect the sexual conflict dynamics between the male and female fish.

- The first assumption is that v_X, v_Y are only functions of the separation $s = Y - X$ of the fish and we write $v_X(s), v_Y(s)$. We make this assumption because we are in a homogeneous 1D environment so the location of either fish is not important. It is the separation between the fish that influences their behaviour. We know that sexual conflict says that the male fish tends to swim towards the female fish and the female fish tends to swim away from the male fish.

- This gives the second assumption on $v_X(s), v_Y(s)$. When the location of the female is to the right of the location of the male, so $s > 0$, both fish tend to swim in the positive direction, so $v_X(s), v_Y(s) > 0$. Similarly, when $s < 0$, $v_X(s), v_Y(s) < 0$. When the fish are at the same location, so $s = 0$, the male fish does not want to move at all while the female fish wants to

move significantly, so $v_X(0) = 0$ and $v_Y(0) > 0$. This assumption can be written concisely as

$$\begin{cases} v_X(s) < 0 & \text{if } s < 0 \\ v_X(s) = 0 & \text{if } s = 0 \\ v_X(s) > 0 & \text{if } s > 0. \end{cases} \quad \text{and} \quad \begin{cases} v_Y(s) < 0 & \text{if } s < 0 \\ v_Y(s) > 0 & \text{if } s \geq 0. \end{cases}$$

- The third assumption is that the male fish swims faster when the female fish is farther away, so $v_X(s)$ increases as $|s|$ increases, and the female fish swims faster when the male fish is closer, so $v_Y(s)$ decreases as $|s|$ increases.
- The final assumption is that the swim speed of the fish should not increase past some maximum speed $v_{\max}$. This ensures that the swim speeds remain biologically realistic.

With these assumptions in mind, the functions we choose for $v_X(s), v_Y(s)$ in (4.4) are given by

$$v_X(s) = \begin{cases} \max\{As, -1\} & \text{if } s < 0 \\ \min\{As, 1\} & \text{if } s \geq 0 \end{cases} \qquad v_Y(s) = \begin{cases} \min\{-1 - s, 0\} & \text{if } s < 0 \\ \max\{1 - s, 0\} & \text{if } s \geq 0 \end{cases} \tag{4.5}$$

where $v_{\max} = 1$ and A is a positive constant that represents the measure of the sexual aggression of the male fish. When A is large, the male fish responds more quickly to the female. When male guppies are raised in environments with a large or small proportion of female guppies, this affects the level of sexual aggression they show other females as they grow older [113].

Before simulating the SDEs in (4.4) using the response functions in (4.5), we note that $v_X(s), v_Y(s)$ have points of intersection where $v_X(s) = v_Y(s)$. At these points, the separation and speed of the fish will remain constant in the absence of noise. We define the mean separation s^* and mean speed v^* of the guppies as the values such that $|v_X(s^*)| = |v_Y(s^*)| =: v^*$. For the response functions in (4.5), we find

$$s^* = \frac{1}{A+1}, \quad v^* = \frac{A}{A+1}, \tag{4.6}$$

so that, as the sexual aggression A increases, the mean separation s^* approaches

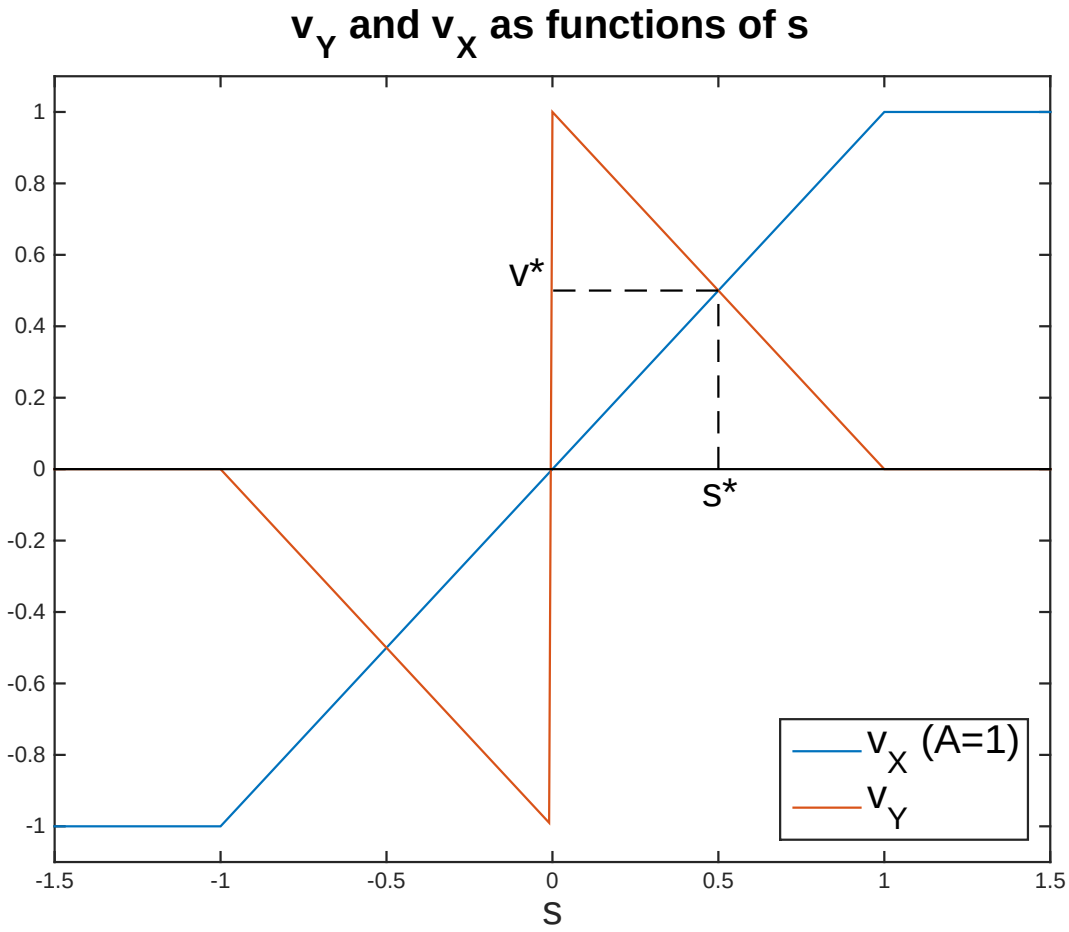

Figure 4-3: The response functions $v_X(s)$ and $v_Y(s)$ as functions of s. s^* is the mean separation and v^* is the mean swim speed of the two fish. $v_X(s)$ is plotted for $A = 1$.

zero and the mean speed v^* approaches $v_{\max} = 1$. This agrees with our concept of A being the sexual aggression of the male fish. These functions are shown in Figure 4-3.

Now we can simulate the SDEs in (4.4) using the response functions in (4.5). We do this using standard Euler-Maruyama time stepping [60]. The results from the simulations are shown in Figure 4-4. In (a), we see the male fish (in blue) and the female fish (in red) swimming on a short time scale. The fish have roughly the same speed with the female in front of the male. Occasionally the stochastic element of the dynamics results in the male fish swimming past the female and the two fish continue the chase in the opposite direction. On a medium timescale in (b), we see the a pattern of coordinated swimming broken by occasional changes

in direction while the movement appears diffusive over much longer timescales in (c).

The movement of the pair of fish is very similar to the 'run and tumble' dynamics of a single fish in Section 4.1. The two fish chasing in a particular direction could be considered 'a run' and a change in direction 'a tumble'. Using the same methods, we can derive a diffusion rate for the pair of fish and compare whether sexual conflict induces a change in the effective diffusion rate of the two fish compared to the diffusion coefficient of the individual fish.

In Section 4.1, we calculated the diffusion coefficient from the 'run and tumble' movement of one fish from the mean speed v and mean time to tumble T. We need to determine the equivalent variables for the pair of fish in order to calculate the effective diffusion coefficient of the pair. We have already stated the mean speed v^* for the pair of fish in (4.6). We now need to derive the mean time T^* for the pair of fish to change directions. This will involve an extensive analysis of (4.4). We begin by rewriting (4.4) in terms of the separation variable $s(t) = Y(t) - X(t)$. We do this because we want to calculate the mean time required for $s(t)$ to move between $s = -s^*$ and $s = s^*$. Then, we will introduce a potential U defined by $U'(s) = v_X(s) - v_Y(s)$. This definition will simplify the notation as we will need to integrate $U'(s)$ and also make it clear that we can use the mean hitting time calculation in Section 2.1.3 in the technical introduction, as we want to know the mean time required for $s(t)$ to hit $s = s^*$ with a reflective boundary at $s = -\infty$, an absorbing boundary at $s = s^*$, and initially starting at $s = -s^*$. This will give us the mean time for the fish to change directions T^*, which we can use with v^* to calculate the effective diffusion coefficient for the pair of fish as a result of sexual conflict.

Now, taking the time derivative and using (4.4) gives the closed expression

$$\frac{ds}{dt} = v_Y(s) - v_X(s) + \sqrt{2D}(\eta_Y(t) - \eta_X(t)) \,.$$

The difference between two Gaussian white noise terms with mean zero and unit variance is a Gaussian white noise term with mean zero and variance two. Hence, we define

$$\eta(t) = \frac{\eta_X(t) + \eta_Y(t)}{\sqrt{2}},$$

(a)

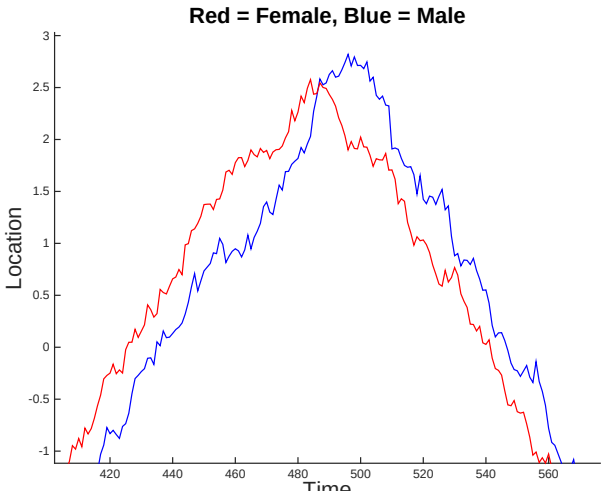

(b)

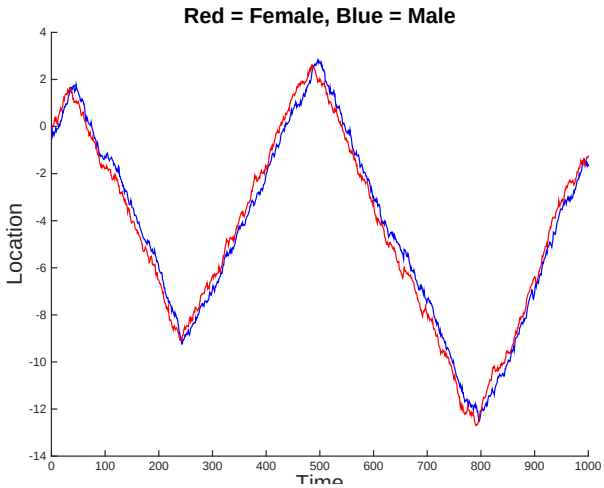

(c)

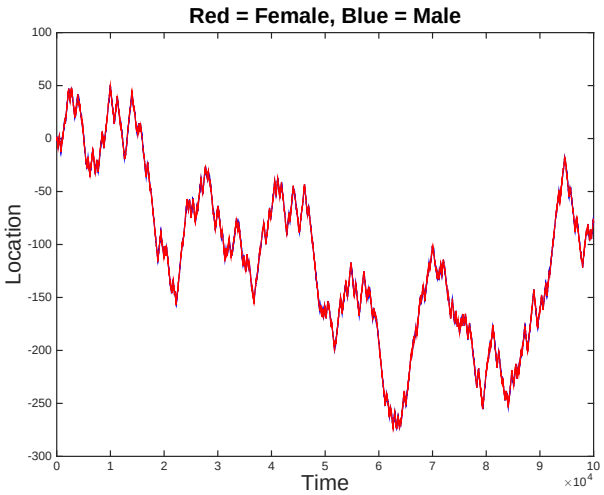

Figure 4-4: (a) Sample trajectories from (4.4) with parameters $D = 0.04$, $A = 1$. The male fish is shown in blue, the female in red. (b) A medium timescale view of the trajectories from (a). (c) A longer timescale view

a Gaussian white noise term with mean zero and unit variance, to get

$$\frac{ds}{dt} = v_Y(s) - v_X(s) + 2\sqrt{D}\eta(t)\,. \tag{4.7}$$

The potential $U(s)$ takes different forms depending on if $A < 1$ or if $A > 1$. Using the definitions in (4.5) and taking $A < 1$ gives

$$U'(s) = \begin{cases} -1 & \text{if } s < -\frac{1}{A} \\ As & \text{if } -\frac{1}{A} \le s < -1 \\ (A+1)s + 1 & \text{if } -1 \le s < 0 \\ (A+1)s - 1 & \text{if } 0 \le s < 1 \\ As & \text{if } 1 \le s < \frac{1}{A} \\ 1 & \text{if } \frac{1}{A} \le s, \end{cases}$$

and integrating gives

$$U(s) = \begin{cases} -s & \text{if } s < -\frac{1}{A} \\ \frac{A}{2}s^2 & \text{if } -\frac{1}{A} \le s < -1 \\ \frac{A+1}{2}s^2 + s & \text{if } -1 \le s < 0 \\ \frac{A+1}{2}s^2 - s & \text{if } 0 \le s < 1 \\ \frac{A}{2}s^2 & \text{if } 1 \le s < \frac{1}{A} \\ s & \text{if } \frac{1}{A} \le s. \end{cases} \tag{4.8}$$

Taking $A > 1$ gives

$$U'(s) = \begin{cases} -1 & \text{if } s < -1 \\ s & \text{if } -1 \le s < -\frac{1}{A} \\ (A+1)s + 1 & \text{if } -\frac{1}{A} \le s < 0 \\ (A+1)s - 1 & \text{if } 0 \le s < \frac{1}{A} \\ s & \text{if } \frac{1}{A} \le s < 1 \\ 1 & \text{if } 1 \le s, \end{cases}$$

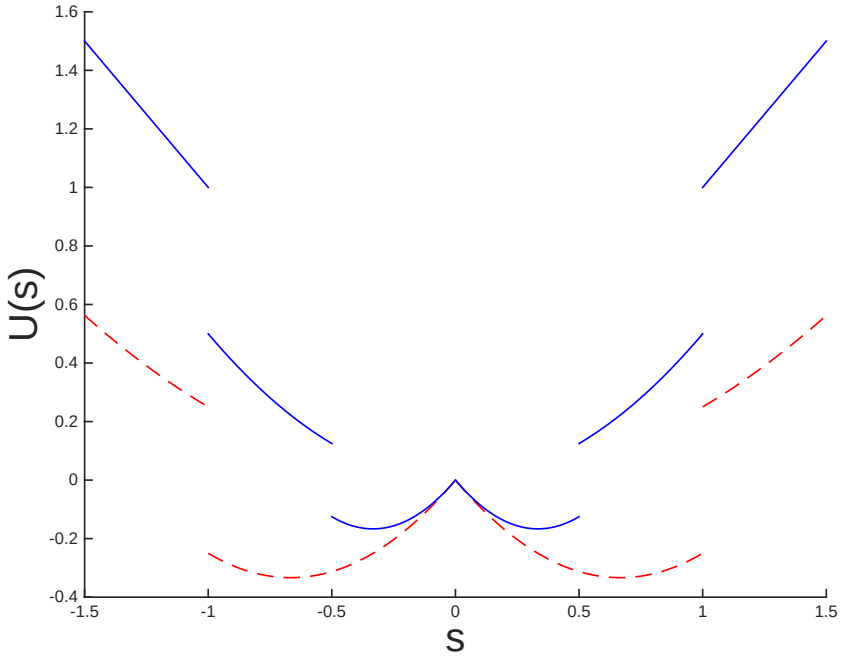

Figure 4-5: The potential $U(s)$ when $A = 0.5$ in red dotted line and $A = 2$ in solid blue line.

and integrating gives

$$U(s) = \begin{cases} -s & \text{if } s < -1 \\ \frac{1}{2}s^2 & \text{if } -1 \le s < -\frac{1}{A} \\ \frac{A+1}{2}s^2 + s & \text{if } -\frac{1}{A} \le s < 0 \\ \frac{A+1}{2}s^2 - s & \text{if } 0 \le s < \frac{1}{A} \\ \frac{1}{2}s^2 & \text{if } \frac{1}{A} \le s < 1 \\ s & \text{if } 1 \le s. \end{cases} \tag{4.9}$$

These two potentials are shown in Figure 4-5.

Using this definition of the potential U, we can rewrite (4.7) as

$$\frac{ds}{dt} = -U'(s) + 2\sqrt{D}\eta(t)\,,$$

so

$$a(x) = -U'(x), \quad b(x) = 2\sqrt{D}, \tag{4.10}$$

in the definition of the mean hitting time calculated in the technical introduction in Section 2.1.3. Here, we want to calculate the mean hitting time for the separation s initially starting at $s = -s^*$ with a reflective boundary at $s = -\infty$ and an absorbing boundary at $s = s^*$. We can simplify this calculation as we know, given the symmetry of the potential $U(x)$, that the mean hitting time of an absorbing boundary at $s = s^*$ is equal to twice the mean hitting time of an absorbing boundary at $s = 0$, hence we will have a coefficient of 4 instead of the coefficient of 2 in (2.14). This mean hitting time is then given by

$$\mathbb{E}[T(-s^*)] = 4 \int_{-s^*}^{0} \frac{1}{\gamma(w)} \int_{-\infty}^{w} \frac{\gamma(z)}{b(z)^2} dz dw,$$

where

$$\gamma(x) = \exp\left(\int_0^x 2 \frac{a(y)}{b(y)^2} dy \right).$$

Using the definitions for $a(x), b(x)$ in (4.10), the equation for $\gamma(x)$ is now

$$\begin{aligned} \gamma(x) &= \exp\left(\int_0^x \frac{-U'(y)}{2D} dy \right) \\ &= \exp\left(\frac{-U(x)}{2D} \right) \end{aligned}$$

and the mean hitting time is given by

$$\mathbb{E}[T(-s^*)] = \frac{1}{D} \int_{-s^*}^{0} \exp\left(\frac{U(w)}{2D} \right) \int_{-\infty}^{w} \exp\left(\frac{-U(z)}{2D} \right) dz dw. \tag{4.11}$$

If the potential $U(x)$ has a big local maximum at zero and D is small, then $\exp\left(\frac{U(z)}{2D}\right)$ has a sharp peak near zero. Hence, $\exp\left(-\frac{U(z)}{2D}\right)$ is very small near zero. Therefore, the integral $\int_{-\infty}^{w} \exp\left(-\frac{U(z)}{2D}\right) dz$ is approximately constant as a function of w near zero. Therefore, we can split the double integral in (4.11) and get the approximation

$$\mathbb{E}[T(-s^*)] \approx \frac{1}{D} \int_{-s^*}^{0} \exp\left(\frac{U(w)}{2D} \right) dw \int_{-\infty}^{0} \exp\left(\frac{-U(z)}{2D} \right) dz. \tag{4.12}$$

To calculate these integrals, we approximate $U(x)$ near $-s^*$ and zero. $U(x)$ is

approximately a positive quadratic near $x = -s^*$, so we use the approximation

$$U(x) \approx U(-s^*) + \frac{1}{2}\left(\frac{x + s^*}{\alpha}\right)^2,$$

for some constant α which is determined by the second derivative of $U(x)$ at $x = -s^*$. Equating the second derivative of $U(x)$ from the definitions in (4.8) and (4.9) and from the approximation gives

$$U''(-s^*) = A + 1 = \frac{1}{\alpha^2} \Rightarrow \alpha = \frac{1}{\sqrt{A+1}}.$$

$U(x)$ is approximately linear near $x = 0$, so we use the approximation

$$U(x) \approx x.$$

Then, the two integrals in (4.12) become

$$\begin{aligned}\int_{-\infty}^{0} \exp\left(-\frac{U(z)}{2D}\right) dz &\approx \int_{-\infty}^{\infty} \exp\left(-\frac{U(-s^*)}{2D} - \frac{1}{4D}\left(\sqrt{A+1}(z+s^*)\right)^2\right) dz \\ &\approx \sqrt{\frac{\pi D}{A+1}} \exp\left(-\frac{U(-s^*)}{2D}\right),\end{aligned}$$

where the second approximation follows from integrating a Gaussian function, and

$$\begin{aligned}\int_{-s^*}^{0} \exp\left(\frac{U(w)}{2D}\right) dw &\approx \int_{-s^*}^{0} \exp\left(\frac{w}{2D}\right) dw \\ &= \left[2D \exp\left(\frac{w}{2D}\right)\right]_{-s^*}^{0} = 2D\left[1 - \exp\left(\frac{-s^*}{2D}\right)\right].\end{aligned}$$

Hence, the mean hitting time is now

$$\begin{aligned}\mathbb{E}[T(-s^*)] &= 2\left[1 - \exp\left(\frac{-s^*}{2D}\right)\right]\sqrt{\frac{\pi D}{A+1}} \exp\left(-\frac{U(-s^*)}{2D}\right) \\ &= 2\sqrt{\frac{\pi D}{A+1}}\left[\exp\left(-\frac{U(-s^*)}{2D}\right) - \exp\left(\frac{-U(-s^*) - s^*}{2D}\right)\right].\end{aligned}$$

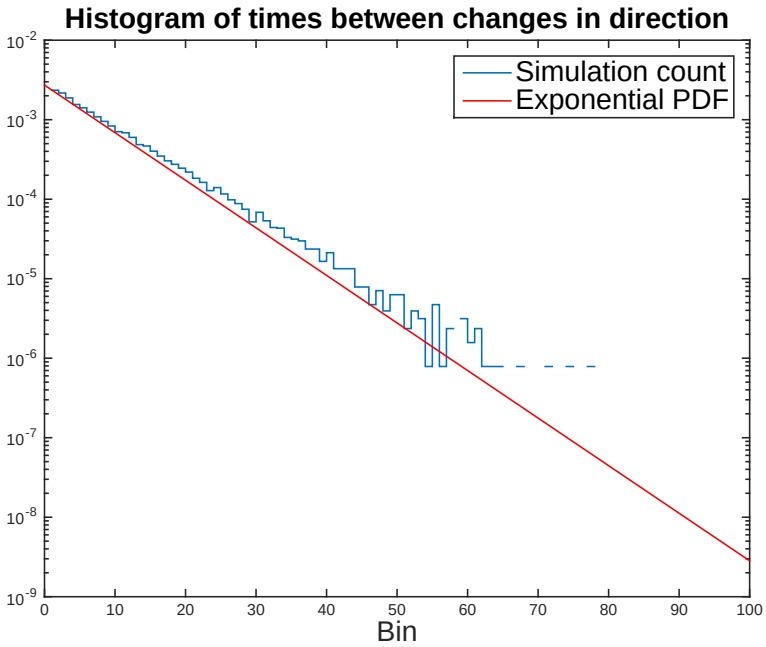

Figure 4-6: Histogram showing the exponential distribution of the periods between direction changes for the male-female pair. $D = 0.02$, $A = 1$, and $t = 10^7$.

Recall from (4.6) that s^* is defined as

$$s^* = \frac{1}{A+1},$$

and returning to the definition of the potential $U(x)$ in (4.8) and (4.9) gives

$$U(-s^*) = \frac{A+1}{2}(-s^*)^2 - s^* = \frac{1}{2(A+1)} - \frac{1}{A+1} = -\frac{1}{2(A+1)}.$$

The equation for the mean hitting time is now

$$\mathbb{E}[T(-s^*)] = 2\sqrt{\frac{\pi D}{A+1}}\left[\exp\left(\frac{1}{4D(A+1)}\right) - \exp\left(\frac{-1}{4D(A+1)}\right)\right],$$

and therefore the mean hitting time T^* for separation starting at $s = -s^*$ with a reflective boundary at $s = -\infty$ and an absorbing boundary at $s = s^*$ is given by

$$T^* = 4\sqrt{\frac{\pi D}{A+1}}\sinh\left(\frac{1}{4D(A+1)}\right). \tag{4.13}$$

When we considered the 'run and tumble' dynamics of one fish, we assumed that the fish swims in the same direction for an exponentially distributed amount of time. In Figure 4-6, we see the distribution for the amount of time the pair of fish swim in the same direction and we see that it has a large tail distribution similar to that of an exponential distribution.

For one fish, we also assumed that, when a tumble occurs, the new direction is chosen uniformly at random. This is currently not the case for the pair of fish as T^* gives the mean time for a change in direction. That is, the new direction is not chosen uniformly at random. To resolve this issue, we use an exponential clock argument. Following the method of Condat et. al.[106], we require that changes in direction are independent from previous changes in direction. Currently, when an exponential clock rings, the pair of guppies start moving in the opposite direction. To make this situation independent, we introduce twice as many exponential clocks with half the mean time of ringing. When one of these clocks ring, we flip a coin. If heads, the guppies change direction. Otherwise, they continue moving in the same direction. With this new perspective, the changes in direction are independent and we have a statistically equivalent situation. Hence, we can indeed use the same arguments in Section 4.1 to calculate the diffusion coefficient of two fish with sexual conflict between them. The mean speed of the two fish is given by v^* in (4.6) and the mean time for a change in direction is given by T^* in (4.13). To model this, we redefine the mean hitting time T^* to $T = T^*/2$. Then, following the calculation in Section 4.1, we find that the large time mean square displacement $Q(t)$ with speed v^* and mean hitting time T is approximately given by

$$Q(t) \approx 2(v^*)^2 T t = (v^*)^2 T^* t,$$

and therefore the effective diffusion rate for a pair of fish is given by

$$D_{\text{eff}} = (v^*)^2 T^*,$$

which depends on the male sexual aggression A and the individual diffusion coefficient of the fish D. The full equation for D_{eff} in terms of A and D is given by

$$D_{\text{eff}} = 4\sqrt{\frac{D\pi}{A+1}} \left(\frac{A}{A+1}\right)^2 \sinh\left(\frac{1}{4D(A+1)}\right). \tag{4.14}$$

Figure 4-7 shows this relationship. We see that, for a given value of D, as A increases from zero, the effective diffusion coefficient peaks and then decreases again. This suggests that there is a level of sexual aggression A that maximises the effective diffusion coefficient D_{eff} for the pair of fish. This level of sexual aggression could be an evolved characteristic that provides an evolutionary benefit to the guppies. For example, a population of guppies with more aggressive males will diffuse more, increasing chances of finding new resources to consume and new environments to invade, all of which is beneficial to the population with more aggressive males. The fact that D_{eff} does not increase monotonically with A can be understood by the fact that, as A gets very large, the male fish is always very close to the female fish. When the noise is added to the system, this results in constant changes in direction. Hence, the pair is unable to travel very far and so has a smaller effective diffusion coefficient. For constant A, as D increases, the effective diffusion coefficient decreases monotonically. This is slightly counterintuitive as it says that when the fish have a small diffusion rate individually, they have a larger diffusion coefficient as a pair. We can make sense of this as, when the individual fish have a small diffusion coefficient, they will swap sides and change the direction of swimming less frequently. With fewer changes in direction, the pair will swim in the same direction for longer periods of time, resulting in a higher diffusion coefficient. The thick black line shows where $D_{\text{eff}} = D$. The parameter space to the left of this curve shows where $D_{\text{eff}} > D$. Hence, we see very clearly that it is possible for sexual conflict to increase the diffusion coefficient for a pair of fish. Note, however, that sexual conflict can also decrease the diffusion coefficient for the pair. When the individual diffusion coefficient $D > 0.5$, the noise in the movement of the fish causes the pair to constantly change direction. These dynamics result in a very small joint diffusion rate as the pair of fish never travel very far in a particular direction.

We have theoretically determined that sexual conflict can increase the effective diffusion coefficient of the pair of fish. We also want to show that this is supported by simulations of the SDEs in (4.4) using the response functions in (4.5). The simulation results are shown in Figure 4-8. We simulate the mean square displacement of the male as a function of sexual aggression A. We only focus on the displacement of the male as the two fish are very close together and the displacement of the male is a suitable approximation for the displacement of

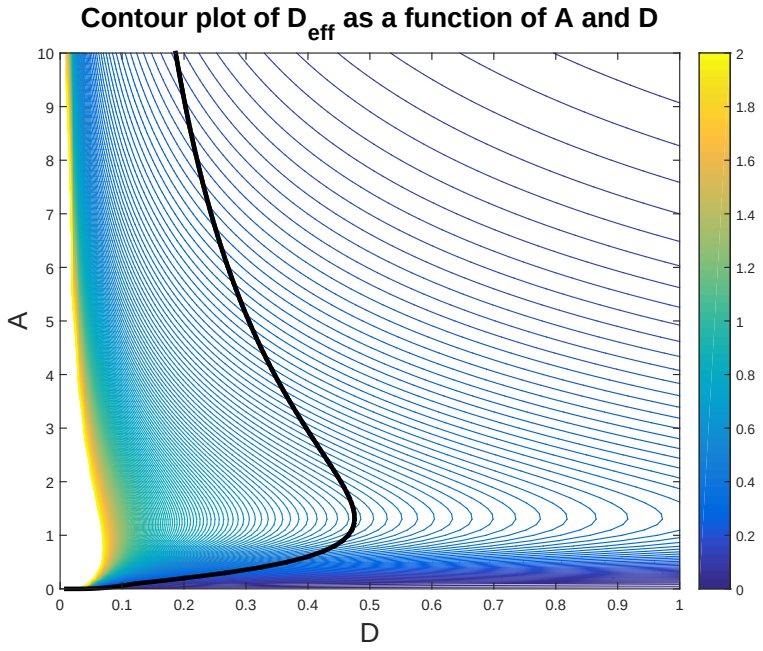

Figure 4-7: The effective diffusion coefficient of the two fish D_{eff} in (4.14) varying with the sexual aggression of the male A and the individual diffusion coefficient D. The thick black line shows where $D_{\text{eff}} = D$. The colour bar shows the effective diffusion coefficient.

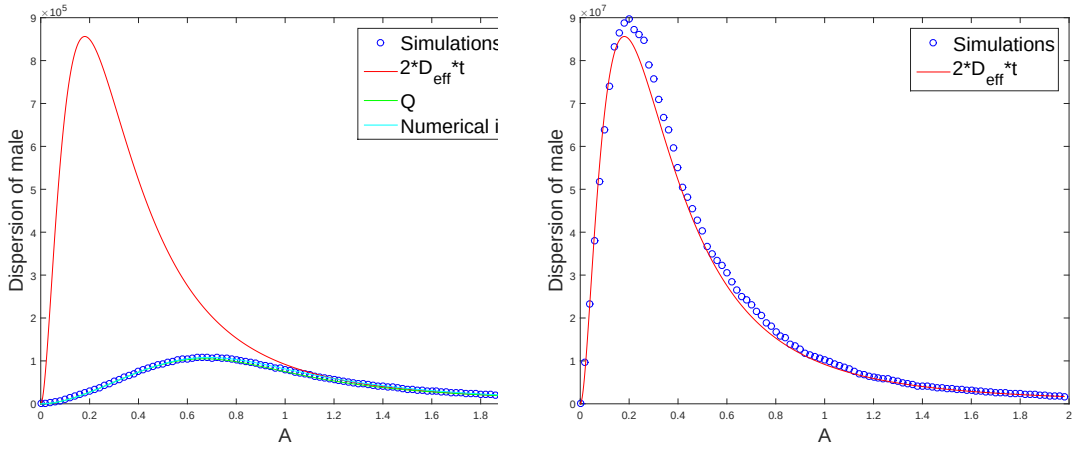

(a) (b)

Figure 4-8: Short time and long time comparisons between simulations of the SDEs for the two fish in (4.4) using the response functions in (4.5) and the theory predicted by the mean square displacement $Q(t)$ and the effective diffusion D_{eff}. The individual diffusion coefficient is $D = 0.02$. (a) Simulation run for time period $t = 10^3$ (b) $t = 10^5$

the two fish. In (a), we simulate over a short time period $t = 10^3$. We plot the simulation results in blue circles, the mean square displacement $Q(t)$ calculated in (4.2) in green, the long time approximation for $Q(t)$ given by $2D_{\text{eff}}t$ in red, and the numerical integration solution for $Q(t)$ in (4.1) in cyan. We see that $Q(t)$ and the numerical integration agree strongly with the simulation results for this short time period. The long time approximation for $Q(t)$ does not agree here as we are in the short time period regime. However, all curves are similar qualitatively with a single peak in A, which agrees with the results in Figure 4-7. In (b), we simulate over a long time scale $t = 10^5$ and see that the long time approximation for $Q(t)$ given by $2D_{\text{eff}}t$ now strongly agrees with the simulations.

We have shown that when sexual conflict is introduced between a male and a female fish, the resulting movement has a diffusion coefficient D_{eff} which can be significantly greater than the diffusion coefficient D of the individual fish. We expect that these results hold in a 2D and 3D environment as well.

4.3 Many Fish

Populations of guppies usually contain significantly more than two fish in a shoal. For this reason, it is more biologically realistic to consider the role sexual conflict plays in populations with lots of fish, with many males and many females. In this Section, we consider a large population of male and female fish in a homogeneous 1D environment. We show that sexual conflict results in fish having a higher diffusion coefficient in the low density region ahead of the front than in the high density region behind the front. We showed in the technical introduction in Section 2.2.2 that the speed of the FKPP is determined ahead of the front in the linearised region. This means that sexual conflict can lead to a faster invasion speed in a guppy population.

In the absence of interaction, we assume all fish move according to a diffusion process with individual diffusion coefficient D. Sexual conflict in female fish tends to cause them to swim away from all male fish. We assume here that female fish respond to the location of all male fish as a first approximation to their behaviour. Sexual conflict in male fish tends to cause them to swim towards the nearest female fish. We make this assumption as male fish are focused on reproducing so only the nearest female fish will hold their attention. In addition to this, the male fish also has a finite attention span which means that it will chase the nearest female for an exponentially distributed amount of time. When a male fish is not chasing, it is moving according to a diffusion process and starts chasing again with a chase rate. We introduce this attention span to create a model that more realistically models the observed behaviour of male guppies.

Consider n male fish and m female fish with locations $X_i(t)$ and $Y_j(t)$ at time t respectively with $i \in \{1, 2, \ldots, n\}, j \in \{1, 2, \ldots, m\}$. We assume each individual fish diffuses with diffusion coefficient D in the absence of interaction and assume that sexual conflict takes the form of response functions v_X, v_Y as in Section 4.2. In addition, for each male fish i, let $Y^i(t)$ be the location of the nearest female fish. Also, let $I^i(t)$ be a discrete Markov process on $\{0, 1\}$. $I^i(t)$ spends an exponentially distributed amount of time with mean c_i^M in state $I^i(t) = 1$, which represents the time when male fish i is chasing, and then jumps to $I^i(t) = 0$, when male fish i is no longer chasing. $I^i(t)$ jumps from state zero to state one

with chase rate c_i. These dynamics are contained in the SDEs as

$$\begin{aligned}\frac{dX_i}{dt} =& v_X(Y^i - X_i)I^i(t) + \sqrt{2D}\eta_X(t)\,,\\ \frac{dY_j}{dt} =& \frac{1}{n}\sum_{i=1}^{n} v_Y(Y_j - X_i) + \sqrt{2D}\eta_Y(t)\,,\end{aligned} \tag{4.15}$$

where $\eta_X\,, \eta_Y$ are independent Gaussian white noise terms with mean zero unit variance, as defined in the technical introduction in Section 2.1.1.We normalise the sum over v_Y to ensure that the max speed of the female fish remains biologically realistic when there is a large group of males to one side of the female fish.

The SDEs in (4.15) provide insights even for very small populations. When we only consider one male fish and one female fish again, taking $n = m = 1$, we can simulate the SDEs and see the male fish chasing and not chasing the female fish. This is shown in Figure 4-9 (a). When we consider one male fish and two female fish, taking $n = 1$ and $m = 2$, the male fish can, due to the fact that it chases the nearest female and has a finite attention span, switch between chasing different female fish. This is shown in Figure 4-9 (b). The male fish starts chasing the female fish in the dashed red line and then with stochastic noise swims closer to the female in the solid red line and continues to chase this new female fish.

Now, we consider the diffusion coefficient of the population ahead of the front where there is a low density of male and female fish and behind the front where there is a high density of male and female fish. Ahead of the front, as there are very few female fish, male fish will spend more time chasing the same female fish instead of switching between them. This will result in longer runs and so a larger diffusion coefficient. Behind the front, male fish will switch between chasing different female fish more often and so the movement of the male fish will be contain more changes in direction and so will result in a smaller diffusion coefficient.

We can model the dynamics in these different regions by considering one male fish with a varying number of female fish in a 1D environment with periodic boundary conditions. We use periodic boundary conditions here because we want to track the displacement of the one male fish over long time periods without any constraints of a boundary while still being able to simulate the environment. We

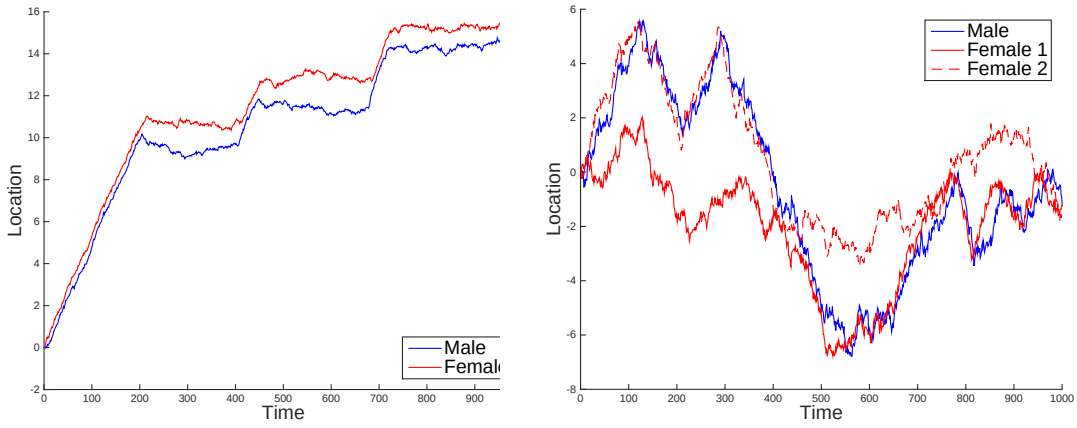

(a) (b)

Figure 4-9: (a) A male fish chasing and not chasing a female fish. Diffusion coefficient $D = 0.01$, chase rate $c_1 = 0.001$, and mean chase time $c_1^M = 10$. (b) A male fish switching between two female fish. Diffusion coefficient $D = 0.1$, chase rate $c_1 = 0.001$, mean chase time $c_1^M = 100$.

vary the number of female fish in the environment to simulate the male fish being ahead of the front where there are few female fish and behind the front where there are many female fish. We track the displacement of the male fish as we vary the number of female fish in the environment and vary the chase rate of the male fish. We vary the chase rate to determine how the displacement of the male fish varies according to how long it spends not chasing in these different regions of the population. The results are shown in Figure 4-10. We see for all cases that the displacement of the male fish increases monotonically with the chase rate. This is expected as, for a higher chase rate, the fish is spending more time chasing. As the number of female fish in the environment decreases, the asymptotic displacement of the male increases. This agrees with our prediction that the male fish will have a higher displacement ahead of the front compared to behind the front. As the invasion speed for the FKPP is determined by the dynamics ahead of the front, we see that sexual conflict can increase the diffusion coefficient of a population and hence the invasion speed of the population.

When male fish move according to the SDEs in (4.15), they switch between chasing and not chasing. If the male fish was always chasing, over a long time period it would have one diffusion coefficient and if the male fish was never

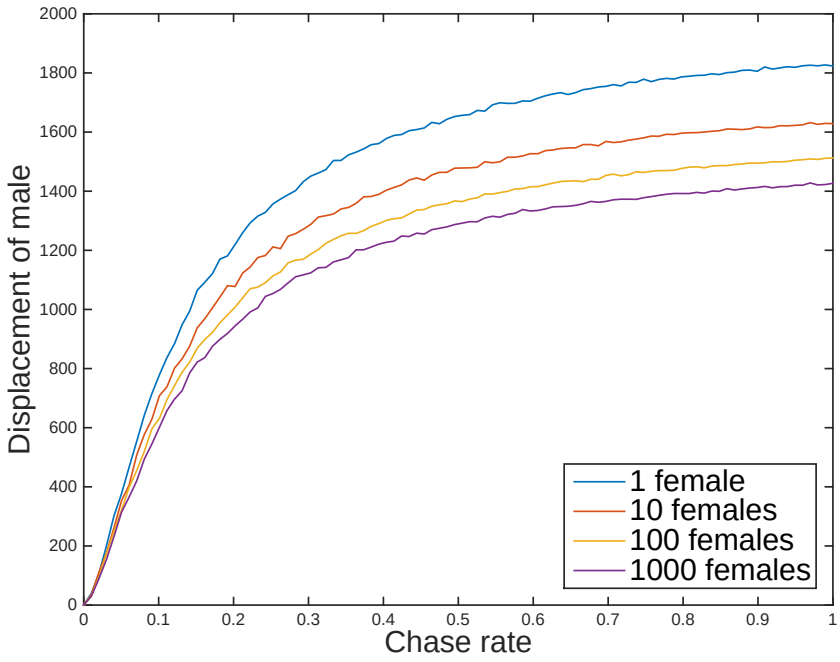

Figure 4-10: The displacement of an individual male fish as a function of its chase rate c_1 and the number of female fish in the environment. Individual diffusion coefficient $D = 0.001$, mean chase time $c_1^M = 1$.

chasing, it would have a different diffusion coefficient. We want to determine the diffusion coefficient D_{swt} for a fish that is switching between diffusion coefficients. We calculate this by calculating the mean square displacement of the fish using an argument similar to the calculation in Section 4.1.

Consider a male fish switching between diffusion rates D_1, D_2 such that it switches from D_1 to D_2 with rate λ_1 and back with rate λ_2. Let $H_i(t)$ be the mean square displacement of a male fish initially diffusing with rate D_i. We begin by conditioning on the first diffusion rate change, given by

$$\begin{aligned} H_1(t) &= \mathbb{P}[\text{no diffusion change in } [0,t]]\mathbb{E}[X(t)^2|\text{no diffusion change in } [0,t]] \\ &\quad + \mathbb{P}[\text{diffusion change in } [0,t]]\mathbb{E}[X(t)^2|\text{diffusion change in } [0,t]] \\ &= e^{-\lambda_1 t}Q_1(t) + \int_0^t \lambda_1 e^{-\lambda_1 \tau}\left(Q_1(\tau) + H_2(t-\tau)\right)\, d\tau\,, \end{aligned}$$

where $Q_1(t) = 2v_1^2T_1\left(t - T_1 + T_1e^{-t/T_1}\right)$ is the mean square displacement only with displacement $D_1 = v_1^2T_1$. As we are interested in the large time mean square displacement, we can make the approximation $Q_1(t) \approx 2D_1t$. Making this

substitution for $Q_1(t)$ gives

$$H_1(t) = e^{-\lambda_1 t} 2D_1 t + \int_0^t \lambda_1 e^{-\lambda_1 \tau} \left(2D_1\tau + H_2(t-\tau)\right)\, d\tau\,,$$

and taking Laplace transforms gives

$$\mathcal{H}_1(s) = \frac{2D_1}{(s+\lambda_1)^2} + \frac{2D_1\lambda_1}{s(s+\lambda_1)^2} + \frac{\lambda_1}{s+\lambda_1}\mathcal{H}_2(s),$$

and similarly

$$\mathcal{H}_2(s) = \frac{2D_2}{(s+\lambda_2)^2} + \frac{2D_2\lambda_2}{s(s+\lambda_2)^2} + \frac{\lambda_2}{s+\lambda_2}\mathcal{H}_1(s).$$

Solving these equations for $\mathcal{H}_1(s)$ gives

$$\mathcal{H}_1(s) = \frac{2}{s+\lambda_1+\lambda_2}\left(\frac{D_1(s+\lambda_2)}{s(s+\lambda_1)} + \frac{D_1\lambda_1(s+\lambda_2)}{s^2(s+\lambda_1)} + \frac{D_2\lambda_1}{s(s+\lambda_2)} + \frac{D_2\lambda_1\lambda_2}{s^2(s+\lambda_2)}\right)$$

and taking inverse Laplace transforms gives

$$H_1(t) = 2\frac{D_1\lambda_2 + D_2\lambda_1}{\lambda_1+\lambda_2}t - \frac{2\lambda_1(D_1-D_2)}{(\lambda_1+\lambda_2)^2}\exp\left(-(\lambda_1+\lambda_2)t\right) + \frac{2\lambda_1(D_1-D_2)}{(\lambda_1+\lambda_2)^2},$$

and similarly

$$H_2(t) = 2\frac{D_1\lambda_2 + D_2\lambda_1}{\lambda_1+\lambda_2}t - \frac{2\lambda_2(D_2-D_1)}{(\lambda_1+\lambda_2)^2}\exp\left(-(\lambda_1+\lambda_2)t\right) + \frac{2\lambda_2(D_2-D_1)}{(\lambda_1+\lambda_2)^2}.$$

After a large time, we see that

$$H_1(t) = H_2(t) \approx 2\frac{D_1\lambda_2 + D_2\lambda_1}{\lambda_1+\lambda_2}t.$$

Therefore, the long time diffusion coefficient of a male fish switching from diffusion coefficient D_1 to D_2 with rate λ_1 and from D_2 to D_1 with rate λ_2 is given by

$$D_{\text{swt}} = \frac{D_1\lambda_2 + D_2\lambda_1}{\lambda_1+\lambda_2}.$$

This is the equation for the diffusion coefficient for a fish that is switching between two different diffusion coefficients. We could apply this to male fish ahead of the

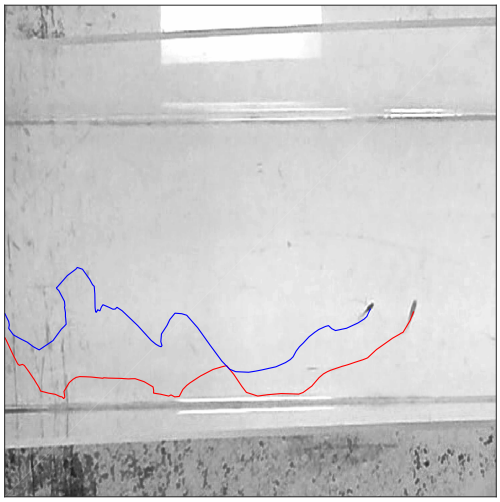

Figure 4-11: The results from the tracking software for one experiment.

population front, as they switch between chasing and not chasing. This would then be used to calculate the population invasion speed $v = 2\sqrt{rD}$ for the 1D FKPP equation. It could also be applied to fish behind the front as well.

4.4 Experiments

Theoretical results are useful to ensure that the model predicts biologically realistic behaviour. So far, we have found theoretical and simulated results for how sexual conflict between male and female guppies affects their diffusion coefficients and hence the invasion speed according to the 1D FKPP equation. These results are more significant when they accurately reflect the observed guppy behaviour. Working with behavioural ecologists Dr Safi Darden and Prof. Darren Croft at the University of Exeter, we organised guppy experiments to help test and inform the models presented above. For the experiments, we chose to use a very long, narrow tank. This simulated the rivers that the guppies live in and allowed us to very clearly see chases along the tank. In the tank, we placed different pairs of fish: either two females, two males, one female and a strongly aggressive male, or one female and one weakly aggressive male. The two female and two male pairs were used as control experiments so that we could determine

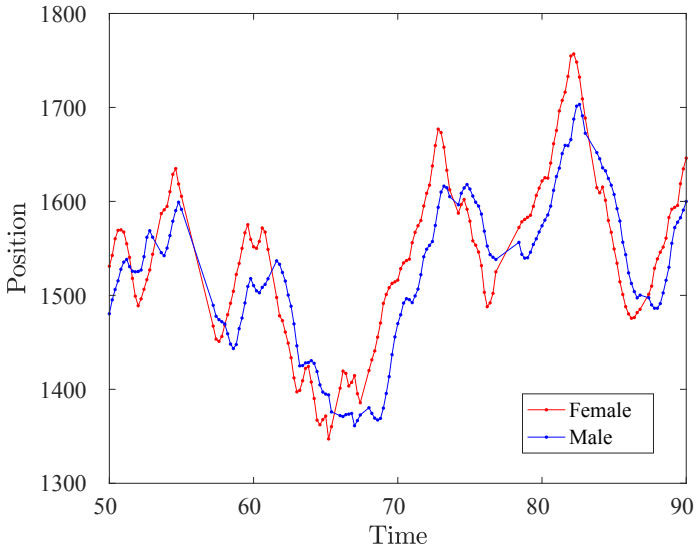

Figure 4-12: The locations of a male and female guppy determined from guppy experiments.

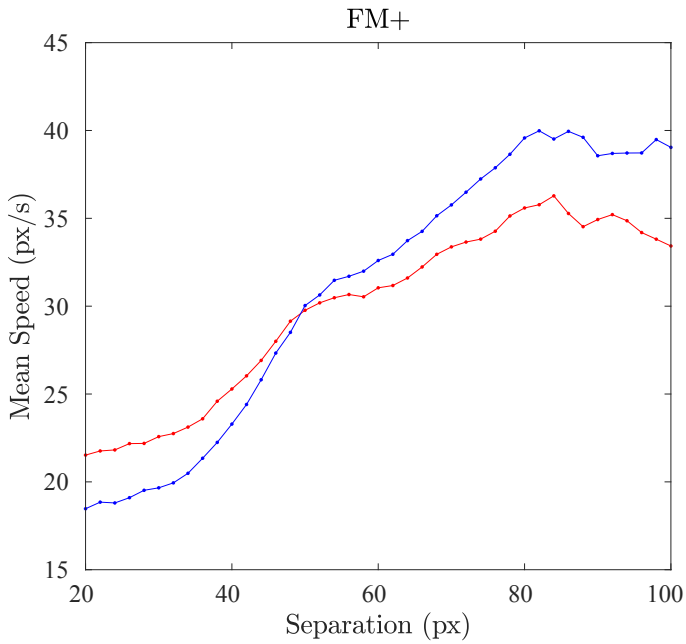

Figure 4-13: The response functions v_X, v_Y as functions of separation s determined from guppy experiments.

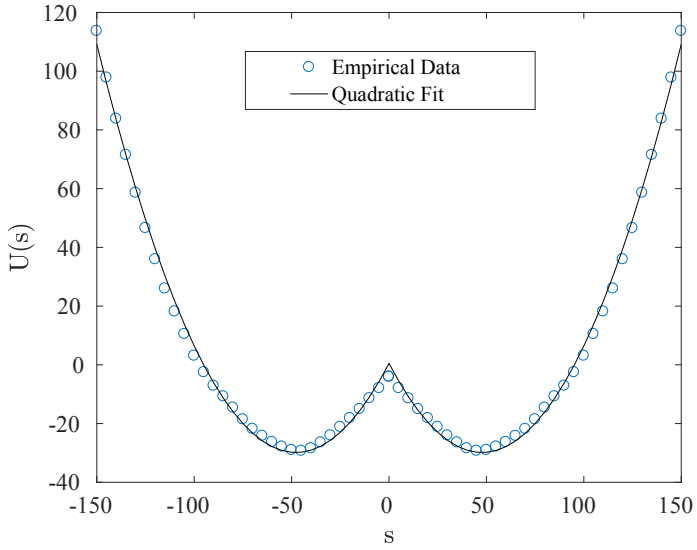

Figure 4-14: The potential $U(s)$ of the guppies plotted as a function of separation s determined from guppy experiments.

if any changes in diffusion are due to sexual conflict between males and females or if it was another interaction due to shoaling that does not depend on the genders involved. The aggression of the males was determined by the gender diversity of the environment the males are raised in. While these pairs were in the tank, there were video cameras recording their movements, which were then tracked using computer software, with an example in Figure 4-11. This software scanned the video for the fish and then recorded their location while also taking into account that they may not always have been visible, e.g. if they crossed over each other in the video. An example of the locations being tracked is shown in Figure 4-12. At the time of writing, these recordings are still being analysed. Once they are done, we can then use the trackings to calculate approximations for the individual diffusion coefficient D, the sexual conflict response functions v_X, v_Y, with an example in Figure 4-13, the mean separation s^*, the mean speed v^*, the potential U, with an example in Figure 4-14, the mean time to change direction T^*, chase rate c, mean chase time c^M, and hence the effective diffusion coefficient D_{eff} and the switching diffusion coefficient D_{swt} for the pair. Results from the tracking can also justify the assumption of run and tumble movement, the zig-zag trajectories, and the exponentially distributed run times. We expect

the experiments will agree with our theoretical results.

4.5 Conclusion

In this Chapter, we have analysed the effect of sexual conflict on the diffusion coefficient of a population, and hence the invasion speed according to the 1D FKPP equation $u_t = Du_{xx} + ru(1-u)$ for diffusion coefficient D and growth rate r. The model for the movement of one fish was introduced using 'run and tumble' dynamics, with the fish having speed v and mean time to change direction T. This resulted in an equation for the large-time mean square displacement of the fish, which grows linearly in time and has diffusion coefficient $D = v^2T$. For two fish, one male and one female, we assumed that on average the male fish swims towards the female, that the female fish swims away from the male, and that the male fish has aggression level A. The stochastic differential equations that captured these dynamics gave the mean speed and mean separation for the pair of fish. Using a similar 'run and tumble' argument, we were able to determine the effective diffusion coefficient D_{eff} for the pair of fish. We found that, in certain parameter regimes, the effective diffusion coefficient for the pair of fish can be much greater than the individual diffusion coefficients. These results were confirmed by simulations. Finally, we extended this framework to include many males and many females and to allow male fish to switch between chasing and not chasing. This large population model introduced variation in the mean square displacement for male fish ahead of the front, where there are few female fish, and behind the front, where there are many female fish. Male fish ahead of the front have a much larger diffusion coefficient.

In order to establish the biological relevance of this work, we carried out experiments tracking the movement of pairs of fish in order to calculate the effect sexual conflict has on the effective diffusion coefficient of the pair. This research can be used to better predict the invasion speed of fish populations. This is significant because we have shown here that the aggression level of the male fish in the population plays a crucial role in determining how quickly the population invades. Behavioural ecologists will now know that understanding the aggression of the males, which is influenced by the environment the fish was raised in, will allow a more accurate prediction of the population invasion speed.

Chapter 5

Invasions and Nonlocal Interaction

Competition within and between populations has been studied for a long time. Classic examples include work that introduced logistic growth and examines populations competing for a finite resource [114, 115, 116]. These models have been used to explain coexisting populations [117, 118, 119], have been studied in field experiments [120], and have been found to influence the community structure within a population [121]. They have been experimentally supported by a wide range of populations, including the growth of yeast [122], herding of African elephants [123], and the density of Peruvian anchovies [124].

These competition models can also be applied to the exchange of opinions within a population, such as political support during an election. Each individual has an opinion and this opinion changes as the individual interacts with others. At any point, they can adopt the opinion of someone else. Understanding these dynamics is crucial for election campaigns and other important decision making processes.

The simplest model that captures these dynamics is the voter model, which belongs to a wider class of models known as interacting particle systems [48]. It is also referred to as a contact process or a stepping stone model [127]. Individuals are modelled by fixed points, so there is no movement, on a lattice, which is usually 1D or 2D. Each point is given a colour representing the opinion of that individual and, at random times, a point adopts the colour of one of its neighbours, simulating the exchange of opinions. The key factors in this model include

the initial distribution of colours on the lattice, the random process for adopting colours, and the condition that colours can only be adopted from neighbours, which is a form of local interaction. Research on the voter model in 2D has found that clusters of opinions form on the lattice, known as coarsening [52, 125, 126].

One important question for the voter model is if the opinions of all individuals agree with each other and, if so, how long does it take? This has been studied for the 1D and 2D voter models [128, 129] and even with the introduction of individuals who never change their opinion, known as zealots [130]. In this Chapter, we analyse the probability of reaching consensus for the 1D voter models with nonlocal interaction and diffusion. We do this because it is very common for individuals to be able to interact with others who are not their neighbours. Who is more likely to convert the other type in a pairwise interaction: a strongly-opinionated individual with a short interaction distance or a weakly-opinionated individual with a large interaction distance? If we had a large population of both types, which type is more likely to reach consensus? What influence does the speed of the individuals have on these scenarios? These are the questions we seek to answer in this Chapter. The answers to these questions will show us how important individual interaction dynamics are in determining the long time evolutionary dynamics of a population.

Consider a population of individuals with two types. The first type has a short range of interaction, but it is very strong. We call this type S. The second type has a long range of interaction, but it is very weak. We call this type W. Individuals of the same type do not interact with each other; the only interactions we consider are between types. Let r_S, r_W be the interaction ranges and let λ_S, λ_W be the interaction rates of the type S, W individuals respectively. We assume $r_S < r_W$ and $\lambda_S > \lambda_W$. When the distance between a S, W pair of individuals is less than r_W, the type W individual converts the type S individual to type W with rate λ_W. Similarly, when a type W individual is within distance r_S of a type S individual, the type S individual converts the type W individual with rate λ_S. These are the only interactions we consider in this Chapter. We also assume that individuals exist in 1D domains because this gives mathematically tractable problems. We expect the results to hold in higher dimensions as well. In particular, we consider the domain $[-\pi, \pi)$. In 1D, the total region of influence for an individual of type W, S is $2r_W, 2r_S$ respectively. We assume another condition

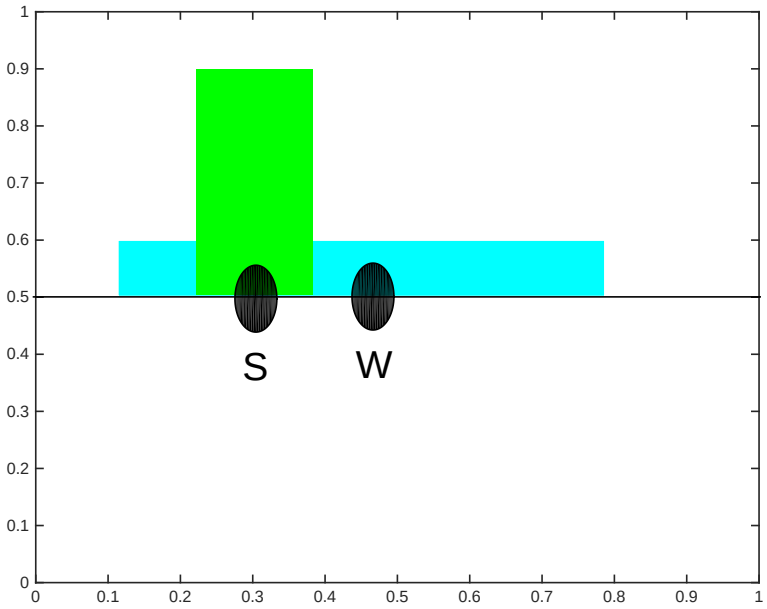

Figure 5-1: A representation of a W-S pair.

$\lambda_S r_S = \lambda_W r_W = 1/2$ so that the product of the region of influence and the interaction rate for each type is equal to one. That is, $2\lambda_S r_S = 2\lambda_W r_W = 1$. This ensures that neither type has an advantage over the other from the choice of parameters. In addition, let D_S, D_W be the diffusion rates of the types. In these 1D domains, individuals are moving and interacting with individuals of a different type. A representation is shown in Figure 5-1. This model could simulate the real-life situation of two political parties on the campaign trail trying to persuade their voters using door-to-door canvassing in one party and social media campaigns in the other.

These interactions end when the entire population consists of one type. We call this reaching consensus because, in the example of voters, this signifies the point when the voting population has reached a consensus. We want to determine which type survives as the population reaches consensus. To do this, we have to consider the number of individuals of each type in the population and the rate at which they convert the other type. These variables depend on the size of the population. In Section 5.1, we consider a small population size and calculate the probability that a particular type converts the other when they meet in a pair and the probability that a particular type survives as the population reaches consensus. When the population size is large, the dynamics are more complicated

and so require a different form of mathematical analysis. In Section 5.2, we consider a large population size and calculate the master equation for the system dynamics in Fourier space and a differential equation for population densities. In both population regimes, we find that the type W individuals with a weak, wide interaction range have an advantage in pair interactions and survive when the population reaches consensus.

5.1 Low-Density Regime

The aim of this Section is to calculate the probability of a particular type surviving to consensus. In the low density regime, a type will survive to consensus if that type has a high probability of converting the other type when a pair meets. This is because surviving to consensus is the result of numerous pair conversions in the low density regime. However, this probability only needs to be greater than 1/2 for large population sizes. We start by considering a single individual and derive a differential equation for the density of individuals of the different type around it. Solving this differential equation provides an equation for the probability that an individual of type S converts the type W individual when a pair meets. Hence, we calculate the probability that type S survives to consensus.

Consider a particular individual, denoted individual I. Let $u(x)$ denote the density of the locations of the individuals of a different type to individual I when an interaction occurs. We only need to consider distances $|x| < r_W$ as, at any larger distances, the individuals cannot interact with each other. Moreover, we only need to consider $x \in [0, r_W)$ as the interactions are symmetric so we can simplify the problem by considering individual I placed at the origin and other individuals at location x. This density is affected by the movement and conversion of individuals. If we take a frame of reference that fixes the location of individual I, individuals of the other type move with diffusion rate $D = D_S + D_W$. When the distance between the individuals is less than r_W and greater than r_S, that is, $r_S < x < r_W$, then the pair reacts with rate λ_W. When $x < r_S$, the pair reacts with rate $\lambda_S + \lambda_W$ as the type S individual could convert to W or the other way around. The type of individual I is not important here as the interactions are symmetric. This reaction rate is summarised by $\lambda(x) = \lambda_S \mathbb{1}_{x<r_S} + \lambda_W \mathbb{1}_{x<r_W}$.

These dynamics of the density $u(x)$ are summarised by the differential equation

$$u_t = Du_{xx} - \lambda(x)u. \tag{5.1}$$

The PDE (5.1) has boundaries at $x = 0, x = r_S, x = r_W$. The boundary condition at $x = 0$ is reflective as we have fixed individual I at the origin and the interactions are symmetric. At $x = r_S$, we need to match the density $u(x)$ and flux $u'(x)$ between the two regions $x \in [0, r_S)$ and $x \in [r_S, r_W)$ as $\lambda(x)$ changes value. Finally, at $x = r_W$, the boundary condition is determined by the rate of occurrence of pairs of different types coming within distance r_W of each other. Define this rate to be κ, which depends on the size of the population, the proportion of different types, and the diffusion rates. We find that we can make analytic progress without knowing the details of κ. These boundary conditions are summarised as

$$u'(0) = 0, \quad \lim_{x \nearrow r_S} u(x) = \lim_{x \searrow r_S} u(x) \quad \lim_{x \nearrow r_S} u'(x) = \lim_{x \searrow r_S} u'(x) \quad u'(r_W) = \kappa. \tag{5.2}$$

Solving (5.1) and (5.2) for $u(x)$ will provide a formula for the probability of a particular type of individual converting the other in a pairwise interaction. Firstly, we only need to consider the stationary solution of (5.1) because we are interested in the long time behaviour of the density, which represents the mean dynamics of a pair interaction. Secondly, as $\lambda(x)$ is a piecewise constant function, we can solve for the stationary solution of (5.1) by considering the constant coefficient ODE $0 = Du_{xx} - \lambda u$ in the two regions $x \in [0, r_S)$ and $x \in [r_S, r_W)$ and taking λ to be the appropriate constant in each region determined by $\lambda(x) = \lambda_S \mathbb{1}_{x<r_S} + \lambda_W \mathbb{1}_{x<r_W}$. Standard calculations give

$$u(x) = \begin{cases} C_1 \cosh\left(\sqrt{\frac{\lambda_S+\lambda_W}{D}}x\right) & \text{for } x \in [0, r_S) \\ C_2 \cosh\left(\sqrt{\frac{\lambda_W}{D}}x\right) + C_3 \sinh\left(\sqrt{\frac{\lambda_W}{D}}x\right) & \text{for } x \in [r_S, r_W), \end{cases} \tag{5.3}$$

where constants C_1, C_2, C_3, which are determined by the last three boundary

conditions in (5.2), are given by

$$C_1 = \frac{\kappa\sqrt{D}}{\sqrt{\lambda_W}\cosh(B_1)\sinh(B_2) - \sqrt{\lambda_S+\lambda_W}\cosh(B_2)\sinh(B_1)}$$
$$C_2 = \frac{-\kappa\sqrt{D\lambda_W}\cosh(B_1)}{\lambda_W\cosh(B_1)\sinh(B_2) - \sqrt{\lambda_W(\lambda_S+\lambda_W)}\cosh(B_2)\sinh(B_1)}$$
$$C_3 = \frac{-\kappa\sqrt{D(\lambda_S+\lambda_W)}\sinh(B_1)}{\lambda_W\cosh(B_1)\sinh(B_2) - \sqrt{\lambda_W(\lambda_S+\lambda_W)}\cosh(B_2)\sinh(B_1)},$$

where

$$B_1 = r_S\sqrt{\frac{\lambda_S+\lambda_W}{D}}$$
$$B_2 = (r_S - r_W)\sqrt{\frac{\lambda_W}{D}}.$$

It is a simple check to see that (5.3) satisfies the first boundary condition.

Now that we have found the solution for $u(x)$, we can determine the probability of a particular type converting the other when a pair of individuals of different types come with interaction range of each other. Define p_S to be the probability that the type S individual wins and converts the other individual in the pair interaction. The fluxes $u'(r_S), u'(r_W)$ are the amount of probability mass moving into the $[0, r_S), [r_S, r_W)$ domains from the right respectively. If the type S individual wins, it will occur in the $[0, r_S)$ domain. If the type W individual wins, it will occur in the $[0, r_W)$ domain. The ratio $u'(r_S)/u'(r_W)$ is the proportion of the probability mass that enters $[r_S, r_W)$ that also enters $[0, r_S)$. This represents all situations when the interaction occurs on $[0, r_S)$. On this domain, the proportion of interactions with the type S individual winning is given by $\lambda_S/\lambda_S + \lambda_W$ and similarly the type W individual winning is given by $\lambda_W/\lambda_S + \lambda_W$. Hence, from the solution for $u(x)$ in (5.3), p_S is given by

$$p_S = \frac{u'(r_S)}{u'(r_W)}\frac{\lambda_S}{\lambda_S+\lambda_W}, \tag{5.4}$$

where the first fraction gives the fraction of reactions occurring within the smaller region of interaction $x \in [0, r_S)$ and the second fraction gives the fraction of interactions that result in the type S individual winning. Similarly, the probability

of the type W individual winning is given by

$$p_W = \frac{u'(r_S)}{u'(r_W)} \frac{\lambda_W}{\lambda_S + \lambda_W} + \frac{u'(r_W) - u'(r_S)}{u'(r_W)}, \tag{5.5}$$

where the first term is the probability of the type W individual winning in the smaller region of interaction $x \in [0, r_S)$ and the second term is for the region $x \in [r_S, r_W)$. Note that we have $p_S + p_W = 1$ as expected. We only consider cases when there is an interaction, that is, when the type of one individual is changed. We do not consider the case when individuals are near each other but do not interact. For the rest of the Section, we only consider p_S.

Using the solution for $u(x)$ in (5.3), we can write down the expressions for p_S in terms of the variables $r_S, r_W, \lambda_S, \lambda_W$. To simplify notation, we introduce $\mu_1 = \sqrt{(\lambda_S + \lambda_W)/D}$ and $\mu_2 = \sqrt{\lambda_W/D}$. Then, we have

$$p_S = \frac{2\mu_1\lambda_S(e^{2\mu_1 r_S} - 1)e^{\mu_2(r_S + r_W)}}{(\lambda_S + \lambda_W)((\mu_1 - \mu_2)(e^{2r_S(\mu_1+\mu_2)} - e^{2\mu_2 r_W}) + (\mu_1 + \mu_2)(e^{2\mu_1 r_S + 2\mu_2 r_W} - e^{2\mu_2 r_S}))}. \tag{5.6}$$

We plot p_S in Figure 5-2 varying the interaction distances and rates. We set $r_W = \lambda_S = 1$ and vary r_S, λ_W in $[0, 1]$. We do this so the conditions $\lambda_W < \lambda_S$ and $r_S < r_W$ are always satisfied. The joint diffusion rate for the types is set at $D = 1$. We see that when $\lambda_W \approx 1$, the probability p_S increases from zero to $1/2$ as r_S increases from zero. This shows that when the interaction rates are approximately the same, the winner of the interaction is determined by the type with the larger interaction distance. Similarly, when $r_S = 1$ and λ_W increases from zero, the probability p_S decreases from one to $1/2$. This shows that when the interaction ranges are approximately the same, the winner is determined by the type with the larger interaction range. We are only interested in the case when the two types are equally effective on average, that is, when $\lambda_S r_S = 1/2 = \lambda_W r_W$. This point of interest is shown by the white x. At this point, the probability p_S of a type S individual winning the pair interaction is given by $p_S = 0.4614$ which shows that the type W individuals have an advantage during the pairwise interactions.

The results in Figure 5-2 are only for the value $D = 1$. To see how the

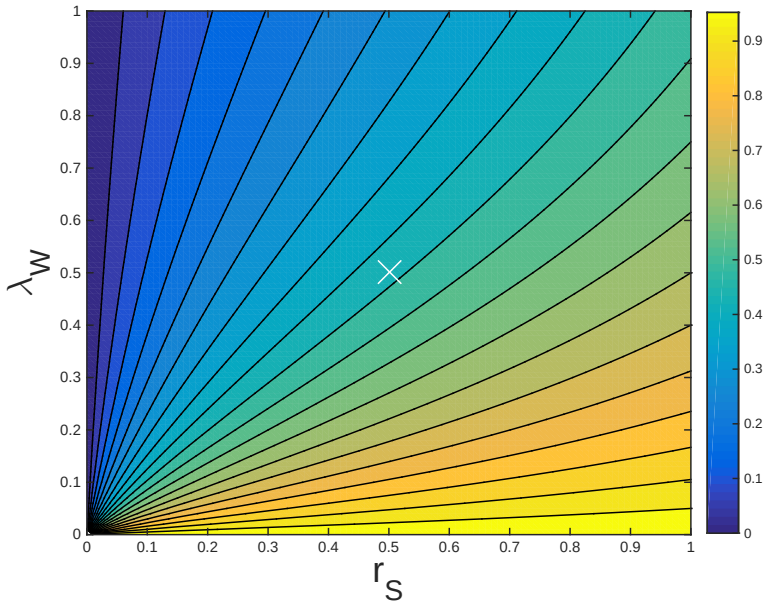

Figure 5-2: The probability p_S in (5.6) of a type S individual winning a pair interaction varying with r_S and λ_W. We set $r_W = \lambda_S = 1$. In order for types to be equally effective on average, we only consider the case when $\lambda_S r_S = 1/2 = \lambda_W r_W$, which is shown by a white x. At their intersection, $p_S = 0.4614$. $D = 1$. The colour bar shows the probability p_S.

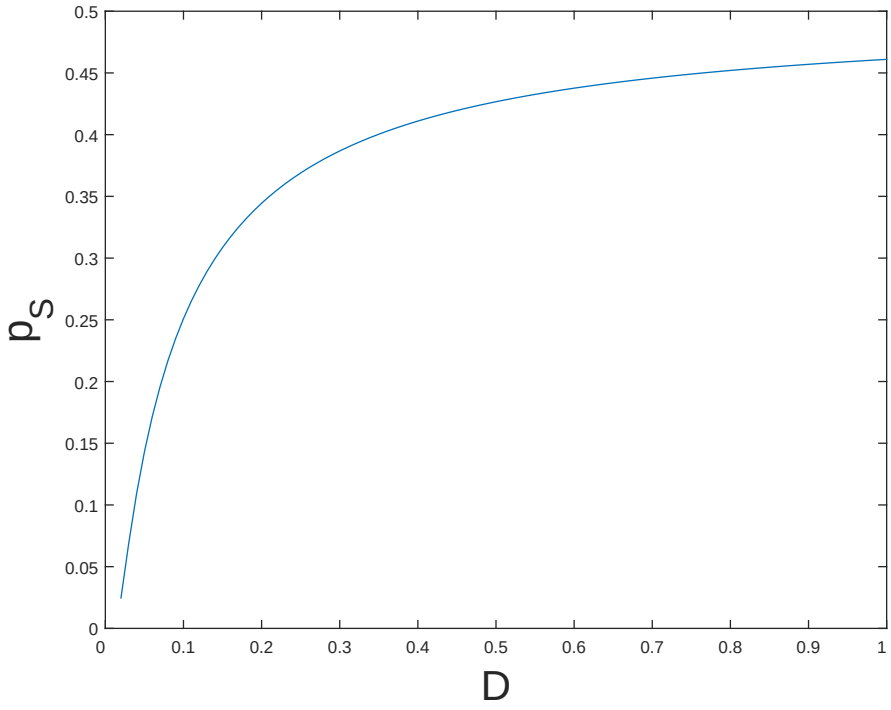

Figure 5-3: The probability p_S as a function of the joint diffusion D. $r_W = \lambda_S = 1, r_S = \lambda_W = 1/2$.

parameter case we are considering varies with D, we plot p_S in Figure 5-3 for different values of D. p_S increases monotonically with D from zero and tends to $1/2$. When D is small, the individuals are moving slowly and when D is large, the individuals are moving quickly. The result we see are expected as, when individuals are moving slowly, type S individuals spend more time within the interaction distance r_W, so they can be converted by the type W individual, before they are ever within distance r_S of the type W individual. This means that there is more time for the type S individual to be converted than there is for it to convert the type W individual. Hence, p_S is small when D is small. When the individuals are moving quickly, they spend very little time within either interaction distance so the effects of different $r_S, r_W, \lambda_S, \lambda_W$ are lost and p_S tends to $1/2$. In Figure 5-4, we replot Figure 5-2 with values $D = 10^3$ and $D = 10^{-2}$. We see in (a) that for large D, the region where $p_S \approx 0.5$ has grown slightly compared to Figure 5-2. In (b), we see that p_S decreases significantly when D is small and individuals move slowly. This agrees with the reasoning above for Figure 5-3.

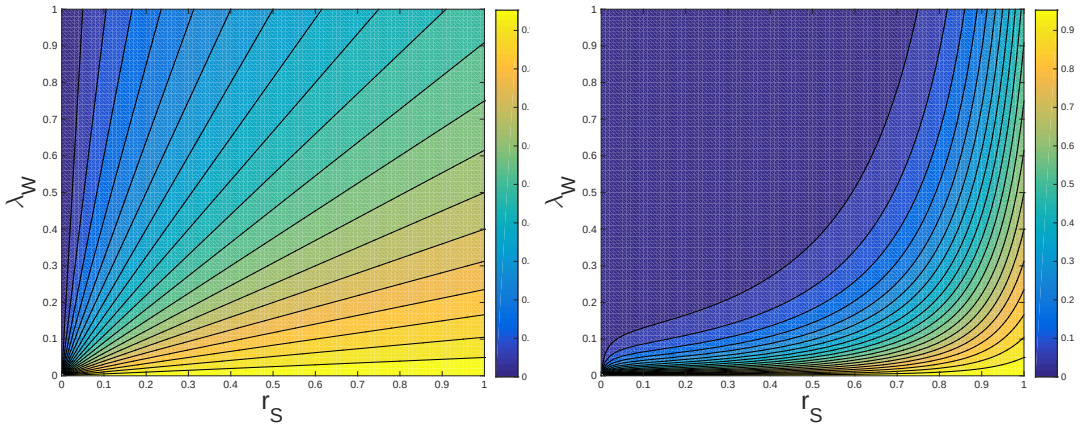

(a) (b)

Figure 5-4: The probability p_S of a type S individual winning a pair interaction varying with r_S and λ_W. The colour bar shows the probability p_S.(a) $D = 10^3$. The case we are interested in gives $p_S = 0.5$. (b) $D = 10^{-2}$. The case we are interested in gives $p_S = 0.0240$.

We have now calculated the probability p_S of an individual of type S winning a pair interaction and shown how this probability varies with the parameters $r_S, r_W, \lambda_S, \lambda_W, D$. For the case we are interested in, which is when $\lambda_W < \lambda_S$, $r_S < r_W$, and $\lambda_S r_S = 1/2 = \lambda_W r_W$, we have seen that $p_S < 1/2$ so the type W individuals always have an advantage in the pair interactions. Using these results, we can calculate the probability that a particular type survives to consensus. We do this by considering a simple birth-death process [131]. Let N be the number of individuals in the population and let $N_S(t_i), N_W(t_i)$ be the number of individuals of type S, W respectively at time t_i of the i-th pairwise meeting. Here we track time in terms of conversions. We then have $N_S(t_i)+N_W(t_i) = N$ for all t_i. Assume initially there are N_S^0 individuals of type S in the population so $N_W^0 = N - N_S^0$ gives the initial number of type W individuals. The birth-death process is then given by

$$\mathbb{P}[N_S(t_{i+1}) = n | N_S(t_i) = m] = \begin{cases} p_S & \text{if } n = m+1 \\ 1 - p_S & \text{if } n = m-1. \end{cases}$$

Now, for this birth-death process, we follow the methods in [132] and calculate

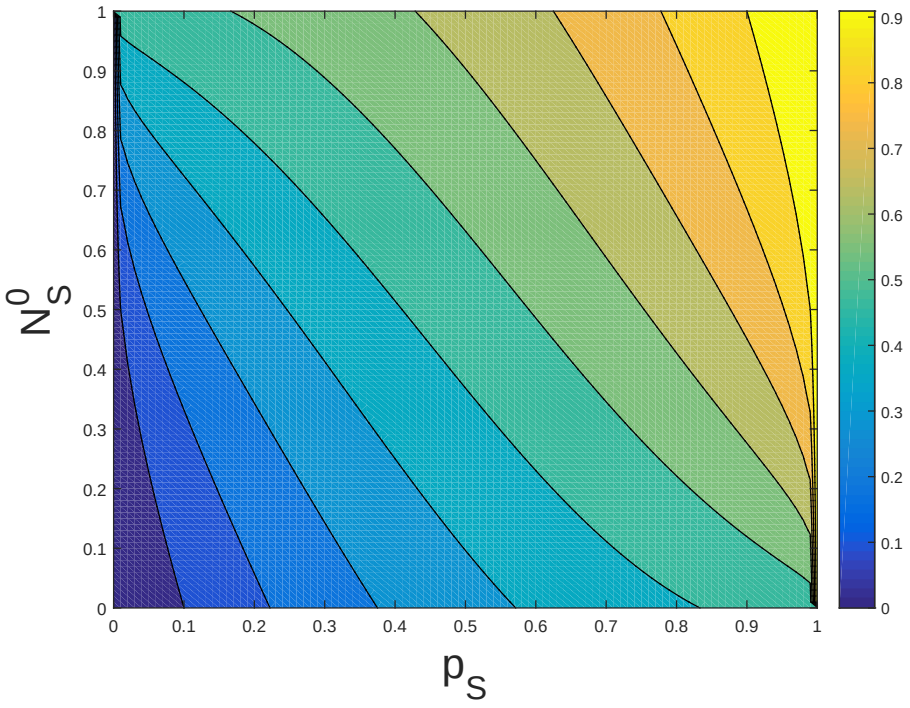

Figure 5-5: The probability P_S, shown in the colour bar, of type S individuals surviving to consensus varying with pairwise win probability p_S and initial population proportion N_S^0/N.

using recursion that the probability P_S of the type S individuals surviving to consensus with initial proportion given by $N_S(0) = N_S^0$ is given by

$$P_S = \frac{p_S^{N-N_S^0}}{p_S^{N-N_S^0} + (1-p_S)^{N_S^0}}. \tag{5.7}$$

We plot P_S in (5.7) in Figure 5-5 as a function of the pairwise win probability p_S and the proportion N_S^0/N of type S individuals initially in the population. We see that the probability of surviving to consensus increases both with pairwise win probability and with initial population proportion. In addition, even if the pairwise win probability is less than $1/2$, the type S individuals can still survive to consensus with probability greater than $1/2$ if the initial proportion is high enough.

We have seen in low density populations that when a type S and type W individual come within interaction distance of each other, the density of the location of interaction solves a stationary, second order differential equation. The

solution to this ODE can be used to determine the probability of either type winning the pairwise interaction. When we assume that the product of the interaction regions and interaction rates are equal, we find that the probability of the type S individual winning is less than $1/2$, for all diffusion rates. Using this probability we can calculate the probability of the type S individual surviving to consensus, which is also less than $1/2$. The type W individuals with a wide region of interaction and a weak interaction rate has an advantage at both the pairwise and population level for low density populations.

5.2 High-Density Regime

In this Section, we consider the same population interactions between type S and type W individuals in a high density population. In Section 5.1, the exact location of the individuals was not important because we only needed to know if a pair were within a certain distance of each other. Now that we are considering a high density population, the locations of individuals is important. For this reason, the mathematical model used for the population dynamics is different here, although we are still considering the 1D domain $[-\pi, \pi)$. We formulate the system in terms of chemical reaction equations that represent the possible interaction and movement events and population density distributions that contain the locations of all individuals of each type. Using these reaction equations and density distributions, we state the chemical master equation for the system, which will be the main focus of this Section. The extensive manipulation of the chemical master equation requires the use of functional operators and Fourier space analysis and ultimately ends with a differential equation for the dynamics of the Fourier modes of the population density distributions. Whether the Fourier modes grow or decay on average over time will determine which type survives to consensus in a high density population. We use the same notation and method used in the technical introduction to derive the FKPP equation in Section 2.2.1.

Consider a population of individuals of two types W and S. Let $W(x), S(y)$ represent individuals of type W, S at location x, y respectively. When a $W(x)$ individual and a $S(y)$ individual interact, the $W(x)$ individual wins with rate $\lambda_W(x-y) = \lambda_W \mathbb{1}_{|x-y|<r_W}$ and the $S(y)$ individual wins with rate $\lambda_S(x-y) =$

$\lambda_S \mathbb{1}_{|x-y|<r_S}$ where λ_W, λ_S are the constant interaction rates and r_W, r_S are the interaction distances. We again assume that the two types satisfy $\lambda_S > \lambda_W$ and $r_S < r_W$. Individuals of type W, S can also move from location x to location y with rate $d_W(x-y)$, $d_S(x-y)$ respectively. We summarise these dynamics using the reaction equations given by

$$\begin{aligned} W(x) + S(y) &\xrightarrow{\lambda_W(x-y)} W(x) + W(y) \\ W(x) + S(y) &\xrightarrow{\lambda_S(x-y)} S(x) + S(y) \\ W(x) &\xrightarrow{d_W(x-y)} W(y) \\ S(x) &\xrightarrow{d_S(x-y)} S(y) \end{aligned} \tag{5.8}$$

where $x, y \in [-\pi, \pi)$. We assume the individuals live on this domain without loss of generality. We are interested in periodic boundaries so that there is no influence from the environment and Fourier series sum over countably many modes, rather than integrate over a continuum.

With the chemical reaction equations for the system now defined in (5.8), we define the population density distributions ϕ_W, ϕ_S for the two types. Let N be the number of individuals in the population. In the future, we will allow $N \to \infty$ as we are interested in modelling the high density regime. To simplify the notation for the density functions, we label the individuals by integers $i \in \mathcal{N} = \{1, \dots, N\}$ and let the individuals have locations $\mathbf{x} = x_1, x_2, \dots, x_N$. Let $\mathcal{S}, \mathcal{W}$ be the set of labels for individuals of type S, W respectively, so that $\mathcal{S} \cup \mathcal{W} = \mathcal{N}$ and $\mathcal{S} \cap \mathcal{W} = \varnothing$. Then, the population density distributions for the system are given by

$$\begin{aligned} \phi_W(x, \mathbf{x}) =& \frac{1}{N} \sum_{i \in \mathcal{W}} \delta(x - x_i) \\ \phi_S(x, \mathbf{x}) =& \frac{1}{N} \sum_{i \in \mathcal{S}} \delta(x - x_i). \end{aligned} \tag{5.9}$$

We drop the $\mathbf{x}$ argument for the rest of the calculation. The coefficient of $1/N$ is required to normalise the distributions over the size of the population, i.e. so that

$$\int_{-\pi}^{\pi} \phi_W(x) dx = |\mathcal{W}|/N, \int_{-\pi}^{\pi} \phi_S(x) dx = |\mathcal{S}|/N. \tag{5.10}$$

At any point in time, the system is completely determined by ϕ_W, ϕ_S.

Recall the notation from (2.2.1) for the birth and death operators Δ_y^+, Δ_y^- at location y defined on an arbitrary function $F[\phi(x,t)]$ given by

$$\Delta_y^{\pm} F[\phi(x,t)] = F\left[\phi(x,t) \pm \frac{1}{N}\delta(x-y)\right].$$

We now define equivalent operators for the births and deaths of a particular type of individual given by $\Delta_y^{W\pm}, \Delta_y^{S\pm}$ for type W, S respectively. Recall also the notation for the movement operator given by $\Delta_{y_1}^- \Delta_{y_2}^+$ for moving from location y_1 to location y_2. We define movement operators for a particular type by $\Delta_{y_1}^{S-}\Delta_{y_2}^{S+}$ and $\Delta_{y_1}^{W-}\Delta_{y_2}^{W+}$. The two events in the system, conversion and movement, can be expressed in terms of these operators. When a type W individual is converted to type S at location y, this can be expressed as the operator $\Delta_y^{W-}\Delta_y^{S+}$. Similarly when a type S is converted to type W at location y, we have $\Delta_y^{S-}\Delta_y^{W+}$. When an individual moves to a new location, we use the movement operators defined above.

The chemical master equation for this system can now be stated using the conversion and movement operators. Let $P(\phi_W, \phi_S, t)$ be the probability of finding the system in state ϕ_W, ϕ_S at time t. There are four ways the system could end up in this state. There could be a conversion from type W to type S, a conversion from type S to type W, movement from a type W individual, or movement from a type S individual. These four events are summarised in the master equation as

$$\frac{\partial P}{\partial t}(\phi_W, \phi_S, t) = N \int_{-\pi}^{\pi}\int_{-\pi}^{\pi} Q(\phi_W, \phi_S, x, y) P(\phi_W, \phi_S, t) dx dy, \tag{5.11}$$

where

$$\begin{aligned} Q(\phi_W, \phi_S, x, y) = &(\Delta_x^{W+}\Delta_x^{S-} - 1)\lambda_S(x-y)\phi_W(x)\phi_S(y) \\ &+ (\Delta_y^{W-}\Delta_y^{S+} - 1)\lambda_W(x-y)\phi_W(x)\phi_S(y) \\ &+ (\Delta_x^{W+}\Delta_y^{W-} - 1)d_W(x-y)\phi_W(x) \\ &+ (\Delta_x^{S-}\Delta_y^{S+} - 1)d_S(x-y)\phi_S(y). \end{aligned} \tag{5.12}$$

We now begin an extensive manipulation of (5.11). We start by using the same variation of the Kramers-Moyal expansion of the conversion and movement op-

erators that we used in the technical introduction in 2.2.1. We can rewrite the operators in terms of a Taylor expansion in N^{-1}, given by

$$\Delta_x^{W\pm} \approx 1 \pm \frac{1}{N}\frac{\delta}{\delta\phi_W(x)} + \frac{1}{2N^2}\frac{\delta^2}{\delta\phi_W(x)^2}$$
$$\Delta_x^{S\pm} \approx 1 \pm \frac{1}{N}\frac{\delta}{\delta\phi_S(x)} + \frac{1}{2N^2}\frac{\delta^2}{\delta\phi_S(x)^2},$$

which ignores higher order terms in N^{-1}, which is appropriate as we are in the high density case. The pair of Δ operators can then be expressed by

$$\begin{aligned}\Delta_x^{W+}\Delta_x^{S-} = 1 &+ \frac{1}{N}\left(\frac{\delta}{\delta\phi_W(x)} - \frac{\delta}{\delta\phi_S(x)}\right) \\ &+ \frac{1}{2N^2}\left(\frac{\delta}{\delta\phi_W(x)} - \frac{\delta}{\delta\phi_S(x)}\right)^2,\end{aligned}$$

with similar expressions for the other combinations. We substitute these expressions into (5.12) to get

$$Q(\phi_W, \phi_S, x, y) = \frac{1}{N}\mathcal{A}(\phi_W, \phi_S, x, y) + \frac{1}{2N^2}\mathcal{B}(\phi_W, \phi_S, x, y),$$

where

$$\begin{aligned}\mathcal{A}(\phi_W, \phi_S, x, y) = &\left(\frac{\delta}{\delta\phi_W(x)} - \frac{\delta}{\delta\phi_S(x)}\right)\lambda_S(x-y)\phi_W(x)\phi_S(y) \\ &+ \left(\frac{\delta}{\delta\phi_S(y)} - \frac{\delta}{\delta\phi_W(y)}\right)\lambda_W(x-y)\phi_W(x)\phi_S(y) \\ &+ \left(\frac{\delta}{\delta\phi_W(x)} - \frac{\delta}{\delta\phi_W(y)}\right)d_W(x-y)\phi_W(x) \\ &+ \left(\frac{\delta}{\delta\phi_S(y)} - \frac{\delta}{\delta\phi_S(x)}\right)d_S(x-y)\phi_S(y),\end{aligned} \tag{5.13}$$

and

$$\begin{aligned}\mathcal{B}(\phi_W,\phi_S,x,y) &= \left(\frac{\delta}{\delta\phi_W(x)}-\frac{\delta}{\delta\phi_S(x)}\right)^2\lambda_S(x-y)\phi_W(x)\phi_S(y)\\ &+\left(\frac{\delta}{\delta\phi_S(y)}-\frac{\delta}{\delta\phi_W(x)}\right)^2\lambda_W(x-y)\phi_W(x)\phi_S(y)\\ &+\left(\frac{\delta}{\delta\phi_W(x)}-\frac{\delta}{\delta\phi_W(y)}\right)^2 d_W(x-y)\phi_W(x)\\ &+\left(\frac{\delta}{\delta\phi_S(y)}-\frac{\delta}{\delta\phi_S(x)}\right)^2 d_S(x-y)\phi_S(y).\end{aligned} \tag{5.14}$$

Substituting this expression for Q into (5.11) gives

$$\begin{aligned}&\frac{\partial P}{\partial t}(\phi_W,\phi_S,t)\\ &\quad=\int_{-\pi}^{\pi}\int_{-\pi}^{\pi}\left[\mathcal{A}(\phi_W,\phi_S,x,y)+\frac{1}{2N}\mathcal{B}(\phi_W,\phi_S,x,y)\right]P(\phi_W,\phi_S,t)dxdy.\end{aligned} \tag{5.15}$$

This is the functional Fokker-Planck equation. In order to make progress with the functional derivatives contained in (5.15), we move to Fourier space. Here we define the inverse Fourier transforms as

$$\phi_W(x)=\sum_n \phi_n^W e^{inx},$$

where $n\in\mathbb{Z}$ and the Fourier transform is given by

$$\phi_n^W=\frac{1}{2\pi}\int_{-\pi}^{\pi}e^{-inx}\phi_W(x)dx, \tag{5.16}$$

so that the functional derivatives are now defined as

$$\frac{\delta}{\delta\phi_W(x)}=\sum_n\frac{\delta\phi_n^W}{\delta\phi_W(x)}\frac{\delta}{\delta\phi_n^W}=\frac{1}{2\pi}\sum_n\frac{\partial}{\partial\phi_n^W}e^{-inx}.$$

The Fourier space definitions for $\phi_S(x)$ and $\delta/\delta\phi_S(x)$ are similar. We also define

$$\begin{aligned}
\lambda_W(x-y) &= \sum_k \lambda_k^W e^{ik(x-y)} \\
\lambda_S(x-y) &= \sum_k \lambda_k^S e^{ik(x-y)} \\
d_W(x-y) &= \sum_k d_k^W e^{ik(x-y)} \\
d_S(x-y) &= \sum_k d_k^S e^{ik(x-y)}.
\end{aligned}$$

Substituting these definitions into (5.13) gives

$$\mathcal{A}(\phi_W, \phi_S, x, y) = \frac{1}{2\pi} \sum_n \frac{\partial}{\partial \phi_n^W} A_n^W(\phi_W, \phi_S) + \frac{1}{2\pi} \sum_n \frac{\partial}{\partial \phi_n^S} A_n^S(\phi_W, \phi_S),$$

where

$$\begin{aligned}
A_n^W(\phi_W, \phi_S) =& \sum_{k,p,q} \lambda_k^S \phi_p^W \phi_q^S e^{i(-n+k+p)x} e^{i(-k+q)y} - \lambda_k^W \phi_p^W \phi_q^S e^{i(k+p)x} e^{i(-n-k+q)y} \\
&+ \sum_p \phi_p^W \left(e^{-inx} - e^{-iny}\right) d_W(x-y) e^{ipx},
\end{aligned}$$

and

$$\begin{aligned}
A_n^S(\phi_W, \phi_S) =& \sum_{k,p,q} \lambda_k^W \phi_p^W \phi_q^S e^{i(k+p)x} e^{i(-n-k+q)y} - \lambda_k^S \phi_p^W \phi_q^S e^{i(-n+k+p)x} e^{i(-k+q)y} \\
&+ \sum_q \phi_q^S \left(e^{-iny} - e^{-inx}\right) d_S(x-y) e^{iqy}.
\end{aligned}$$

Substituting these Fourier space definitions into (5.14) gives

$$\begin{aligned}
\mathcal{B}(\phi_W, \phi_S, x, y) =& \frac{1}{4\pi^2} \sum_{n,m} \frac{\partial}{\partial \phi_n^W} \frac{\partial}{\partial \phi_m^W} B_{n,m}^{W,W}(\phi_W, \phi_S) \\
&- \frac{1}{2\pi^2} \sum_{n,m} \frac{\partial}{\partial \phi_n^W} \frac{\partial}{\partial \phi_m^S} B_{n,m}^{W,S}(\phi_W, \phi_S) \\
&+ \frac{1}{4\pi^2} \sum_{n,m} \frac{\partial}{\partial \phi_n^S} \frac{\partial}{\partial \phi_m^S} B_{n,m}^{S,S}(\phi_W, \phi_S),
\end{aligned}$$

where

$$B^{W,W}_{n,m}(\phi_W,\phi_S) = \sum_{k,p,q} \phi^W_p \phi^S_q [\lambda^S_k e^{i(-n-m+k+p)x} e^{i(-k+q)y} + \lambda^W_k e^{i(k+p)x} e^{i(-n-m-k+q)y}] + \sum_p \phi^W_p e^{ipx} d_W(x-y)[e^{i(-n-m)x} - 2e^{-inx}e^{-imy} + e^{i(-n-m)y}],$$

$$B^{W,S}_{n,m}(\phi_W,\phi_S) = \sum_{k,p,q} \lambda^S_k \phi^W_p \phi^S_q e^{i(-n-m+k+p)x} e^{i(-k+q)y} + \sum_{k,p,q} \lambda^W_k \phi^W_p \phi^S_q e^{i(k+p)x} e^{i(-n-m-k+q)y},$$

and

$$B^{S,S}_{n,m}(\phi_W,\phi_S) = \sum_{k,p,q} \phi^W_p \phi^S_q [\lambda^S_k e^{i(-n-m+k+p)x} e^{i(-k+q)y} + \lambda^W_k e^{i(k+p)x} e^{i(-n-m-k+q)y}] + \sum_q \phi^S_q e^{iqy} d_S(x-y)[e^{i(-n-m)y} - 2e^{-iny}e^{-imx} + e^{i(-n-m)x}].$$

Substituting these equations for $\mathcal{A}(\phi_W,\phi_S,x,y)$ and $\mathcal{B}(\phi_W,\phi_S,x,y)$ into (5.15) gives

$$\begin{aligned}
\frac{\partial P}{\partial t}(\phi_W,\phi_S,t) =& \frac{1}{2\pi}\sum_n \frac{\partial}{\partial \phi^W_n} P(\phi_W,\phi_S,t) \int_{-\pi}^{\pi}\int_{-\pi}^{\pi} A^W_n(\phi_W,\phi_S)dxdy \\
&+ \frac{1}{2\pi}\sum_n \frac{\partial}{\partial \phi^S_n} P(\phi_W,\phi_S,t) \int_{-\pi}^{\pi}\int_{-\pi}^{\pi} A^S_n(\phi_W,\phi_S)dxdy \\
&+ \frac{1}{8N\pi^2}\sum_{n,m} \frac{\partial}{\partial \phi^W_n}\frac{\partial}{\partial \phi^W_m} P(\phi_W,\phi_S,t) \int_{-\pi}^{\pi}\int_{-\pi}^{\pi} B^{W,W}_{n,m}(\phi_W,\phi_S)dxdy \\
&- \frac{1}{8N\pi^2}\sum_{n,m} \frac{\partial}{\partial \phi^W_n}\frac{\partial}{\partial \phi^S_m} P(\phi_W,\phi_S,t) \int_{-\pi}^{\pi}\int_{-\pi}^{\pi} B^{W,S}_{n,m}(\phi_W,\phi_S)dxdy \\
&+ \frac{1}{8N\pi^2}\sum_{n,m} \frac{\partial}{\partial \phi^S_n}\frac{\partial}{\partial \phi^S_m} P(\phi_W,\phi_S,t) \int_{-\pi}^{\pi}\int_{-\pi}^{\pi} B^{S,S}_{n,m}(\phi_W,\phi_S)dxdy,
\end{aligned}$$

and substituting the expressions for $A^W_n, A^S_n, B^{W,W}_{n,m}, B^{W,S}_{n,m}, B^{S,S}_{n,m}$ into this equation

gives

$$
\begin{aligned}
&\frac{\partial P}{\partial t}(\phi_W,\phi_S,t) = \\
&\frac{1}{2\pi}\sum_{n,k,p,q}\lambda_k^S\phi_p^W\phi_q^S\frac{\partial}{\partial\phi_n^W}P(\phi_W,\phi_S,t)\int_{-\pi}^{\pi}\int_{-\pi}^{\pi}z_{-n+k+p,-k+q}dxdy \\
&-\frac{1}{2\pi}\sum_{n,k,p,q}\lambda_k^W\phi_p^W\phi_q^S\frac{\partial}{\partial\phi_n^W}P(\phi_W,\phi_S,t)\int_{-\pi}^{\pi}\int_{-\pi}^{\pi}z_{k+p,-n-k+q}dxdy \\
&+\sum_{n,p}\phi_p^W\frac{\partial}{\partial\phi_n^W}P(\phi_W,\phi_S,t)P_{n,p}^W(\phi_W,\phi_S) \\
&+\frac{1}{2\pi}\sum_{n,k,p,q}\lambda_k^W\phi_p^W\phi_q^S\frac{\partial}{\partial\phi_n^S}P(\phi_W,\phi_S,t)\int_{-\pi}^{\pi}\int_{-\pi}^{\pi}z_{k+p,-n-k+q}dxdy \\
&-\frac{1}{2\pi}\sum_{n,k,p,q}\lambda_k^S\phi_p^W\phi_q^S\frac{\partial}{\partial\phi_n^S}P(\phi_W,\phi_S,t)\int_{-\pi}^{\pi}\int_{-\pi}^{\pi}z_{-n+k+p,-k+q}dxdy \\
&+\sum_{n,q}\phi_q^S\frac{\partial}{\partial\phi_n^S}P(\phi_W,\phi_S,t)P_{n,q}^S(\phi_W,\phi_S) \\
&+\frac{1}{8N\pi^2}\sum_{n,m,k,p,q}\lambda_k^S\phi_p^W\phi_q^S\frac{\partial}{\partial\phi_n^W}\frac{\partial}{\partial\phi_m^W}P(\phi_W,\phi_S,t)\int_{-\pi}^{\pi}\int_{-\pi}^{\pi}z_{-n-m+k+p,-k+q}dxdy \\
&+\frac{1}{8N\pi^2}\sum_{n,m,k,p,q}\lambda_k^W\phi_p^W\phi_q^S\frac{\partial}{\partial\phi_n^W}\frac{\partial}{\partial\phi_m^W}P(\phi_W,\phi_S,t)\int_{-\pi}^{\pi}\int_{-\pi}^{\pi}z_{k+p,-n-m-k+q}dxdy \\
&+\frac{1}{4N\pi}\sum_{n,m,p}\phi_p^W\frac{\partial}{\partial\phi_n^W}\frac{\partial}{\partial\phi_m^W}P(\phi_W,\phi_S,t)P_{n,m,p}^{W,W}(\phi_W,\phi_S) \\
&-\frac{1}{8N\pi^2}\sum_{n,m,k,p,q}\lambda_k^S\phi_p^W\phi_q^S\frac{\partial}{\partial\phi_n^W}\frac{\partial}{\partial\phi_m^S}P(\phi_W,\phi_S,t)\int_{-\pi}^{\pi}\int_{-\pi}^{\pi}z_{-n-m+k+p,-k+q}dxdy \\
&-\frac{1}{8N\pi^2}\sum_{n,m,k,p,q}\lambda_k^W\phi_p^W\phi_q^S\frac{\partial}{\partial\phi_n^W}\frac{\partial}{\partial\phi_m^S}P(\phi_W,\phi_S,t)\int_{-\pi}^{\pi}\int_{-\pi}^{\pi}z_{k+p,-n-m-k+q}dxdy \\
&+\frac{1}{8N\pi^2}\sum_{n,m,k,p,q}\lambda_k^S\phi_p^W\phi_q^S\frac{\partial}{\partial\phi_n^S}\frac{\partial}{\partial\phi_m^S}P(\phi_W,\phi_S,t)\int_{-\pi}^{\pi}\int_{-\pi}^{\pi}z_{-n-m+k+p,-k+q}dxdy \\
&+\frac{1}{8N\pi^2}\sum_{n,m,k,p,q}\lambda_k^W\phi_p^W\phi_q^S\frac{\partial}{\partial\phi_n^S}\frac{\partial}{\partial\phi_m^S}P(\phi_W,\phi_S,t)\int_{-\pi}^{\pi}\int_{-\pi}^{\pi}z_{k+p,-n-m-k+q}dxdy \\
&+\frac{1}{4N\pi}\sum_{n,m,q}\phi_q^S\frac{\partial}{\partial\phi_n^S}\frac{\partial}{\partial\phi_m^S}P(\phi_W,\phi_S,t)P_{n,m,q}^{S,S}(\phi_W,\phi_S),
\end{aligned}
\tag{5.17}
$$

where

$$z_{n,m} = e^{inx}e^{imy}$$

and where

$$\begin{aligned}
P^W_{n,p}(\phi_W,\phi_S) =& \frac{1}{2\pi}\int_{-\pi}^{\pi}\int_{-\pi}^{\pi} e^{ipx}\left(e^{-inx}-e^{-iny}\right)d_W(x-y)dxdy\\
P^S_{n,q}(\phi_W,\phi_S) =& \frac{1}{2\pi}\int_{-\pi}^{\pi}\int_{-\pi}^{\pi} e^{iqy}\left(e^{-iny}-e^{-inx}\right)d_S(x-y)dxdy\\
P^{W,W}_{n,m,p}(\phi_W,\phi_S) =& \frac{1}{2\pi}\int_{-\pi}^{\pi}\int_{-\pi}^{\pi} e^{ipx}[(e^{-inx}-e^{-iny})(e^{-imx}-e^{-imy})]d_W(x-y)dxdy\\
P^{S,S}_{n,m,q}(\phi_W,\phi_S) =& \frac{1}{2\pi}\int_{-\pi}^{\pi}\int_{-\pi}^{\pi} e^{iqy}[(e^{-iny}-e^{-inx})(e^{-imy}-e^{-imx})]d_S(x-y)dxdy
\end{aligned}$$

In order to simplify $P^W_{n,p}, P^S_{n,q}, P^{W,W}_{n,m,p}, P^{S,S}_{n,m,q}$, we need to define the diffusion rates d_W, d_S. In this high density regime, we are assuming that individuals remain static at some location x and then move to location y with rate $d_W(x-y)$ or $d_S(x-y)$ for either type. To model this here we assume that type W and type S individuals remain static at some location x and then move to location y with rate $d_W(x-y), d_S(x-y)$ respectively. In order to resolve the difference between the microscopic Brownian motion we want to model and the framework we are using here, we assume that individuals move at random times that are exponentially distributed with rates γ_W, γ_S. The distance traveled is a normal random variable with mean zero and variance $D_W/\gamma_W, D_S/\gamma_S$. In the limit $\gamma_W, \gamma_S \to \infty$, the movement of the individuals converges to Brownian motion with diffusion coefficients D_W, D_S, which is the movement we want to model. Hence, we set

$$\begin{aligned}
d_W(x-y) =& \frac{\gamma_W}{\sqrt{2\pi D_W/\gamma_W}}\exp\left(\frac{-\gamma_W(x-y)^2}{2D_W}\right)\\
d_S(x-y) =& \frac{\gamma_S}{\sqrt{2\pi D_S/\gamma_S}}\exp\left(\frac{-\gamma_S(x-y)^2}{2D_S}\right).
\end{aligned}$$

This choice means that we can approximate $P^W_{n,p}, P^S_{n,q}$ by

$$\begin{aligned}
P^W_{n,p}(\phi_W,\phi_S) &\approx \frac{D_W}{2}n^2\delta_{n,p}\\
P^S_{n,q}(\phi_W,\phi_S) &\approx \frac{D_S}{2}n^2\delta_{n,q}
\end{aligned}$$

which follows from

$$\begin{aligned} P^W_{n,p}(\phi_W,\phi_S) =& \frac{1}{2\pi}\int_{-\pi}^{\pi}\int_{-\pi}^{\pi} e^{ipx}\left(e^{-inx}-e^{-iny}\right) d_W(x-y)dxdy \\ =& \frac{\gamma_W}{2\pi\sqrt{2\pi D_W/\gamma_W}}\int_{-\pi}^{\pi}\int_{-\pi}^{\pi} e^{ipx-inx-\frac{\gamma_W(x-y)^2}{2D_W}}dxdy \\ -& \frac{\gamma_W}{2\pi\sqrt{2\pi D_W/\gamma_W}}\int_{-\pi}^{\pi}\int_{-\pi}^{\pi} e^{ipx-iny-\frac{\gamma_W(x-y)^2}{2D_W}}dxdy. \end{aligned} \tag{5.18}$$

For the first integral in the last line of (5.18), after switching the order of integration, we have

$$\begin{aligned} &\frac{\gamma_W}{2\pi\sqrt{2\pi D_W/\gamma_W}}\int_{-\pi}^{\pi}\int_{-\pi}^{\pi} e^{ipx-inx-\frac{\gamma_W(x-y)^2}{2D_W}}dydx \\ &= \frac{\gamma_W}{2\pi\sqrt{2\pi D_W/\gamma_W}}\int_{-\pi}^{\pi} e^{ipx-inx}\int_{-\pi}^{\pi} e^{-\frac{\gamma_W(x-y)^2}{2D_W}}dydx \\ &\approx \frac{\gamma_W}{2\pi\sqrt{2\pi D_W/\gamma_W}}\int_{-\pi}^{\pi} e^{ipx-inx}\int_{-\infty}^{\infty} e^{-\frac{\gamma_W(x-y)^2}{2D_W}}dydx \\ &= \frac{\gamma_W}{2\pi}\int_{-\pi}^{\pi} e^{ipx-inx}dx = \gamma_W\delta_{n,p}, \end{aligned}$$

where the third line follows from the large γ_W approximation and the fourth line from the Gaussian curve integrating to one. For the second integral in the last

line of (5.18), also switching the order of integration, we have

$$
\begin{aligned}
&-\frac{\gamma_W}{2\pi\sqrt{2\pi D_W/\gamma_W}}\int_{-\pi}^{\pi}\int_{-\pi}^{\pi} e^{ipx-iny-\frac{\gamma_W(x-y)^2}{2D_W}}dydx\\
&=-\frac{\gamma_W}{2\pi\sqrt{2\pi D_W/\gamma_W}}\int_{-\pi}^{\pi}\int_{-\pi}^{\pi} e^{-\frac{\gamma_W}{2D_W}\left[(y-x+in\frac{\gamma_W}{D_W})^2-ip\frac{2D_W}{\gamma_W}x+x^2-\frac{1}{4}(2x-2in\frac{D_W}{\gamma_W})^2\right]}dydx\\
&=-\frac{\gamma_W}{2\pi\sqrt{2\pi D_W/\gamma_W}}\int_{-\pi}^{\pi} e^{-\frac{\gamma_W}{2D_W}\left[-ip\frac{2D_W}{\gamma_W}x+x^2-\frac{1}{4}(2x-2in\frac{D_W}{\gamma_W})^2\right]}\\
&\qquad\qquad\qquad\qquad\qquad\qquad\qquad\qquad\qquad\qquad\int_{-\pi}^{\pi} e^{-\frac{\gamma_W}{2D_W}(y-x+in\frac{\gamma_W}{D_W})^2}dydx\\
&=-\frac{\gamma_W}{2\pi}\int_{-\pi}^{\pi} e^{-\frac{\gamma_W}{2D_W}\left[-ip\frac{2D_W}{\gamma_W}x+x^2-\frac{1}{4}(2x-2in\frac{D_W}{\gamma_W})^2\right]}dx\\
&=-\frac{\gamma_W}{2\pi}\int_{-\pi}^{\pi} e^{-\frac{\gamma_W}{2D_W}\left[\frac{D_W^2}{\gamma_W^2}n^2+\frac{2D_W}{\gamma_W}x(n-p)i\right]}dx=-\frac{\gamma_W}{2\pi}\int_{-\pi}^{\pi} e^{-\frac{D_W}{2\gamma_W}n^2-x(n-p)i}dx\\
&=-\frac{\gamma_W}{2\pi}e^{-\frac{D_W}{2\gamma_W}n^2}\int_{-\pi}^{\pi} e^{-x(n-p)i}dx=-\gamma_W e^{-\frac{D_W}{2\gamma_W}n^2}\delta_{n,p}.
\end{aligned}
$$

Hence,

$$
\begin{aligned}
P^W_{n,p}(\phi_W,\phi_S)&=\gamma_W\delta_{n,p}-\gamma_W e^{-\frac{D_W}{2\gamma_W}n^2}\delta_{n,p}=\gamma_W(1-e^{-\frac{D_W}{2\gamma_W}n^2})\delta_{n,p}\\
&\approx\gamma_W\frac{D_W}{2\gamma_W}n^2\delta_{n,p}=\frac{D_W}{2}n^2\delta_{n,p},
\end{aligned}
$$

where the approximation follows as we only need to consider small $1/\gamma_W$ as we are only interested in the case when $\gamma_W\to\infty$. The calculation for $P^S_{n,q}$ is similar. We can approximate $P^{W,W}_{n,m,p}, P^{S,S}_{n,m,q}$ by

$$
\begin{aligned}
P^{W,W}_{n,m,p}(\phi_W,\phi_S)&\approx -D_W mn\delta_{n+m,p}\\
P^{S,S}_{n,m,q}(\phi_W,\phi_S)&\approx -D_S mn\delta_{n+m,q},
\end{aligned}
$$

which follows from

$$
\begin{aligned}
P^{W,W}_{n,m,p}(\phi_W,\phi_S) &= \frac{1}{2\pi}\int_{-\pi}^{\pi}\int_{-\pi}^{\pi} e^{ipx}[(e^{-inx}-e^{-iny})(e^{-imx}-e^{-imy})]d_W(x-y)dxdy \\
&= \frac{\gamma_W}{2\pi\sqrt{2\pi D_W/\gamma_W}}\int_{-\pi}^{\pi}\int_{-\pi}^{\pi} e^{ipx}[e^{i(-n-m)x}-e^{-inx}e^{-imy}-e^{-imx}e^{-iny}+e^{i(-n-m)y}] \\
&\qquad\qquad \exp\left(\frac{-\gamma_W(x-y)^2}{2D_W}\right)dxdy \\
&= \frac{\gamma_W}{2\pi\sqrt{2\pi D_W/\gamma_W}}\int_{-\pi}^{\pi}\int_{-\pi}^{\pi} e^{ipx-\frac{\gamma_W(x-y)^2}{2D_W}-ix(n+m)} - e^{ipx-\frac{\gamma_W(x-y)^2}{2D_W}-ixn-imy} \\
&\qquad\qquad - e^{ipx-\frac{\gamma_W(x-y)^2}{2D_W}-imx-iny} + e^{ipx-\frac{\gamma_W(x-y)^2}{2D_W}-iy(n+m)}dxdy \\
&= \frac{\gamma_W}{2\pi\sqrt{2\pi D_W/\gamma_W}}\int_{-\pi}^{\pi}\int_{-\pi}^{\pi} e^{ipx-\frac{\gamma_W(x-y)^2}{2D_W}-ix(n+m)}dxdy \\
&- \frac{\gamma_W}{2\pi\sqrt{2\pi D_W/\gamma_W}}\int_{-\pi}^{\pi}\int_{-\pi}^{\pi} e^{ipx-\frac{\gamma_W(x-y)^2}{2D_W}-inx-imy}dxdy \\
&- \frac{\gamma_W}{2\pi\sqrt{2\pi D_W/\gamma_W}}\int_{-\pi}^{\pi}\int_{-\pi}^{\pi} e^{ipx-\frac{\gamma_W(x-y)^2}{2D_W}-imx-iny}dxdy \\
&+ \frac{\gamma_W}{2\pi\sqrt{2\pi D_W/\gamma_W}}\int_{-\pi}^{\pi}\int_{-\pi}^{\pi} e^{ipx-\frac{\gamma_W(x-y)^2}{2D_W}-iy(n+m)}dxdy.
\end{aligned}
\tag{5.19}
$$

The first integral in the last line of (5.19) follows the calculation of the first integral in the last line of (5.18) to get

$$
\frac{\gamma_W}{2\pi\sqrt{2\pi D_W/\gamma_W}}\int_{-\pi}^{\pi}\int_{-\pi}^{\pi} e^{ipx-\frac{\gamma_W(x-y)^2}{2D_W}-ix(n+m)}dxdy = \gamma_W\delta_{n+m,p}.
$$

The second, third, and fourth integrals in the last line of (5.19) follow the calculation of the second integral in the last line of (5.18) to get

$$
\begin{aligned}
&- \frac{\gamma_W}{2\pi\sqrt{2\pi D_W/\gamma_W}}\int_{-\pi}^{\pi}\int_{-\pi}^{\pi} e^{ipx-\frac{\gamma_W(x-y)^2}{2D_W}-inx-imy}dxdy = -\gamma_W e^{-\frac{D_W}{2\gamma_W}m^2}\delta_{m,p-n} \\
&- \frac{\gamma_W}{2\pi\sqrt{2\pi D_W/\gamma_W}}\int_{-\pi}^{\pi}\int_{-\pi}^{\pi} e^{ipx-\frac{\gamma_W(x-y)^2}{2D_W}-imx-iny}dxdy = -\gamma_W e^{-\frac{D_W}{2\gamma_W}n^2}\delta_{n,p-m} \\
&\frac{\gamma_W}{2\pi\sqrt{2\pi D_W/\gamma_W}}\int_{-\pi}^{\pi}\int_{-\pi}^{\pi} e^{ipx-\frac{\gamma_W(x-y)^2}{2D_W}-iy(n+m)}dxdy = \gamma_W e^{-\frac{D_W}{2\gamma_W}(n+m)^2}\delta_{n+m,p}.
\end{aligned}
$$

Hence, $P^{W,W}_{n,m,p}(\phi_W, \phi_S)$ is given by

$$\begin{aligned}
P^{W,W}_{n,m,p}(\phi_W, \phi_S) &= \gamma_W \delta_{n+m,p} - \gamma_W e^{-\frac{D_W}{2\gamma_W} m^2} \delta_{m,p-n} - \gamma_W e^{-\frac{D_W}{2\gamma_W} n^2} \delta_{n,p-m} \\
&\quad + \gamma_W e^{-\frac{D_W}{2\gamma_W}(n+m)^2} \delta_{n+m,p} \\
&= \gamma_W (1 - e^{-\frac{D_W}{2\gamma_W} m^2} - e^{-\frac{D_W}{2\gamma_W} n^2} + e^{-\frac{D_W}{2\gamma_W}(n+m)^2}) \delta_{n+m,p} \\
&\approx \frac{D_W}{2} (m^2 + n^2 - (n+m)^2) \delta_{n+m,p} \\
&= -D_W mn \delta_{n+m,p},
\end{aligned}$$

where the approximation follows as we only need to consider small $1/\gamma_W$ as we are only interested in the case when $\gamma_W \to \infty$. The result for $P^{S,S}_{n,m,q}(\phi_W, \phi_S)$ is

similar. Using these results, the master equation is now given by

$$
\begin{aligned}
&\frac{\partial P}{\partial t}(\phi_W,\phi_S,t) = \\
&\frac{1}{2\pi}\sum_{n,k,p,q}\lambda_k^S\phi_p^W\phi_q^S\frac{\partial}{\partial\phi_n^W}P(\phi_W,\phi_S,t)\int_{-\pi}^{\pi}\int_{-\pi}^{\pi}z_{-n+k+p,-k+q}dxdy \\
&-\frac{1}{2\pi}\sum_{n,k,p,q}\lambda_k^W\phi_p^W\phi_q^S\frac{\partial}{\partial\phi_n^W}P(\phi_W,\phi_S,t)\int_{-\pi}^{\pi}\int_{-\pi}^{\pi}z_{k+p,-n-k+q}dxdy \\
&+\sum_{n,p}\phi_p^W\frac{\partial}{\partial\phi_n^W}P(\phi_W,\phi_S,t)\frac{D_W}{2}n^2\delta_{n,p} \\
&+\frac{1}{2\pi}\sum_{n,k,p,q}\lambda_k^W\phi_p^W\phi_q^S\frac{\partial}{\partial\phi_n^S}P(\phi_W,\phi_S,t)\int_{-\pi}^{\pi}\int_{-\pi}^{\pi}z_{k+p,-n-k+q}dxdy \\
&-\frac{1}{2\pi}\sum_{n,k,p,q}\lambda_k^S\phi_p^W\phi_q^S\frac{\partial}{\partial\phi_n^S}P(\phi_W,\phi_S,t)\int_{-\pi}^{\pi}\int_{-\pi}^{\pi}z_{-n+k+p,-k+q}dxdy \\
&+\sum_{n,q}\phi_q^S\frac{\partial}{\partial\phi_n^S}P(\phi_W,\phi_S,t)\frac{D_S}{2}n^2\delta_{n,q} \\
&+\frac{1}{8N\pi^2}\sum_{n,m,k,p,q}\lambda_k^S\phi_p^W\phi_q^S\frac{\partial}{\partial\phi_n^W}\frac{\partial}{\partial\phi_m^W}P(\phi_W,\phi_S,t)\int_{-\pi}^{\pi}\int_{-\pi}^{\pi}z_{-n-m+k+p,-k+q}dxdy \\
&+\frac{1}{8N\pi^2}\sum_{n,m,k,p,q}\lambda_k^W\phi_p^W\phi_q^S\frac{\partial}{\partial\phi_n^W}\frac{\partial}{\partial\phi_m^W}P(\phi_W,\phi_S,t)\int_{-\pi}^{\pi}\int_{-\pi}^{\pi}z_{k+p,-n-m-k+q}dxdy \\
&-\frac{1}{4N\pi}\sum_{n,m,p}\phi_p^W\frac{\partial}{\partial\phi_n^W}\frac{\partial}{\partial\phi_m^W}P(\phi_W,\phi_S,t)D_W mn\delta_{n+m,p} \\
&-\frac{1}{8N\pi^2}\sum_{n,m,k,p,q}\lambda_k^S\phi_p^W\phi_q^S\frac{\partial}{\partial\phi_n^W}\frac{\partial}{\partial\phi_m^S}P(\phi_W,\phi_S,t)\int_{-\pi}^{\pi}\int_{-\pi}^{\pi}z_{-n-m+k+p,-k+q}dxdy \\
&-\frac{1}{8N\pi^2}\sum_{n,m,k,p,q}\lambda_k^W\phi_p^W\phi_q^S\frac{\partial}{\partial\phi_n^W}\frac{\partial}{\partial\phi_m^S}P(\phi_W,\phi_S,t)\int_{-\pi}^{\pi}\int_{-\pi}^{\pi}z_{k+p,-n-m-k+q}dxdy \\
&+\frac{1}{8N\pi^2}\sum_{n,m,k,p,q}\lambda_k^S\phi_p^W\phi_q^S\frac{\partial}{\partial\phi_n^S}\frac{\partial}{\partial\phi_m^S}P(\phi_W,\phi_S,t)\int_{-\pi}^{\pi}\int_{-\pi}^{\pi}z_{-n-m+k+p,-k+q}dxdy \\
&+\frac{1}{8N\pi^2}\sum_{n,m,k,p,q}\lambda_k^W\phi_p^W\phi_q^S\frac{\partial}{\partial\phi_n^S}\frac{\partial}{\partial\phi_m^S}P(\phi_W,\phi_S,t)\int_{-\pi}^{\pi}\int_{-\pi}^{\pi}z_{k+p,-n-m-k+q}dxdy \\
&-\frac{1}{4N\pi}\sum_{n,m,q}\phi_q^S\frac{\partial}{\partial\phi_n^S}\frac{\partial}{\partial\phi_m^S}P(\phi_W,\phi_S,t)D_S mn\delta_{n+m,q},
\end{aligned}
$$

For the remaining integrals, we note that they will vanish unless both exponential

powers are equal to zero because we are not integrating around any poles in the complex plane according to the Cauchy Theorem [66]. Hence, we require the powers to be equal to zero. When the powers are equal to zero, each integral for the x and y variables is equal to 2π. This considerably simplifies the master equation to give

$$\begin{aligned}
&\frac{\partial P}{\partial t}(\phi_W, \phi_S, t) = \\
&-\sum_n \frac{\partial}{\partial \phi_n^W} P(\phi_W, \phi_S, t) \left[\sum_k 2\pi(\lambda_k^W \phi_{-k}^W \phi_{n+k}^S - \lambda_k^S \phi_{n-k}^W \phi_k^S) - \phi_n^W D_W \frac{n^2}{2} \right] \\
&-\sum_n \frac{\partial}{\partial \phi_n^S} P(\phi_W, \phi_S, t) \left[\sum_k 2\pi(\lambda_k^S \phi_{n-k}^W \phi_k^S - \lambda_k^W \phi_{-k}^W \phi_{n+k}^S) - \phi_n^S D_S \frac{n^2}{2} \right] \\
&+\frac{1}{2N} \sum_{n,m} \frac{\partial}{\partial \phi_n^W} \frac{\partial}{\partial \phi_m^W} P(\phi_W, \phi_S, t) \left[\sum_k \eta(n,m,k) - \frac{1}{2\pi} \phi_{n+m}^W D_W nm \right] \\
&-\frac{1}{2N} \sum_{n,m} \frac{\partial}{\partial \phi_n^W} \frac{\partial}{\partial \phi_m^S} P(\phi_W, \phi_S, t) \left[\sum_k \lambda_k^S \phi_{n+m-k}^W \phi_k^S + \lambda_k^W \phi_{-k}^W \phi_{n+m+k}^S \right] \\
&+\frac{1}{2N} \sum_{n,m} \frac{\partial}{\partial \phi_n^S} \frac{\partial}{\partial \phi_m^S} P(\phi_W, \phi_S, t) \left[\sum_k \eta(n,m,k) - \frac{1}{2\pi} \phi_{n+m}^S D_S nm \right],
\end{aligned} \tag{5.20}$$

where

$$\eta(n,m,k) = \phi_{n+m-k}^W \phi_k^S \lambda_k^S + \phi_{-k}^W \phi_{n+m+k}^S \lambda_k^W .$$

This is the Fourier Fokker-Planck equation for the system in terms of functional derivatives and Fourier modes. We can now use this master equation to derive differential equations for the Fourier modes ϕ_n^W, ϕ_n^S. To do this, we let $N \to \infty$ for a high density population to get

$$\begin{aligned}
&\frac{\partial P}{\partial t}(\phi_W, \phi_S, t) = \\
&-\sum_n \frac{\partial}{\partial \phi_n^W} P(\phi_W, \phi_S, t) \left[\sum_k 2\pi(\lambda_k^W \phi_{-k}^W \phi_{n+k}^S - \lambda_k^S \phi_{n-k}^W \phi_k^S) - \phi_n^W D_W \frac{n^2}{2} \right] \\
&-\sum_n \frac{\partial}{\partial \phi_n^S} P(\phi_W, \phi_S, t) \left[\sum_k 2\pi(\lambda_k^S \phi_{n-k}^W \phi_k^S - \lambda_k^W \phi_{-k}^W \phi_{n+k}^S) - \phi_n^S D_S \frac{n^2}{2} \right].
\end{aligned}$$

The functional master equation for our system is now in the form of the Liouville

equation [60], which is a special case of the forward Fokker-Planck equation (2.5) when $b(x,t) = 0$. This high density master equation has solutions ϕ_n^W, ϕ_n^S when

$$\begin{aligned} \frac{d}{dt}\phi_n^W &= \sum_k 2\pi(\lambda_k^W \phi_{-k}^W \phi_{n+k}^S - \lambda_k^S \phi_{n-k}^W \phi_k^S) - \phi_n^W D_W \frac{n^2}{2} \\ \frac{d}{dt}\phi_n^S &= \sum_k 2\pi(\lambda_k^S \phi_{n-k}^W \phi_k^S - \lambda_k^W \phi_{-k}^W \phi_{n+k}^S) - \phi_n^S D_S \frac{n^2}{2}\,. \end{aligned} \tag{5.21}$$

These differential equations show how the Fourier modes depend on conversion and diffusion. We note that $\frac{d}{dt}(\phi_0^W + \phi_0^S) = 0$ so $\phi_0^W + \phi_0^S$ is a constant. To determine this constant, recall from (5.10) that

$$\int_{-\pi}^{\pi} \phi_W(x)dx = |\mathcal{W}|/N, \int_{-\pi}^{\pi} \phi_S(x)dx = |\mathcal{S}|/N$$

and recall the definitions for ϕ_0^W, ϕ_0^S in (5.16) so that

$$\phi_0^W + \phi_0^S = \frac{1}{2\pi}\int_{-\pi}^{\pi} \phi_W(x) + \phi_S(x)dx = \frac{1}{2\pi}.$$

For $n \neq 0$, we have $\frac{d}{dt}(\phi_n^W + \phi_n^S) = -Dn^2(\phi_n^W + \phi_n^S)/2$ which has solution $\phi_n^W + \phi_n^S = Ae^{-Dn^2t/2}$ for some constant A. As time increases, $\phi_n^W + \phi_n^S$ quickly decays to zero, so we have the condition $\phi_n^W + \phi_n^S = 0$. A simple check shows that (5.21) has a family of solutions given by

$$\phi_n^W = \frac{\tau}{2\pi}\delta_{n,0}, \quad \phi_n^S = \frac{1-\tau}{2\pi}\delta_{n,0},$$

for all $\tau \in [0,1]$. These solutions correspond to the scenario where a proportion τ of individuals are of type W and the remaining $1-\tau$ proportion are of type S. There may be other solutions but we focus only on this family of solutions here as they are an example of how demographic noise can influence the stability of a solution, which will be shown in the rest of this Section. Each of these solutions is linearly stable in this $N \to \infty$ regime. If instead N is large but finite, there will be small fluctuations in the Fourier modes which could result in a change in the solutions and in their stability. To explore this possibility, we consider an

ansatz given by

$$\phi_n^W = \frac{\tau}{2\pi}\delta_{n,0} + \frac{1}{\sqrt{N}}\alpha_n\,, \quad \phi_n^S = \frac{1-\tau}{2\pi}\delta_{n,0} - \frac{1}{\sqrt{N}}\alpha_n\,, \tag{5.22}$$

where α_n is Gaussian white noise with mean zero and unit variance, as defined in the technical introduction in Section 2.1.1. The noise terms have opposite signs to ensure that we still satisfy the condition $\phi_n^W + \phi_n^S = \delta_{n,0}/2\pi$. Also, we only need to consider ϕ_n^W as we can use this condition to work out ϕ_n^S. Recall as well from the Chapter introduction that we choose the two types so that the product of the interaction distance and interaction rate is equal. This means that we choose $\lambda_W, \lambda_S, r_W, r_S$ such that

$$\int_{-\pi}^{\pi} \lambda_W(x)dx = \int_{-r_W}^{r_W} \lambda_W dx = 2r_W\lambda_W = 2r_S\lambda_S = \int_{-r_S}^{r_S} \lambda_S dx = \int_{-\pi}^{\pi} \lambda_S(x)dx.$$

Hence, we have that $\lambda_0^W = \lambda_0^S$ as

$$\lambda_0^W = \frac{1}{2\pi}\int_{-\pi}^{\pi} \lambda_W(x)dx = \frac{1}{2\pi}\int_{-\pi}^{\pi} \lambda_S(x)dx = \lambda_0^S.$$

Now, substituting the ansatz (5.22) into (5.21) gives

$$\frac{d}{dt}\tau = \frac{1}{N}\sum_{k\neq 0}(\lambda_k^S - \lambda_k^W)|\alpha_k|^2. \tag{5.23}$$

The sign of the summand in this equation is determined by the sign of $\lambda_k^S - \lambda_k^W$ as $|\alpha_k|^2$ is positive. If $\lambda_k^S - \lambda_k^W$ is always positive, then the sum and the right hand side of that equation are positive and the proportion of the population of type W increases. If $\lambda_k^S - \lambda_k^W$ is always negative, the proportion of the population decreases. The sign of this factor is determined by the interaction functions $\lambda_W(x), \lambda_S(x)$. Recall from (5.16) that the Fourier modes are defined by

$$\begin{aligned}
\lambda_0^W &= \frac{1}{2\pi}\int_{-\pi}^{\pi} \lambda_W(x)dx = \frac{\lambda_W}{2\pi}\int_{-r_W}^{r_W} dx = \frac{\lambda_W r_W}{\pi} \\
\lambda_k^W &= \frac{1}{2\pi}\int_{-\pi}^{\pi} e^{-ikx}\lambda_W(x)dx = \frac{\lambda_W}{2\pi}\int_{-r_W}^{r_W} e^{-ikx}dx \\
&= \frac{\lambda_W}{2\pi}\frac{-1}{ik}(e^{ikr_W} - e^{-ikr_W}) = -\frac{\lambda_W}{k\pi}\sin(kr_W),
\end{aligned}$$

and similarly $\lambda_0^S = \frac{\lambda_S r_S}{\pi}, \lambda_k^S = -\lambda_S \sin(kr_S)/k\pi$ for $k \neq 0$. Substituting these values into (5.23) gives

$$\frac{d}{dt}\tau = \frac{1}{N}\sum_{k\neq 0}\frac{1}{k\pi}(\lambda_W \sin(kr_W) - \lambda_S \sin(kr_S))|\alpha_k|^2.$$

The term $\lambda_W \sin(kr_W) - \lambda_S \sin(kr_S)$ is not always positive or always negative. In order to determine if the proportion of type W individuals increases or decreases, we have to calculate the value of the full sum, which cannot be done until we have an equation for $|\alpha_k|^2$. To calculate this, we return to (5.20). Multiplying by $\phi_n^W \phi_{-n}^S$ and integrating gives

$$\begin{aligned}\frac{d}{dt}\phi_n^W\phi_{-n}^S &= \phi_{-n}^S\left(\sum_k 2\pi(\lambda_k^W\phi_{-k}^W\phi_{n+k}^S - \lambda_k^S\phi_{n-k}^W\phi_k^S) - \phi_n^W D_W\frac{n^2}{2}\right)\\ &\quad + \phi_n^W\left(\sum_k 2\pi(\lambda_k^S\phi_{n-k}^W\phi_k^S - \lambda_k^W\phi_{-k}^W\phi_{n+k}^S) - \phi_n^S D_S\frac{n^2}{2}\right)\\ &\quad - \frac{1}{N}\left(\sum_k \lambda_k^S\phi_{-k}^W\phi_k^S + \lambda_k^W\phi_{-k}^W\phi_k^S\right).\end{aligned} \tag{5.24}$$

Now for $n \neq 0$ the ansatz (5.22) gives us $\phi_n^W\phi_{-n}^S = -|\alpha_n|^2/N$. Substituting the ansatz into (5.24) gives

$$\begin{aligned}\frac{d}{dt}|\alpha_n|^2 &= -N\frac{d}{dt}\phi_n^W\phi_{-n}^S\\ &= -N\phi_{-n}^S\left(\sum_k 2\pi(\lambda_k^W\phi_{-k}^W\phi_{n+k}^S - \lambda_k^S\phi_{n-k}^W\phi_k^S) - \phi_n^W D_W\frac{n^2}{2}\right)\\ &\quad - N\phi_n^W\left(\sum_k 2\pi(\lambda_k^S\phi_{n-k}^W\phi_k^S - \lambda_k^W\phi_{-k}^W\phi_{n+k}^S) - \phi_n^S D_S\frac{n^2}{2}\right)\\ &\quad + \left(\sum_k \lambda_k^S\phi_{-k}^W\phi_k^S + \lambda_k^W\phi_{-k}^W\phi_k^S\right)\\ &= -|\alpha_n|^2\left(4\pi[(\lambda_{-n}^W - \lambda_0^S)(1-\tau) + (\lambda_n^S - \lambda_0^W)\tau] + (D_W + D_S)\frac{n^2}{2}\right)\\ &\quad + (\lambda_0^S + \lambda_0^W)\tau(1-\tau) + \mathcal{O}(N^{-1/2}),\end{aligned}$$

so we have a differential equation for the noise α_n for large but finite N given by

$$\frac{d}{dt}|\alpha_n|^2 = -\psi_n|\alpha_n|^2 + \sigma \tag{5.25}$$

where we note that $\lambda^W_{-n} = \lambda^W_n$ and $\lambda^S_{-n} = \lambda^S_n$ and where

$$\begin{aligned}\psi_n &= 4\pi[(\lambda^W_n - \lambda^S_0)(1-\tau) + (\lambda^S_n - \lambda^W_0)\tau] + (D_W + D_S)\frac{n^2}{2} \\ \sigma &= (\lambda^S_0 + \lambda^W_0)\tau(1-\tau)\ .\end{aligned}$$

The solution to (5.25) is given by

$$|\alpha_n|^2 = \frac{\sigma - e^{-\psi_n(t-C)}}{\psi_n},$$

for some constant C. The noise equilibrates quickly for $\psi_n > 0$ so we can make the approximation $|\alpha_n|^2 \approx \sigma/\psi_n$ and substitute into (5.23) to get

$$\frac{d}{dt}\tau = \frac{1}{N}\sum_{k\neq 0}\frac{(\lambda^S_k - \lambda^W_k)(\lambda^S_0 + \lambda^W_0)\tau(1-\tau)}{4\pi[(\lambda^W_k - \lambda^S_0)(1-\tau) + (\lambda^S_k - \lambda^W_0)\tau] + (D_W + D_S)\frac{k^2}{2}} \tag{5.26}$$

Substituting the Fourier modes into (5.26) gives

$$\frac{d}{dt}\tau = \frac{(\lambda_S r_S + \lambda_W r_W)\tau(1-\tau)}{N\pi^2}$$
$$\sum_{k\neq 0}\frac{\lambda_W \sin(kr_W) - \lambda_S \sin(kr_S)}{(D_W + D_S)\frac{k^3}{2} - 4k[(\frac{\lambda_W}{k}\sin(kr_W) + \lambda_S r_S)(1-\tau) + (\frac{\lambda_S}{k}\sin(kr_S) + \lambda_W r_W)\tau]}$$

This is now an ODE for the zero mode in terms of the Fourier modes λ^S_k, λ^W_k and the diffusion rates D_W, D_S. Recall from the Chapter introduction that we are interested in the case where $\lambda_W < \lambda_S$, $r_S < r_W$, and $\lambda_S r_S = \lambda_W r_W = 1/2$ so we can set $\lambda_S = 1/2r_S, \lambda_W = 1/2r_W$. Making this substitution gives

$$\frac{d}{dt}\tau = \frac{\tau(1-\tau)}{N\pi^2}$$
$$\sum_{k\neq 0}\frac{\frac{1}{2r_W}\sin(kr_W) - \frac{1}{2r_S}\sin(kr_S)}{(D_W + D_S)\frac{k^3}{2} - 4k[(\frac{1}{2kr_W}\sin(kr_W) + 1/2)(1-\tau) + (\frac{1}{2kr_S}\sin(kr_S) + 1/2)\tau]}. \tag{5.27}$$

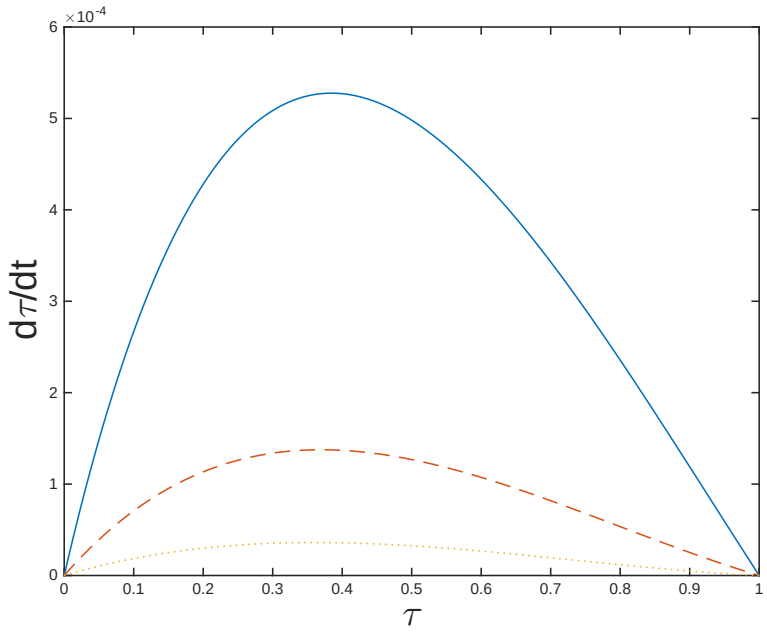

Figure 5-6: The value of $d\tau/dt$ in (5.27) as a function of τ for different values of r_S. $r_W = 1, \lambda_W = 1/2r_W, \lambda_S = 1/2r_S, D = 0, N = 100$ and we take the first 1000 positive and negative modes. Solid line $r_S = 0.2$, dashed line $r_S = 0.5$, dotted line $r_S = 0.8$.

We plot (5.27) as a function of τ in Figure 5-6 for different values of r_S. We see that $d\tau/dt$ is always positive and that when r_S is closer to $r_W = 1$, the effects of the noise is weakened. It then follows that introducing noise for large but finite N results in the proportion of individuals of type W always increasing. Hence, the type W individuals will survive to consensus in this regime.

When $D = 0$, $d\tau/dt$ is always positive. For small but positive values of D, the sign of $d\tau/dt$ changes depending on the value of τ. This is shown in Figure 5-7.

5.3 Conclusion

In this Chapter, we have considered the novel model of nonlocal interaction and diffusion in the voter model. One type of individual has a high interaction rate with individuals very close while the other type has a low interaction rate with individuals very far away. The mathematics required for low density and high density population are very different. For a low density population,

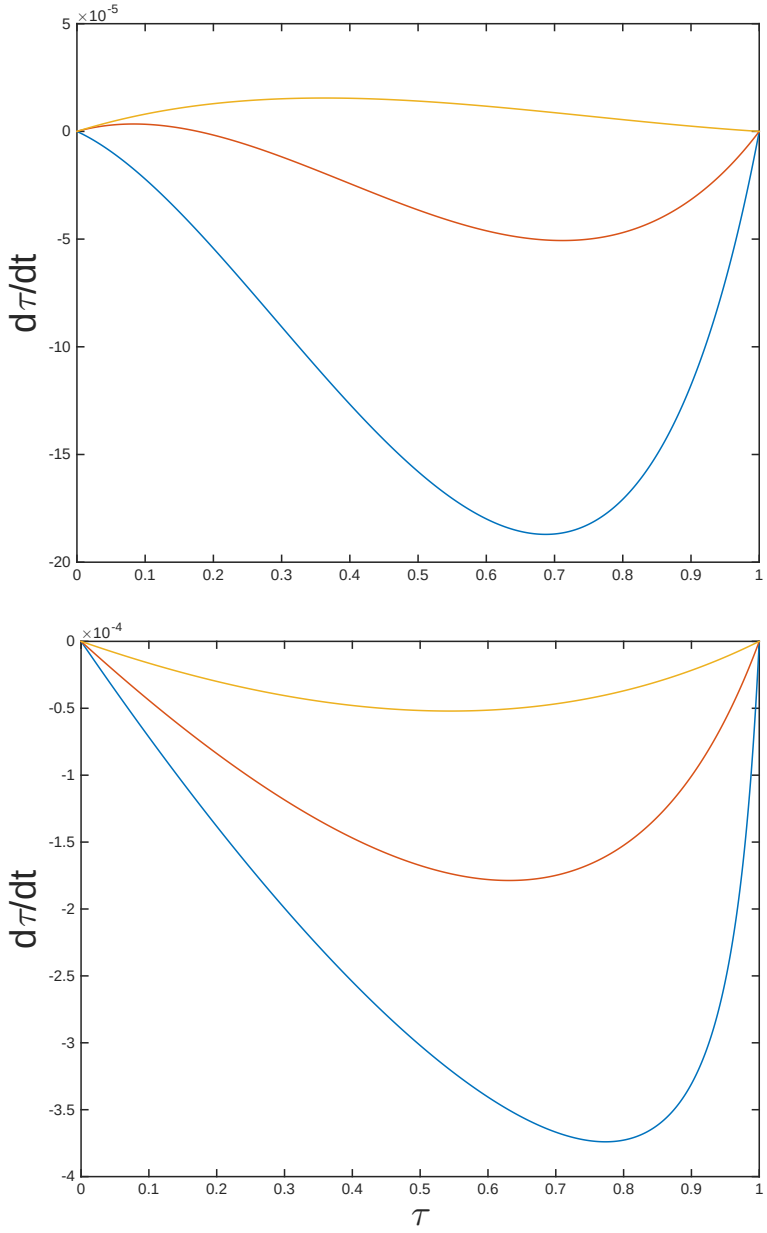

Figure 5-7: The value of $d\tau/dt$ for $D = 1$ and $D = 2$. See Figure 5-6 for caption details.

we summarised the dynamics using a second-order partial differential equation. Using this PDE, we showed that in a pairwise interaction, the wide and weak type individual has a better chance of winning the interaction. In a high density population, we determined using an intensive Fourier space argument that noise changes the stability of steady states in the system. This instability also results in the wide and weak type individuals reaching consensus overall.

These results can be applied to the real world in any situation where decisions are being made on two options and individuals have the opportunity to persuade each other. In our research, when an individual switches types, the individuals method of interaction also changes. This can be applied to the development of election campaign strategies. For example, if there are two political parties. One party prefers to use online advertising, a wide and weak form of interaction, while the other prefers door-to-door canvassing, a short and strong form of interaction. Our work here shows that the wide and weak political party has a better chance of winning the election, regardless of the size of the population, with everything else being equal. Our results hold only in very particular real world scenarios.

Chapter 6

General Conclusion and Outlook for Future Research

Populations are very complicated. The factors that influence a population and how they do so are still not fully understood. In this thesis, we have seen some examples of ways we can better understand these factors. We conclude by restating the new results presented here.

In Chapter 3, we considered a population moving in 2D according to the FKPP equation in the presence of mixed boundaries. In a corridor C_L of width L, we apply the mixed boundary conditions $u_y = \alpha u$ at $y = 0$ and $u_y = -\beta u$ at $y = L$. In the half plane C_∞, we only need the former as there is only one boundary in this domain. Ahead of the front, the linearised 2D FKPP equation allowed us to calculate the dependence of the population structure on the y domain and the resulting invasion speed. The critical corridor width $L^m_{\infty,\beta}$, such that if $L > L^m_{\infty,\beta}$, the population will always have a positive invasion speed for any value of α, is given by

$$L^m_{\infty,\beta} = \frac{1}{\sqrt{2}}\left[\pi + \tan^{-1}\left(-\frac{\sqrt{2}}{\beta}\right)\right].$$

When $\beta = 0$, we have a reflective boundary at $y = L$ and $L^m_{\infty,0} = \pi/2\sqrt{2}$. When $\beta \to \infty$, we have an absorbing boundary at $y = L$ and $L^m_{\infty,\infty} = \pi/\sqrt{2}$. Each of these critical corridor widths ahead of the front also have a corresponding curve in the (L, α) plane that represent where each population invasion achieves invasion

speed zero. For a mixed boundary at $y = L$, this is given by

$$(2 - \alpha\beta)\tan(\sqrt{2}L) = \sqrt{2}(\alpha + \beta).$$

Ahead of the front in the half plane, we were able to calculate explicitly a formula for the 2D invasion front, given by

$$u(x, y, t) = u_0 \exp(-(x - 2t))(1 + \alpha y),$$

for some constant u_0 and we showed that the level sets of this equation meet the mixed boundary at $y = 0$ with gradient $1/\alpha$ which is independent of the level set chosen. Also, we found that the level sets never become parallel with the y axis as $y \to \infty$. This shows that the effects of the mixed boundary at $y = 0$ are felt very far away from the boundary. Behind the front, the problem is fully nonlinear and we show that solutions exist for all $L > 0$ using a phase plane argument and we derive the condition for these solutions behind the front to be stable, which is given by

$$(1 - \alpha\beta)\tan(L) = \alpha + \beta.$$

Comparing these conditions for stability behind the front and the conditions for achieving zero invasion speed ahead of the front in the (L, α) plane show that, as α increases, the population invasion collapses behind the front before it can ever reach zero invasion speed. Hence, the invasion collapses and reaches zero invasion speed before the linear prediction. From this, we can conclude that the invasion speed for the 2D FKPP equation in the presence of mixed boundaries is not fully determined by the low density linear calculations ahead of the front, as it is for the 1D FKPP equation, which we showed in 2.2.2. It is indeed a nonlinear process. Future work includes:

- Recording the invasion speed for the stochastic individual based simulations in Section 3.3.1 and comparing them to the deterministic simulations and the predicted theory.

- Extending the speed simulations in Figures 3-13,3-14,3-15 to include mixed and absorbing boundaries at $y = L$.

- Considering a population that is invading at some angle θ with a hostile

boundary. That is, replacing the hostile boundary condition $u_y = \alpha u$ on $y = 0$ with the same condition on $y = \tan(\theta)x$.

- Exploring population invading past a spatially heterogeneous hostile boundary, such as $u_y = \alpha(1 - \sin(x))u/2$, or past a generation-varying hostile boundary, such as $u_y^i = \alpha_i u^i$ where u^i, α_i are the population density and reaction rate of the i-th generation respectively.

The future outlook for this research includes calibrating bacteriophage detection devices to the existence of low density populations near hostile boundaries and the effects of antibiotic medicine just outside the regions of influence. In the mathematics literature, this work provides new insight for the 2D FKPP equation.

In Chapter 4, we analysed how a population moving in 1D according to the FKPP equation is affected by the introduction of sexual conflict, in particular how this influences the population invasion speed. Starting with an introduction of 'run and tumble' movement, we calculated the mean square displacement of one fish, given by

$$Q(t) = 2v^2T\left(t - T + Te^{-t/T}\right),$$

and showed how this leads to diffusive movement for large times with diffusion rate $D = v^2T$ and to the stochastic differential equation

$$\frac{dX}{dt} = \sqrt{2D}\eta_X(t)$$

for the location of the fish. We then introduced the response functions v_X, v_Y for sexual conflict between two fish as

$$\begin{aligned}\frac{dX}{dt} &= v_X(X,Y) + \sqrt{2D}\eta_X(t)\,,\\ \frac{dY}{dt} &= v_Y(X,Y) + \sqrt{2D}\eta_Y(t)\,.\end{aligned}$$

The movement of the two fish is very similar to the 'run and tumble' movement of one fish so we use similar methods to calculate the diffusion rate for the pair. We found that for a particular level of male aggression A and individual diffusion rate D, the effective diffusion rate D_{eff} of the pair of fish is given by

$$D_{\text{eff}} = 4\sqrt{\frac{D\pi}{A+1}}\left(\frac{A}{A+1}\right)^2 \sinh\left(\frac{1}{4D(A+1)}\right),$$

and that it can be significantly larger than the individual diffusion rate D. Since the invasion speed for the 1D FKPP equation is given by $v = 2\sqrt{rD}$, we have shown that sexual conflict between male and female fish can increase the invasion speed of the population. This contrasts very nicely with the work in Chapter 3, where we saw that interactions with the environment can slow down a population. Here we saw that coupled interactions within a population can speed it up. Finally, we showed that sexual conflict in populations with lots of fish can result in male fish having a higher diffusion rate ahead of the front where there are fewer female fish compared to behind the front where there are many female fish. This agrees with our conclusion as the FKPP equation has a pulled front so the invasion speed is determined by the dynamics ahead of the front. We also derived the equation for the diffusion coefficient of a fish switching between two different diffusion coefficients, which is given by

$$D_{\text{swt}} = \frac{D_1\lambda_2 + D_2\lambda_1}{\lambda_1 + \lambda_2}.$$

In order to inform and test the model, we carried out experiments tracking the movement of pairs of guppies in a tank. The results from the experiment qualitatively agree with the assumptions we made in our model. Future work includes:

- Exploring the case of male and female fish having different diffusion rates, which is very likely as female fish are, on average, bigger than the male fish
- Using the data we have collected from the pair experiments, we can explore different interaction functions v_X, v_Y that more closely reflect the observed behaviour
- Consider more variations of guppy behaviour, such as guppies of the same gender interacting with each other and female fish only interacting with the nearest male in the large population case

This work contributes to the literature surrounding *Poecilia Reticulata* and the factors that contribute to it being so successful at establishing an invasive population. This also addresses the wider influence of coupled, nonlinear interactions within a population and the role they play in determining population density level characteristics that cannot be accounted for at the individual or linear level.

In Chapter 5, we examined the voter model with nonlocal interaction and diffusion. The population contained two types: type W individuals with a wide region of interaction that is very weak and type S individuals with a short region of interaction that is very strong. We assumed the interaction ranges satisfy $r_S < r_W$ and the interaction rates satisfy $\lambda_W < \lambda_S$. The success of either type surviving to consensus varies with the density of the population. For a low density population, we derive a differential equation for the density of pairs of different types and calculate the probability of either type winning a interaction from the stationary solution of the ODE. We see that the probability p_S of a type S individual winning in a pairwise interaction is given by

$$p_S = \frac{2\mu_1\lambda_S(e^{2\mu_1 r_S} - 1)e^{\mu_2(r_S+r_W)}}{(\lambda_S+\lambda_W)((\mu_1-\mu_2)(e^{2r_S(\mu_1+\mu_2)} - e^{2\mu_2 r_W}) + (\mu_1+\mu_2)(e^{2\mu_1 r_S+2\mu_2 r_W} - e^{2\mu_2 r_S}))},$$

where $\mu_1 = \sqrt{(\lambda_S+\lambda_W)/D}$ and $\mu_2 = \sqrt{\lambda_W/D}$. It is less than $1/2$ when we assume $\lambda_S r_S = \lambda_W r_W = 1/2$ and $D = 1$. In order for a type to survive to consensus, it must repeatedly win these pairwise interactions. We calculate that the probability P_S for the survival of type S individuals to consensus is given by

$$P_S = \frac{p_S^{N-N_S^0}}{p_S^{N-N_S^0} + (1-p_S)^{N_S^0}}.$$

We see that the type W individuals always have an advantage in low density populations. However, in high density populations, we formulate the model in terms of chemical reaction equations and a chemical master equation. After a long analysis of the chemical master equation, involving Fourier space expansions, Kramers-Moyal operator expansions, diffusion rate approximations, and complex integrals, we find that there is a family of solutions where the proportion of type W individuals is τ and the proportion of type S individuals is $1-\tau$ for all $\tau \in [0,1]$. When we add noise to these steady states with large but finite populations, we

find that the density of the type W individuals satisfies the equation

$$\frac{d}{dt}\tau = \frac{\tau\,(1-\tau)}{N\pi^2}$$
$$\sum_{k\neq 0} \frac{\frac{1}{2r_W}\sin(kr_W) - \frac{1}{2r_S}\sin(kr_S)}{(D_W+D_S)\frac{k^3}{2} - 4k[(\frac{1}{2kr_W}\sin(kr_W)+1/2)\,(1-\tau) + (\frac{1}{2kr_S}\sin(kr_S)+1/2)\tau]}.$$

When we assume $\lambda_S r_S = \lambda_W r_W = 1/2$, this equation is always positive as we vary τ. Hence, in a large but finite population, the type W individuals also survive to consensus. Future work includes:

- Allowing individuals of the same type to interact with each other either in a competitive or mutualistic way
- Extending calculations to two and three dimensions and determining if the results still hold
- Exploring more complicated interaction rates, such as spatially and temporally varying, and more complicated interaction regions, such as circles and squares in two dimensions, spheres and cubes in three dimensions
- Considering populations of more than two types
- Exploring nonzero diffusion rates in the high density case

This work contributes to the literature surrounding the voter model, interacting particle systems, and contact processes. More generally, it provides insight into optimum strategies for decision making events, such as elections.

Appendix A

Mean Hitting Time For Alternative Boundary Conditions

Here, we calculate the mean hitting time for alternative boundary conditions. For an absorbing boundary at $x = A$ and at $x = B$, the boundary conditions on $\mathcal{P}(x,t)$ are given by

$$\mathcal{P}(A,t) = \mathcal{P}(B,t) = 0,$$

so the boundary conditions on $\mathbb{E}[T(x)]$ are given by

$$\mathbb{E}[T(A)] = \mathbb{E}[T(B)] = 0.$$

Applying these boundary conditions to

$$\mathbb{E}[T(x)] = -2\int_A^x \frac{1}{\gamma(w)}\int_A^w \frac{\gamma(z)}{b(z)^2}dzdw + \int_A^A \frac{C_1}{\gamma(w)}dw + C_2,$$

gives

$$0 = \mathbb{E}[T(A)] = -2\int_A^A \frac{1}{\gamma(w)}\int_A^w \frac{\gamma(z)}{b(z)^2}dzdw + \int_A^x \frac{C_1}{\gamma(w)}dw + C_2 = C_2$$

and

$$0 = \mathbb{E}[T(B)] = -2\int_A^B \frac{1}{\gamma(w)}\int_A^w \frac{\gamma(z)}{b(z)^2}dzdw + \int_A^B \frac{C_1}{\gamma(w)}dw$$

so

$$C_1 = \frac{-2\int_A^B \frac{1}{\gamma(w)}\int_A^w \frac{\gamma(z)}{b(z)^2}dzdw}{\int_A^B \frac{1}{\gamma(w)}dw}.$$

Hence,

$$\begin{aligned}
\mathbb{E}[T(x)] =& -2\int_A^x \frac{1}{\gamma(w)}\int_A^w \frac{\gamma(z)}{b(z)^2}dzdw \\
&+\frac{-2\int_A^B \frac{1}{\gamma(w)}\int_A^w \frac{\gamma(z)}{b(z)^2}dzdw}{\int_A^B \frac{1}{\gamma(w)}dw}\int_A^x \frac{1}{\gamma(w)}dw \\
=& -2\frac{\int_A^x \frac{1}{\gamma(w)}\int_A^w \frac{\gamma(z)}{b(z)^2}dzdw \int_A^B \frac{1}{\gamma(w)}dw}{\int_A^B \frac{1}{\gamma(w)}dw} \\
&-2\frac{\int_A^B \frac{1}{\gamma(w)}\int_A^w \frac{\gamma(z)}{b(z)^2}dzdw \int_A^x \frac{1}{\gamma(w)}dw}{\int_A^B \frac{1}{\gamma(w)}dw} \\
=& -2\frac{\int_A^x \frac{1}{\gamma(w)}\int_A^w \frac{\gamma(z)}{b(z)^2}dzdw \int_A^B \frac{1}{\gamma(w)}dw}{\int_A^B \frac{1}{\gamma(w)}dw} \\
&-2\frac{\int_A^x \frac{1}{\gamma(w)}\int_A^w \frac{\gamma(z)}{b(z)^2}dzdw \int_A^x \frac{1}{\gamma(w)}dw}{\int_A^B \frac{1}{\gamma(w)}dw} \\
&-2\frac{\int_x^B \frac{1}{\gamma(w)}\int_A^w \frac{\gamma(z)}{b(z)^2}dzdw \int_A^x \frac{1}{\gamma(w)}dw}{\int_A^B \frac{1}{\gamma(w)}dw} \\
=& -\frac{2}{\int_A^B \frac{1}{\gamma(w)}dw}\int_A^x \frac{1}{\gamma(w)}\int_A^w \frac{\gamma(z)}{b(z)^2}dzdw \int_x^B \frac{1}{\gamma(w)}dw \\
&-\frac{2}{\int_A^B \frac{1}{\gamma(w)}dw}\int_x^B \frac{1}{\gamma(w)}\int_A^w \frac{\gamma(z)}{b(z)^2}dzdw \int_A^x \frac{1}{\gamma(w)}dw,
\end{aligned}$$

which is the mean hitting time for two absorbing boundaries at A and B.

For one absorbing boundary at A and one reflecting boundary at B, the boundary conditions for $\mathcal{P}(x', t')$ become

$$\mathcal{P}(A, t') = \frac{\partial}{\partial x}\mathcal{P}(B, t') = 0,$$

so the boundary conditions for $\mathbb{E}[T(x)]$ become

$$\mathbb{E}[T(A)] = \frac{\partial}{\partial x}\mathbb{E}[T(B)] = 0.$$

Now, solving

$$\mathbb{E}[T(x)] = -2\int_A^x \frac{1}{\gamma(w)}\int_A^w \frac{\gamma(z)}{b(z)^2}dzdw + \int_A^x \frac{C_1}{\gamma(w)}dw + C_2,$$

with these boundary conditions gives $C_2 = 0$ again and

$$\begin{aligned}
0 = \frac{\partial}{\partial x}\mathbb{E}[T(B)] =& \frac{\partial}{\partial x}\left[-2\int_A^x \frac{1}{\gamma(w)}\int_A^w \frac{\gamma(z)}{b(z)^2}dzdw + \int_A^x \frac{C_1}{\gamma(w)}dw\right]\Bigg|_{x=B} \\
=& \left[-2\frac{1}{\gamma(x)}\int_A^x \frac{\gamma(z)}{b(z)^2}dz + \frac{C_1}{\gamma(x)}\right]\Bigg|_{x=B} \\
=& -2\frac{1}{\gamma(B)}\int_A^B \frac{\gamma(z)}{b(z)^2}dz + \frac{C_1}{\gamma(B)},
\end{aligned}$$

so

$$C_1 = 2\int_A^B \frac{\gamma(z)}{b(z)^2}dz.$$

Hence

$$\begin{aligned}
\mathbb{E}[T(x)] =& -2\int_A^x \frac{1}{\gamma(w)}\int_A^w \frac{\gamma(z)}{b(z)^2}dzdw + 2\int_A^B \frac{\gamma(z)}{b(z)^2}dz\int_A^x \frac{1}{\gamma(w)}dw \\
=& \int_A^x \left[-2\int_A^w \frac{\gamma(z)}{b(z)^2}dz + 2\int_A^B \frac{\gamma(z)}{b(z)^2}dz\right]\frac{1}{\gamma(w)}dw \\
=& 2\int_A^x \frac{1}{\gamma(w)}\int_w^B \frac{\gamma(z)}{b(z)^2}dzdw,
\end{aligned}$$

which is the mean hitting time for an absorbing boundary at A and a reflective boundary at B.

Appendix B

Calculation of Sexual Conflict as a Second Order Interaction

In this Section, we show that sexual conflict between individuals of two different types is a second order, nonlinear interaction. To see this, assume we have a population with N males with locations $X_1, \ldots, X_N$ and M females with locations $Y_1, \ldots, Y_M$. We assume that the male response to other male fish is given by f_{xx}, the male response to female fish is given by f_{xy}, the male response to other male fish as a coefficient of the noise is given by g_{xx}, and the male response to female fish as a coefficient of the noise is given by g_{xy}. There are similar functions for the female responses. We also assume all fish have diffusion coefficient D. These dynamics for the i-th male and female are given by

$$\begin{aligned}
\frac{dX_i}{dt} &= \frac{1}{N}\sum_{j=1}^{N} f_{xx}(X_i(t) - X_j(t)) + \frac{1}{M}\sum_{k=1}^{M} f_{xy}(X_i(t) - Y_k(t)) \\
&\quad + \sqrt{2D}\eta_i(t)\left(\frac{1}{N}\sum_{j=1}^{N} g_{xx}(X_i(t) - X_j(t)) + \frac{1}{M}\sum_{k=1}^{M} g_{xy}(X_i(t) - Y_k(t))\right), \\
\frac{dY_i}{dt} &= \frac{1}{N}\sum_{j=1}^{N} f_{yx}(Y_i(t) - X_j(t)) + \frac{1}{M}\sum_{k=1}^{M} f_{yy}(Y_i(t) - Y_k(t)) \\
&\quad + \sqrt{2D}\eta_i(t)\left(\frac{1}{N}\sum_{j=1}^{N} g_{yx}(Y_i(t) - X_j(t)) + \frac{1}{M}\sum_{k=1}^{M} g_{yy}(Y_i(t) - Y_k(t))\right),
\end{aligned}$$

where $\eta_i(t)$ is Gaussian white noise with mean zero and unit variance. For the rest of this calculation, we only focus on $\frac{dX_i}{dt}$. The calculations for $\frac{dY_i}{dt}$ are similar. Define the location distribution ρ_i^x for the i-th male fish as

$$\rho_i^x(x,t) = \delta(X_i(t) - x), \tag{B.1}$$

so that, for arbitrary function h^x, we have

$$h^x(X_i(t)) = \int \rho_i^x(x,t) h^x(x) dx. \tag{B.2}$$

We will use the fact that h^x is arbitrary to derive a partial differential equation for ρ_i^x. Summing over i will then provide a PDE for the population density of male fish. Firstly, we need to calculate the derivative of $h^x(X_i(t))$. To do this, we use Itô's formula from Section 2.1.2, to get

$$\begin{aligned}
\frac{\partial h^x}{\partial t} = &\left(\frac{1}{N} \sum_{j=1}^{N} f_{xx}(X_i(t) - X_j(t)) + \frac{1}{M} \sum_{k=1}^{M} f_{xy}(X_i(t) - Y_k(t)) \right) \frac{\partial h^x}{\partial x} \\
&+ D \left(\frac{1}{N} \sum_{j=1}^{N} g_{xx}(X_i(t) - X_j(t)) + \frac{1}{M} \sum_{k=1}^{M} g_{xy}(X_i(t) - Y_k(t)) \right)^2 \frac{\partial^2 h^x}{\partial x^2} \\
&+ \sqrt{2D} \left(\frac{1}{N} \sum_{j=1}^{N} g_{xx}(X_i(t) - X_j(t)) + \frac{1}{M} \sum_{k=1}^{M} g_{xy}(X_i(t) - Y_k(t)) \right) \frac{\partial h^x}{\partial x} \eta_i.
\end{aligned}$$

We replace the location $X_i(t)$ using (B.2) to get

$$\begin{aligned}
\frac{\partial h^x}{\partial t} = \int \rho_i^x(x,t) \Bigg[&\frac{\partial h^x}{\partial x} \left(\frac{1}{N} \sum_{j=1}^{N} f_{xx}(x - X_j(t)) + \frac{1}{M} \sum_{k=1}^{M} f_{xy}(x - Y_k(t)) \right. \\
&\left. + \sqrt{2D} \eta_i \left(\frac{1}{N} \sum_{j=1}^{N} g_{xx}(x - X_j(t)) + \frac{1}{M} \sum_{k=1}^{M} g_{xy}(x - Y_k(t)) \right) \right) \\
&+ D \left(\frac{1}{N} \sum_{j=1}^{N} g_{xx}(x - X_j(t)) + \frac{1}{M} \sum_{k=1}^{M} g_{xy}(x - Y_k(t)) \right)^2 \frac{\partial^2 h^x}{\partial x^2} \Bigg] dx,
\end{aligned}$$

and integrating by parts gives

$$\frac{\partial h^x}{\partial t} = \int h^x(x) \left[-\frac{\partial}{\partial x} \left(\left[\frac{1}{N} \sum_{j=1}^{N} f_{xx}(x - X_j(t)) + \frac{1}{M} \sum_{k=1}^{M} f_{xy}(x - Y_k(t)) \right] \rho_i^x(x,t) \right.\right.$$
$$+ \sqrt{2D}\eta_i \left(\frac{1}{N} \sum_{j=1}^{N} g_{xx}(x - X_j(t)) + \frac{1}{M} \sum_{k=1}^{M} g_{xy}(x - Y_k(t)) \right) \rho_i^x(x,t) \Bigg)$$
$$\left. + D \frac{\partial^2}{\partial x^2} \left(\left(\frac{1}{N} \sum_{j=1}^{N} g_{xx}(x - X_j(t)) + \frac{1}{M} \sum_{k=1}^{M} g_{xy}(x - Y_k(t)) \right)^2 \rho_i^x(x,t) \right) \right] dx. \tag{B.3}$$

We now compare (B.3) to the time derivative of (B.2), which is given by

$$\frac{dh^x}{dt} = \int h^x(x) \frac{\partial \rho_i^x}{\partial t} dx.$$

Because h^x is arbitrary, we must have that

$$\frac{\partial \rho_i^x}{\partial t} = -\frac{\partial}{\partial x} \left(\left[\frac{1}{N} \sum_{j=1}^{N} f_{xx}(x - X_j(t)) + \frac{1}{M} \sum_{k=1}^{M} f_{xy}(x - Y_k(t)) \right] \rho_i^x(x,t) \right.$$
$$+ \sqrt{2D}\eta_i \left(\frac{1}{N} \sum_{j=1}^{N} g_{xx}(x - X_j(t)) + \frac{1}{M} \sum_{k=1}^{M} g_{xy}(x - Y_k(t)) \right) \rho_i^x(x,t) \Bigg)$$
$$\left. + D \frac{\partial^2}{\partial x^2} \left(\left(\frac{1}{N} \sum_{j=1}^{N} g_{xx}(x - X_j(t)) + \frac{1}{M} \sum_{k=1}^{M} g_{xy}(x - Y_k(t)) \right)^2 \rho_i^x(x,t) \right) \right.$$

We now define the population distribution for all male fish

$$\rho^x(x,t) = \sum_{i=1}^{N} \rho_i^x(x,t),$$

so that

$$\begin{aligned}
\frac{\partial \rho^x}{\partial t} &= \sum_{i=1}^{N} \frac{\partial \rho_i^x}{\partial t} \\
&= -\frac{\partial}{\partial x}\left(\left[\frac{1}{N}\sum_{j=1}^{N} f_{xx}(x - X_j(t)) + \frac{1}{M}\sum_{k=1}^{M} f_{xy}(x - Y_k(t))\right]\rho^x(x,t)\right) \\
&- \frac{\partial}{\partial x}\left(\sqrt{2D}\left(\frac{1}{N}\sum_{j=1}^{N} g_{xx}(x - X_j(t)) \right.\right. \\
&\qquad \left.\left. + \frac{1}{M}\sum_{k=1}^{M} g_{xy}(x - Y_k(t))\right)\sum_{i=1}^{N}\eta_i(t)\rho_i^x(x,t)\right) \\
&+ D\frac{\partial^2}{\partial x^2}\left(\left(\frac{1}{N}\sum_{j=1}^{N} g_{xx}(x - X_j(t)) + \frac{1}{M}\sum_{k=1}^{M} g_{xy}(x - Y_k(t))\right)^2 \rho^x(x,t)\right).
\end{aligned}$$

Using the fact that

$$\begin{aligned}
\int \rho^x(y,t) f_{xx}(x-y)dy &= \int \sum_{j=1}^{N} \rho_j^x(y,t) f_{xx}(x-y)dy \\
&= \sum_{j=1}^{N} \int \rho_j^x(y,t) f_{xx}(x-y)dy \\
&= \sum_{j=1}^{N} f_{xx}(x - X_j(t)),
\end{aligned}$$

we integrate against $\rho(y,t)$ giving

$$\begin{aligned}\frac{\partial \rho^x}{\partial t} = &-\frac{\partial}{\partial x}\left(\left[\frac{1}{N}\int \rho^x(y,t) f_{xx}(x-y)dy \right.\right. \\ &\left.\left. +\frac{1}{M}\int \rho^y(y,t) f_{xy}(x-y)dy\right]\rho^x(x,t)\right) \\ &-\frac{\partial}{\partial x}\left(\sqrt{2D}\left(\frac{1}{N}\int \rho^x(y,t) g_{xx}(x-y)dy \right.\right. \\ &\left.\left. +\frac{1}{M}\int \rho^y(y,t) g_{xy}(x-y)dy\right)\sum_{i=1}^{N}\eta_i(t)\rho_i^x(x,t)\right) \\ &+D\frac{\partial^2}{\partial x^2}\left(\left(\frac{1}{N}\int \rho^x(y,t) g_{xx}(x-y)dy \right.\right. \\ &\left.\left. +\frac{1}{M}\int \rho^y(y,t) g_{xy}(x-y)dy\right)^2 \rho^x(x,t)\right).\end{aligned}$$

At this point, we have to mention that the noise terms are uncorrelated so the correlation function is

$$\mathbb{E}[\eta_i(t)\eta_j(t')] = \delta_{i,j}\delta(t-t').$$

Define the noise term as

$$\xi(x,t) = -\frac{\partial}{\partial x}\left(A(x,\rho^x,\rho^y,g_{xx},g_{xy})\sum_{i=1}^{N}\eta_i(t)\rho_i^x(x,t)\right),$$

where

$$\begin{aligned}A(x,\rho^x,\rho^y,g_{xx},g_{xy}) = \sqrt{2D}&\left(\frac{1}{N}\int \rho^x(y,t) g_{xx}(x-y)dy \right. \\ &\left. +\frac{1}{M}\int \rho^y(y,t) g_{xy}(x-y)dy\right).\end{aligned}$$

Then, we can derive the correlation function for $\xi(x,t)$ by noting that

$$\begin{aligned}\xi(x,t)\xi(z,t') = \frac{\partial}{\partial x}\frac{\partial}{\partial z}&A(x,\rho^x,\rho^y,g_{xx},g_{xy})A(z,\rho^x,\rho^y,g_{xx},g_{xy}) \\ &\sum_{i=1}^{N}\sum_{j=1}^{N}\rho_i^x(x,t)\rho_j^x(z,t')\eta_i(t)\eta_j(t').\end{aligned}$$

Taking averages then gives

$$\begin{aligned}\mathbb{E}[\xi(x,t)\xi(z,t')] &= \frac{\partial}{\partial x}\frac{\partial}{\partial z}A(x,\rho^x,\rho^y,g_{xx},g_{xy})A(z,\rho^x,\rho^y,g_{xx},g_{xy}) \\ &\qquad \sum_{i=1}^{N}\sum_{j=1}^{N}\rho_i^x(x,t)\rho_j^x(z,t')\mathbb{E}[\eta_i(t)\eta_j(t')] \\ &= \frac{\partial}{\partial x}\frac{\partial}{\partial z}A(x,\rho^x,\rho^y,g_{xx},g_{xy})A(z,\rho^x,\rho^y,g_{xx},g_{xy}) \\ &\qquad \sum_{i=1}^{N}\sum_{j=1}^{N}\rho_i^x(x,t)\rho_j^x(z,t')\delta_{i,j}\delta(t-t') \\ &= \frac{\partial}{\partial x}\frac{\partial}{\partial z}A(x,\rho^x,\rho^y,g_{xx},g_{xy})A(z,\rho^x,\rho^y,g_{xx},g_{xy}) \\ &\qquad \sum_{i=1}^{N}\rho_i^x(x,t)\rho_i^x(z,t).\end{aligned}$$

Recalling the definition of ρ_i^x from (B.1), we see that

$$\rho_i^x(x,t)\rho_i^x(z,t) = \delta(X_i(t)-x)\delta(X_i(t)-z) = \delta(x-z)\rho_i^x(x,t),$$

so we have

$$\begin{aligned}&\mathbb{E}[\xi(x,t)\xi(z,t')] \\ &= \frac{\partial}{\partial x}\frac{\partial}{\partial z}A(x,\rho^x,\rho^y,g_{xx},g_{xy})A(z,\rho^x,\rho^y,g_{xx},g_{xy})\sum_{i=1}^{N}\delta(x-z)\rho_i^x(x,t) \\ &= \frac{\partial^2}{\partial x^2}A(x,\rho^x,\rho^y,g_{xx},g_{xy})^2\sum_{i=1}^{N}\rho_i^x(x,t) \\ &= \frac{\partial^2}{\partial x^2}A(x,\rho^x,\rho^y,g_{xx},g_{xy})^2\rho^x(x,t).\end{aligned}$$

We now define the global uncorrelated white noise field $\eta(x,t)$, such that the correlation function is

$$\mathbb{E}[\eta(x,t)\eta(z,t')] = \delta(t-t')\delta(x-z),$$

and define the global noise field $\xi'(x,t)$ by

$$\xi'(x,t) = -\frac{\partial}{\partial x}\left(A(x,\rho^x,\rho^y,g_{xx},g_{xy})\eta(x,t)\rho^{1/2}(x,t)\right).$$

We show now that $\xi(x,t)$ and $\xi'(x,t)$ have the same correlation function. Note that

$$\xi'(x,t)\xi'(z,t') = \frac{\partial}{\partial x}\frac{\partial}{\partial z}A(x,\rho^x,\rho^y,g_{xx},g_{xy})A(z,\rho^x,\rho^y,g_{xx},g_{xy}) \\ \rho^{1/2}(x,t)\rho^{1/2}(z,t')\eta(x,t)\eta(z,t'),$$

and taking averages gives

$$\begin{aligned}\mathbb{E}[\xi'(x,t)\xi'(z,t')] &= \frac{\partial}{\partial x}\frac{\partial}{\partial z}A(x,\rho^x,\rho^y,g_{xx},g_{xy})A(z,\rho^x,\rho^y,g_{xx},g_{xy}) \\ &\qquad \rho^{1/2}(x,t)\rho^{1/2}(z,t')\mathbb{E}[\eta(x,t)\eta(z,t')] \\ &= \frac{\partial}{\partial x}\frac{\partial}{\partial z}A(x,\rho^x,\rho^y,g_{xx},g_{xy})A(z,\rho^x,\rho^y,g_{xx},g_{xy}) \\ &\qquad \rho^{1/2}(x,t)\rho^{1/2}(z,t')\delta(t-t')\delta(x-z), \\ &= \frac{\partial^2}{\partial x^2}A(x,\rho^x,\rho^y,g_{xx},g_{xy})^2\rho(x,t).\end{aligned}$$

Hence, $\xi(x,t)$ and $\xi'(x,t)$ are statistically equivalent. Then we have

$$\begin{aligned}\frac{\partial\rho^x}{\partial t} &= -\frac{\partial}{\partial x}\left(\left[\frac{1}{N}\int\rho^x(y,t)f_{xx}(x-y)dy + \frac{1}{M}\int\rho^y(y,t)f_{xy}(x-y)dy\right]\rho^x(x,t)\right) \\ &\quad -\frac{\partial}{\partial x}\left(\sqrt{2D}\left(\frac{1}{N}\int\rho^x(y,t)g_{xx}(x-y)dy\right.\right. \\ &\qquad \left.\left.+\frac{1}{M}\int\rho^y(y,t)g_{xy}(x-y)dy\right)\eta(x,t)\rho^{1/2}(x,t)\right) \\ &\quad + D\frac{\partial^2}{\partial x^2}\left(\left(\frac{1}{N}\int\rho^x(y,t)g_{xx}(x-y)dy\right.\right. \\ &\qquad \left.\left.+\frac{1}{M}\int\rho^y(y,t)g_{xy}(x-y)dy\right)^2\rho^x(x,t)\right)\end{aligned}$$

Defining

$$\phi^x = \frac{\rho^x}{N}, \phi^y = \frac{\rho^y}{M}$$

gives

$$\frac{\partial \phi^x}{\partial t} = \frac{1}{N}\frac{\partial \rho^x}{\partial t}$$

and

$$\begin{aligned}
\frac{\partial \phi^x}{\partial t} &= \frac{1}{N}\frac{\partial \rho^x}{\partial t} \\
&= -\frac{1}{N}\frac{\partial}{\partial x}\left(\left[\int \phi^x(y,t) f_{xx}(x-y)dy + \int \phi^y(y,t) f_{xy}(x-y)dy\right] N\phi^x(x,t)\right) \\
&- \frac{1}{N}\frac{\partial}{\partial x}\left(\sqrt{2D}\left(\int \phi^x(y,t) g_{xx}(x-y)dy\right.\right. \\
&\qquad\qquad \left.\left. + \int \phi^y(y,t) g_{xy}(x-y)dy\right)\eta(x,t) N^{1/2}\phi^{1/2}(x,t)\right) \\
&+ \frac{D}{N}\frac{\partial^2}{\partial x^2}\left(\left(\int \phi^x(y,t) g_{xx}(x-y)dy + \int \phi^y(y,t) g_{xy}(x-y)dy\right)^2 N\phi^x(x,t)\right) \\
&= -\frac{\partial}{\partial x}\left(\left[\int \phi^x(y,t) f_{xx}(x-y)dy + \int \phi^y(y,t) f_{xy}(x-y)dy\right]\phi^x(x,t)\right) \\
&- \frac{1}{N^{1/2}}\frac{\partial}{\partial x}\left(\sqrt{2D}\left(\int \phi^x(y,t) g_{xx}(x-y)dy\right.\right. \\
&\qquad\qquad \left.\left. + \int \phi^y(y,t) g_{xy}(x-y)dy\right)\eta(x,t)\phi^{1/2}(x,t)\right) \\
&+ D\frac{\partial^2}{\partial x^2}\left(\left(\int \phi^x(y,t) g_{xx}(x-y)dy + \int \phi^y(y,t) g_{xy}(x-y)dy\right)^2 \phi^x(x,t)\right)
\end{aligned}$$

Letting $N \to \infty$ gives

$$\begin{aligned}
\frac{\partial \phi^x}{\partial t} &= -\frac{\partial}{\partial x}\left(\left[\int \phi^x(y,t) f_{xx}(x-y)dy + \int \phi^y(y,t) f_{xy}(x-y)dy\right]\phi^x(x,t)\right) \\
&+ D\frac{\partial^2}{\partial x^2}\left(\left(\int \phi^x(y,t) g_{xx}(x-y)dy + \int \phi^y(y,t) g_{xy}(x-y)dy\right)^2 \phi^x(x,t)\right)
\end{aligned}$$

As the calculation for the population invasion only depends on the linearisation of these equations, it is clear that the invasion speed is unaffected by sexual conflict as these terms are all nonlinear.

Bibliography

[1] Katz V. J., 2007. *The Mathematics of Egypt, Mesopotamia, China, India, and Islam*. USA: Princeton University Press.

[2] Shu J., 2012. On Generalized Tian Ji's Horse Racing Strategy. *Interdisciplinary Science Reviews*, **37** (2), 187–193.

[3] Bhanu Murthy T. S., 2009. *A Modern Introduction to Ancient Indian Mathematics*. New Delhi: New Age International.

[4] Closs M., 1996. *Native American Mathematics*. Texas: University of Texas Press.

[5] Ossendrijver M., 2016. Ancient Babylonian Astronomers Calculated Jupiter's Position From the Area Under a Time-Velocity Graph. *Science*, **351** (6272), 482–484.

[6] Mohamad N., Said F., 2011. A Mathematical Programming Approach to Crop Mix Problem. *African Journal of Agricultural Research*, **6** (1), 191–197.

[7] Sparavigna A., Baldi M., (2016). Overlapping Circles Grid Drawn With Compass and Straightedge on an Egyptian Artefact of 14th Century BC. *SSRN* https://ssrn.com/abstract=2750125.

[8] Darwin C., 1859. *The Origin of Species by Means of Natural Election, or the Preservation of Favoured Races in the Struggle for Life.* New York: AL Burt.

[9] Erlang A., 1909. The Theory of Probabilities and Telephone Conversations. *Nyt Tidsskrift for Matematik B*, **20**, 33–39.

[10] Hethcote H., 1989. Three Basic Epidemiological Models. *Springer Berlin Heidelberg*, **18**, 119–144.

[11] Sanders N., 2003. Community Disassembly by an Invasive Species. *PNAS* , **100** (5), 2474–2477.

[12] Williamson M., 1996. *Biological Invasions.* Netherlands: Springer Netherlands.

[13] Shigesada N., Kawasaki K., 1997. *Biological Invasions: Theory and Practice.* England: Oxford University Press.

[14] Murray J., 2002. *Mathematical Biology: I. An Introduction.* USA: Springer-Verlag New York.

[15] Kot M., 2008. *Elements of Mathematical Ecology.* England: Cambridge University Press.

[16] Volpert V., Petrovskii S., 2009. Reaction-Diffusion Waves in Biology. *Physics of Life Reviews*, **6**(4), 267–310.

[17] Simberloff D., Rejmanek M., 2011. *Encyclopaedia of Biological Invasions.* USA: University of California Press.

[18] Lewis M., Petrovskii S., Potts J., 2016. *The Mathematics Behind Biological Invasions.* Switzerland: Springer International Publishing.

[19] Fisher R., 1937. The Wave of Advance of Advantageous Genes. *Annals of Eugenics*, **7** (4), 355–369.

[20] Kolmogorov A., Petrovskii I., Piscounov I., 1937. A Study of the Diffusion Equation With Increase in the Amount of Substance and Its Application to a Biology Problem. *Mathematical Bulletin Moscow University*, **1**(6), 1–26.

[21] van Saarloos W., 2003. Front Propagation Into Unstable States. *Physics Reports*, **386**(2-6), 29–222.

[22] Sherratt J., 1998. On the Transition From Initial Data to Travelling Waves in the Fisher-KPP Equation. *Dynamics and Stability of Systems*, **13** (2), 167-174.

[23] Evans M., 2013. *Speed Selection in Coupled Fisher Waves* [Online]. UK: University of Edinburgh. Available from: *https://warwick.ac.uk/fac/sci/maths/research/events/2013-2014/statmech/ght/programme/evans.pdf*[Accessed 12 January 2018].

[24] Volpert A., Volpert V., Volpert V., 1994. *Traveling Wave Solutions of Parabolic Systems.* USA: American Mathematical Society.

[25] Habbal A., Barelli H., Malandain G., 2014. Assessing the Ability of the 2D Fisher-KPP Equation to Model Cell-Sheet Wound Closure. *Mathematical Biosciences* , **252**(1), 45–59.

[26] Steele J., 2009. Human Dispersals: Mathematical Models and the Archaeological Record. *Human Biology*, **81** (2), 121–140.

[27] Mansour M., 2007. Traveling Wave Solutions of a Reaction-Diffusion Model for Bacterial Growth. *Physica A: Statistical Mechanics and its Applications*, **383**(2), 466–472.

[28] Brazhnik P., Tyson J., 1999. On Traveling Wave Solutions of Fisher's Equation in Two Spatial Dimensions. *Journal of Applied Mathematics*, **60**(2), 371–391.

[29] Aronson D., Weinberger H., 1978. Multidimensional Nonlinear Diffusion Arising in Population Genetics. *Advances in Mathematics*, **30**(1), 33–76.

[30] Gardner R., 1986. Existence of Multidimensional Travelling Waves Solutions of an Initial Boundary Value Problem. *Journal of Differential Equations*, **61**(1), 335–379.

[31] Tzella A., Vanneste J., 2015. FKPP Fronts in Cellular Flows: The Large-Peclet Regime. *SIAM Journal of Applied Mathematics*, **75**(4), 1789–1816.

[32] Andow D., Kareiva P., Levin S., Okubo A., 1990. Spread of Invading Organisms. *Landscape Ecology*, **4**(2–3), 177–188.

[33] Higgins S., Richardson D., 1996. A Review of Models of Alien Plant Spread. *Ecological Modelling*, **87**(1–3), 249–265.

[34] Higgins S., Richardson D., Cowling R., 1996. Modelling Invasive Plant Spread: The Role of Plant Environment Interactions and Model Structure. *Ecological Society of America*, **77**(7), 2043-2054.

[35] Kinezaki N., Kawasaki K., Shigesada N., 2010. The Effect of the Spatial Configuration of Habitat Fragmentation on Invasive Spread. *Theoretical Population Biology*, **78**(4), 298–308.

[36] Möbius W., Murray A., Nelson D., 2015. How Obstacles Perturb Population Fronts and Alter Their Genetic Structure. *PLoS Computational Biology*, **11**(12), e1004615. *https://doi.org/10.1371/journal.pcbi.1004615*.

[37] Sanchez-Garduno F., Maini P., 1994. Existence and Uniqueness of a Sharp Travelling Wave in Degenerate Non-Linear Diffusion Fisher-KPP Equations. *Journal of Mathematical Biology*, **33**(2),163–192.

[38] Mansour M., 2010. Traveling Wave Solutions for the Extended Fisher-KPP Equation. *Reports on Mathematical Physics*, **66**(3), 375–383.

[39] Li W., Sun Y., Wang Z., 2010. Entire Solutions in the Fisher-KPP Equation With Nonlocal Dispersal. *Nonlinear Analysis: Real World Applications*, **11**(4), 2302–2313.

[40] Berestycki H., Roquejoffre J., Rossi L., 2016. The Shape of Expansion Induced by a Line With Fast Diffusion in Fisher-KPP Equations. *Communications in Mathematical Physics*, **343**(1), 207–232.

[41] Endler J., 1980. Natural Selection on Color Patterns in Poecilia Reticulata. *Evolution*, **34**(1), 76–91.

[42] Endler J., 1987. Predation, Light Intensity and Courtship Behaviour in Poecilia Reticulata. *Animal Behaviour*, **35**(5), 1376–1385.

[43] Hughes K., Du L., Rodd F., Reznick D., 1999. Familiarity Leads to Female Mate Preference for Novel Males in the Guppy, Poecilia Reticulata. *Animal Behaviour*, **58**(4), 907–916.

[44] Seghers B., 1974. Schooling Behaviour in the Guppy (Poecilia Reticulata): An Evolutionary Response to Predation. *Evolution*, **28**(3), 486–489.

[45] Reynolds J., Gross M., 1992. Female Mate Preference Enhances Offspring Growth and Reproduction in a Fish, Peocilia Reticulata. *Proceedings of The Royal Society B: Biological Sciences*, **250**(1327), 57–62.

[46] Endler J., Houde A., 1995. Geographic Variation in Female Preferences for Male Traits in Poecilia Reticulata. *Evolution*, **49**(3), 456–468.

[47] Bartlett M., 1971. Physical Nearest-Neighbour Models and Non-Linear Time-Series. *Journal of Applied Probability*, **8**(2), 222–232.

[48] Liggett T., 2005. *Interacting Particle Systems.* Berlin: Springer-Verlag Berlin Heidelberg.

[49] Lanchier N., Neuhauser C., 2007. Voter Model and Biased Voter Model in Heterogeneous Environments. *Journal of Applied Probability*, **44**(3), 770–787.

[50] Granovsky B., Madras N., 1995. The Noisy Voter Model. *Stochastic Processes and their Applications*, **55**(1), 23–43.

[51] Durrett R., 1980. On the Growth of One Dimensional Contact Processes. *The Annals of Probability*, **8**(5), 890–907.

[52] Cox J., Griffeath D., 1986. Diffusive Clustering in the Two Dimensional Voter Model. *The Annals of Probability*, **14**(2), 347–370.

[53] Harris T., 1974. Contact Interactions on a Lattice. *The Annals of Probability*, **2**(6), 969–988.

[54] Sood V., Antal T., Redner S., 2008. Voter Models on Heterogeneous Networks. *Physical Review E*, **77**(4), 041121.

[55] Sawyer S., 1976. Results for the Stepping Stone Model for Migration in Population Genetics. *The Annals of Probability*, **4**(5), 699–728.

[56] Bramson M., Griffeath D., 1981. On the Williams-Bjerknes Tumour Growth Model. *The Annals of Probability*, **9**(2), 173–185.

[57] Clifford P., Sudbury A., 1973. A Model for Spatial Conflict. *Biometrika*, **60**(3), 581–588.

[58] Krapivsky P., 1992. Kinetics of Monomer-Monomer Surface Catalytic Reactions. *Physical Review A*, **45**(2), 1067–1072.

[59] Hida T., 1980. *Brownian Motion.* New York: Springer-Verlag.

[60] Gardiner C., 2009. *Stochastic Methods.* Berlin Heidelberg: Springer-Verlag.

[61] Rogers T., McKane A., Rossberg A., 2012. Demographic Noise Can Lead to the Spontaneous Formation of Species. *Europhysics Letters*, **97**(4), 40008.

[62] Kramers H., 1940. Brownian Motion in a Field of Force and the Diffusion Model of Chemical Reactions. *Physica*, **7**(4), 284–304.

[63] Moyal J., 1949. Quantum Mechanics as a Statistical Theory. *Mathematical Proceedings of the Cambridge Philosophical Society*, **45**(1), 99–124.

[64] Van Kampen N., 2007. *Stochastic Processes in Physics and Chemistry.* Netherlands: Elsevier.

[65] Lang S., 2013. *Complex Analysis* . US: Springer Science and Business Media.

[66] Carrier G., Krook M., Pearson C., 2005. *Functions of a Complex Variable: Theory and Technique.* USA: SIAM.

[67] Agarwal R., Perera K., Pinelas S., 2011. *An Introduction to Complex Analysis.* US: Springer.

[68] Brooks R., Corey A., 1966. Properties of Porous Media Affecting Fluid Flow. *Journal of the Irrigation and Drainage Division*, **92**(2), 61–90.

[69] Bear J., 2013. *Dynamics of Fluids in Porous Media.* Courier Corporation.

[70] Fletcher M., 1991. The Physiological Activity of Bacteria Attached to Solid Surfaces. *Advances in Microbial Physiology*, **32**(1), 53–85.

[71] Costerton J., Lewandowski Z., Caldwell D., Korber D., Lappin-Scott H., 1995. Microbial Biofilms. *Annual Review of Microbiology*, **49**(1), 711–745.

[72] Christen D., Matlack G., 2006. The Role of Roadsides in Plant Invasions: A Demographic Approach. *Conservation Biology*, **20**(2), 385–391.

[73] Berestycki H., Roquejoffre J., Rossi L., 2013. The Influence of a Line With Fast Diffusion on Fisher-KPP Propagation. *Journal of Mathematical Biology*, **66**(4-5), 743–766.

[74] Excoffier L., Foll M., Petit R., 2009. Genetic Consequences of Range Expansions. *Annual Review of Ecology*, **40**(1), 481–501.

[75] Korolev K., Avlund M., Hallatschek O., Nelson D., 2010. Genetic Demixing and Evolution in Linear Stepping Stone Models. *Reviews of Modern Physics*, **82**(2), 1691–1718.

[76] Erban R., Chapman S., Maini P., 2007. A Practical Guide to the Stochastic Simulations of Reaction-Diffusion Processes. *arXiv*, 0704.1908 [q-bio.SC].

[77] Perko, L., 2008. *Differential Equations and Dynamical Systems.* Springer Science & Business Media.

[78] Butcher J., 2016. *Numerical Methods for Ordinary Differential Equations.* John Wiley & Sons.

[79] Bertness M., Leonard G., 1997. The Role of Positive Interactions in Communities: Lessons From Intertidal Habitats. *Ecology* , **78**(7), 1976–1989.

[80] Wilson J., Agnew A., 1992. Positive-Feedback Switches in Plant Communities. *Advances in Ecological Research*, **23**(1), 263–336.

[81] Way M., 1962. Mutualism Between Ants and Honeydew-Producing Homoptera. *Annual Review of Entomology*, **8**(1), 307–344.

[82] Gross K., 2008. Positive Interactions Among Competitors Can Produce Species-Rich Communities. *Ecology Letters*, **11**(9), 929–936.

[83] Soll D., 2002. Candida Commensalism and Virulence: The Evolution of Phenotypic Plasticity. *Acta Tropica* , **81**(2), 101–110.

[84] Holland J., DeAngelis D., Bronstein J., 2002. Population Dynamics and Mutualism: Functional Responses of Benefits and Costs. *The American Naturalist*, **159**(3), 231–244.

[85] Brown S., Le Chat L., De Paepe M., Taddei F., 2006. Ecology of Microbial Invasions: Amplification Allows Virus Carriers to Invade More Rapidly When Rare. *Current Biology* , **16**(20), 2048–2052.

[86] Bourgeois K., Suehs C., Vidal E., Mèdail F., 2005. Invasional Meltdown Potential: Facilitation Between Introduced Plants and Mammals on French Mediterranean Islands. *Ecoscience*, **12**(2), 248–256.

[87] Elliott E., Cornell S., 2012. Dispersal Polymorphism and the Speed of Biological Invasions. *PLoS ONE*, **7**(7), e40496.

[88] Elliott E., Cornell S., 2013. Are Anomalous Invasion Speeds Robust to Demographic Stochasticity? *PLoS ONE*, **8**(7), e67871.

[89] Deacon A., Ramnarine I., Magurran A., 2011. How Reproductive Ecology Contributes to the Spread of a Globally Invasive Fish. *PLoS ONE*, **6**(9), e24416.

[90] Manna B., Aditya G., Banerjee S., 2008. Vulnerability of the Mosquito Larvae to the Guppies (Poecilia Reticulata) in the Presence of Alternative Preys. *Journal of Vector Borne Diseases*, **45**(3), 200–206.

[91] El-Sabaawi R., Frauendorf T., Marques P., Mackenzie R., Manna L., Mazzoni R., Phillip D., Warbanski M., Zandona E., 2016. Biodiversity and Ecosystem Risks Arising From Using Guppies to Control Mosquitos. *Biology Letters*, **12**(10), 20160590.

[92] Houde A., 1987. Mate Choice Based Upon Naturally Occurring Color-Pattern Variation in a Guppy Population. *Evolution*, **41**(1), 1–10.

[93] Magurran A., Nowak M., 1991. Another Battle of the Sexes: The Consequences of Sexual Asymmetry in the Mating Costs and Predation Risk in the Guppy, Poecilia Reticulata. *Proceedings Biological Sciences*, **246**(1315), 31–38.

[94] Darden S., Watts L., 2011. Male Sexual Harassment Alters Female Social Behaviour Towards Other Females. *Biology Letters*, **8**(1), 186–188.

[95] Brask J., Croft D., Thompson K., Dabelsteen T., Darden S., 2011. Social Preferences Based on Sexual Attractiveness: A Female Strategy to Reduce Male Sexual Attention. *Proceedings of The Royal Society B: Biological Sciences*, **279**(1), 1748–1753.

[96] Darden S., James R., Ramnarine I., Croft D., 2009. Social Implications of the Battle of the Sexes: Sexual Harassment Disrupts Female Sociality and Social Recognition. *Proceedings of The Royal Society B: Biological Sciences*, **276** (1667), 2651–2656.

[97] Darden S., Croft D., 2008. Male Harassment Drives Females to Alter Habitat Use and Leads to Segregation of the Sexes. *Biology Letters*, **4**(5), 449–451.

[98] Heathcote R., Darden S., Franks D., Ramnarine I., Croft D., 2017. Fear of Predation Drives Stable and Differentiated Social Relationships in Guppies. *Scientific Reports*, **7** DOI: 10.1038/srep41679.

[99] Pizzari T., Snook R., 2003. Perspective: Sexual Conflict and Sexual Selection: Chasing Away Paradigm Shifts. *Evolution*, **57**(6), 1223–1236.

[100] Magurran A., Seghers B., 1994. Sexual Conflict as a Consequence of Ecology: Evidence From Guppy, Poecilia Reticulata, Populations in Trinidad. *Proceedings of the Royal Society London B*, **255**(1342), 31–36.

[101] Faugeras B., Maury O., 2007. Modelling Fish Population Movements: From an Individual-Based Representation to an Advection-Diffusion Equation. *Journal of Theoretical Biology*, **247**(4), 837–848.

[102] Bertignac M., Lehodey P., Hampton J., 1998. A Spatial Population Dynamics Simulation Model of Tropical Tunas Using a Habitat Index Based on Environmental Parameters. *Fisheries Oceanography* , **7**(1), 326–334.

[103] Faugeras B., Maury O., 2005. An Advection-Diffusion-Reaction Size-Structured Fish Population Dynamics Model Combined With a Statistical Parameter Estimation Procedure: Application to the Indian Ocean Skipjack Tuna Fishery. *Mathematical Biosciences and Engineering*, **2**(4), 719–741.

[104] Lehodey P., Chai F., Hampton J., 2003. Modelling Climate-Related Variability of Tuna Populations From a Coupled Ocean, Biogeochemical-Populations Dynamics Model. *Fisheries Oceanography*, **12**(45), 483–494.

[105] Maury O., 2000. *A Habitat-Based Simulation Framework to Design Tag-Recapture Experiments for Tunas in the Indian Ocean. Application to the Skipjack (Katsuwonus Pelamis) Population.* Seychelles: Indian Ocean Tuna Commission.

[106] Condat C., Jàckle J., Menchòn S., 2005. Randomly Curved Runs Interrupted by Tumbling: A Model for Bacterial Motion. *Physical Review E*, **72** (2), 021909.

[107] Tailleur J., Cates M., 2008. Statistical Mechanics of Interacting Run-and-Tumble Bacteria. *Physical Review Letters* , **100**(21), 218103.

[108] Cates M., Tailleur J., 2013. When Are Active Brownian Particles and Run-and-Tumble Particles Equivalent? Consequences for Motility-Induced Phase Separation. *Europhysics Letters*, **101**(2), 20010.

[109] Bearon R., Pedley T., 2000. Modelling Run-and-Tumble Chemotaxis in a Shear Flow. *Bulletin of Mathematical Biology*, **62**(4), 775–791.

[110] Kehr K., Richter D., Swendsen R., 1978. The Influence of Impurities on Interstitial Diffusion. *Journal of Physics F: Metal Physics*, **8**(3), 433-446.

[111] Haus J., Kehr K., Lyklema J., 1982. Diffusion in a Disordered Medium. *Physical Review B*, **25**(1), 2905–2907.

[112] Clutton-Brock T., Parker G., 1995. Sexual Coercion in Animal Societies. *Animal Behaviour*, **49**(5), 1345–1365.

[113] Ross P., 2002. *Causes and Consequences of Variation in the Mating Behaviour of the Male Guppy, Poecilia Reticulata.* Thesis (PhD). University of California, Santa Barbara, CA.

[114] Verhulst P., 1838. Notice Sur La Loi Que La Population Suit Dans Son Accroissement. *Correspondance Mathématique et Physique*, **10**(1), 113–121.

[115] Lotka A., 1923–1940. The Growth of Mixed Populations: Two Species Competing for a Common Food Supply. *The Golden Age of Theoretical Ecology*, **22**, Lecture notes in Biomathematics 274–286.

[116] Volterra V., 1927. Variazioni E Fluttuazioni Del Numero D'individui in Specie Animali Conviventi. *Memoria della Reale Accademia Nazionale dei Lincei* , **2** , 31–113.

[117] Gause G., 1934. *The Struggle for Existence.* New York: Hafner.

[118] Hutchinson G., Homage to Santa Rosalia or Why Are There So Many Kinds of Animals? *The American Naturalist*, **93**(870), 145–159.

[119] MacArthur R., Levins R., 1967. The Limiting Similarity, Convergence and Divergence of Coexisting Species. *The American Naturalist*, **101**(921), 363–375.

[120] Schoener T., 1983. Field Experiments on Interspecific Competition. *The American Naturalist*, **122**(2), 240–285.

[121] Hairston N., Smith F., Slobodkin L., 1960. Community Structure, Population Control, and Competition. *The American Naturalist*, **94**(879), 421–425.

[122] Carlson T., 1913. Ber Geschwindigkeit Und GrSse Der Hefevermehrung in WRze. *Biochemische Zeitschrift*, **57**, 313–334.

[123] Morgan B., 1976. Stochastic Models of Groupings Changes. *Advances in Applied Probability*, **8** (1), 30–57.

[124] Krebs C., 1985. *The Experimental Analysis of Distribution and Abundance.* New York: Harper and Row.

[125] Scheucher M., Spohn H., 1988. A Soluble Kinetic Model for Spinodal Decomposition. *Journal of Statistical Physics*, **53**(1–2), 279–294.

[126] Dornic I., Chatè H. , Chave J., Hinrichsen H., 2001. Critical Coarsening Without Surface Tension: The Universality Class of the Voter Model. *Physical Review Letters*, **87**(4), 045701.

[127] Kimura M., Weiss G., 1964. The Stepping Stone Model of Population Structure and the Decrease of Genetic Correlation With Distance. *Genetics* , **49**(4), 561–576.

[128] Cox J., 1989. Coalescing Random Walks and Voter Model Consensus Times on the Torus in Z^D. *The Annals of Probability*, **17**(4), 1333–1366.

[129] Behera L., Schweitzer F., 2003. On Spatial Consensus Formation: Is the Sznajd Model Different From a Voter Model? *International Journal of Modern Physics C*, **14**(10), 1331–1354.

[130] Mobilia M., Petersen A., Redner S., 2007. On the Role of Zealotry in the Voter Model. *Journal of Statistical Mechanics*, **2007**(8), 8029.

[131] Kendall D., 1948. On the Generalised "Birth-and-Death" Process. *The Annals of Mathematical Statistics*, **19**(1), 1–15.

[132] Norris J., 1998. *Markov Chains.* England: Cambridge University Press.